CHAPTER 3

ABSORPTION AND DISPERSION OF ULTRASOUND IN BIOLOGICAL MEDIA

Floyd Dunn, Peter D. Edmonds, and William J. Fry†‡

1. INTRODUCTION

After the introduction of the piezoelectric element into acoustics by Langevin [1918] and the subsequent rapid development of electronics in the next 30 years, it became feasible to construct instruments for precise measurement of the velocity of propagation and the absorption coefficient of ultrasonic waves. A notable advance occurred after 1945 when the adaptation of radar techniques yielded pulsed ultrasonic equipment operating in the multimegahertz range. Since that time numerous techniques have been developed which permit utilization of ultrasound in the frequency range from about 2×10^4 Hz (the arbitrary boundary with the "sonic" range) to 10^9 Hz. The extension of the effective range to 10^{11} Hz can be foreseen with the further development of Brillouin scattering techniques (Chiao and Stoicheff, 1964; Benedek et al., 1964).

Two distinct groups of investigators pursuing their individual research interests have employed ultrasonic methods in biologically oriented studies. On the one hand, these techniques have been employed as a means of studying fast physical and chemical reactions, with the objective of obtaining detailed information about the time course of overall and intermediate reactions for the complete kinetic description of reaction mechanisms (Eigen and de Maeyer, 1963; Eigen and Hammes, 1963). Ultrasound offers access to the determination of time constants, ranging from 10^{-3} to 10^{-9} s, for the approach to equilibrium by physical-chemical reactions for which both reactants and products are present in comparable concentrations. It is of interest to note that the fastest rate constant for a diffusion-controlled reaction is 10^{11} l/(mole)(s) for H^+ recombining with OH^- in water. In combination with stopped flow, pressure—and temperature—jump, and pulsed

† The authors gratefully acknowledge the support of the following organizations for portions of the work, described in this chapter, accomplished in the laboratories with which the authors are affiliated: Aero-Medical Laboratory of the Wright-Patterson Air Force Base, American Thoracic Society, Office of Naval Research, National Institutes of Health, National Science Foundation, University of Illinois, and University of Pennsylvania.

‡ Deceased July 21, 1968.

electric field methods, ultrasound and Brillouin scattering methods bridge the considerable gap in time constants which cannot be determined by the more conventional mixing procedures ($\tau_r > 10^{-3}$ s) and the spectroscopic techniques ($\tau_r < 10^{-10}$ s).†

Biochemical reactions involving macromolecules are remarkable for their high degree of specificity. In the presence of a large variety of available chemical substances, only a single one may be selected for a specific chemical reaction in the course of a biochemical sequence. This behavior is distinctly different from the variation in chemical reactivity observed for reactions of simpler chemical species. Therefore, much attention is centered on "active sites," i.e., regions of the exterior of macromolecules where specific recognition of molecular species and subsequent reactions are envisaged to take place. Such sites and generally the entire exterior of a macromolecule will be hydrated, since by binding a layer of relatively immobile water to its exterior, a macromolecule becomes a soluble entity in an aqueous environment. Thus the exteriors of biological macromolecules tend to be hydrophilic, while hydrophobic regions tend to be buried in the interior, thereby achieving remoteness from the aqueous environment.

As a result of hydration, reaction at an active site will require initial disturbance of, or reaction with, water molecules and may involve any ionic species that may be present in the vicinity. Such disturbance or reaction may be involved in one or more of the intermediate steps in the overall reaction scheme at the site in question. It is within the realm of profitable investigation to consider the details of these and other intermediate steps in certain reactions (Eigen and Hammes, 1963). As examples we may cite enzyme-substrate reactions, which include those responsible for the feedback control of important metabolic cycles; the interaction of small molecules such as O_2, CO, H_2O with hemoglobin, which is a constituent part of the heme-heme interaction problem concerning the transport of oxygen by the blood; the conformational changes concerned in the denaturation of proteins and the transport of hydrated ions through membranes.

On the other hand, the second group of investigators who have required ultrasonic velocity and absorption measurements have been those concerned with the use of ultrasound for fundamental studies in cellular organization (Fry et al., 1966) and as tools in medical practice. In medical diagnosis, a pulse-echo technique is employed to obtain information regarding the static and dynamic state of gross tissue structures (Franklin, Schlegel, and Rushmer, 1961; Howry, 1957; Holmes, 1964; Reid and Joyner, 1965). As a therapeutic agent, ultrasound is utilized in two distinct ways: first, as a deep heating agent wherein low intensities (about 1 W/cm² or less) are employed

† A list of symbols is given in Appendix A.

(Aldes, 1957) and secondly, as a selective tissue-modifying agent, wherein very high intensities (approximately 10^3 W/cm^2) are used in the form of pulses of short duration (about 1 s) (Fry and Meyers, 1962). For the successful employment of all these techniques it is essential to have available detailed information on the bulk acoustic properties of specific tissues. More detailed information relating to the modes of interaction of ultrasonic energy with tissue structures is continually being sought.

Although this chapter is not intended to be a comprehensive treatment, the authors have attempted to produce a survey of the pertinent data on ultrasonic velocity and absorption, which bears on the entire spectrum of biological interest. This ranges from the acoustic properties of water to those of discrete tissue structures. The chapter is organized as follows: First, in Sec. 2 ultrasonic fields are described in terms of the basic physics necessary to relate the physical parameters to the propagation parameters; special emphasis is placed here on absorption mechanisms. Also included in this section are brief discussions of effects at large acoustic amplitudes. Section 3 is devoted to selected methods of measuring acoustic velocity and absorption for liquid and liquidlike media. It includes discussions of precision and limitations of the methods and a brief account of the technology of transducers. Section 4 summarizes available acoustic data on aqueous solutions of amino acids, peptides, polypeptides, proteins, and nucleic acids, on liquid media during phase transitions between states, and on tissues. It includes interpretations, where possible, in terms of specific mechanisms of absorption, and distributions of relaxation spectra, etc. The brief concluding remarks indicate deficiencies in our present knowledge with a view to suggesting future directions for fruitful research.

2. PHYSICAL DESCRIPTION OF ULTRASONIC FIELDS

Development of Propagation Relations

The propagation of an acoustic disturbance or the presence of an acoustic field in an elastic medium is characterized by changes in a number of the physical variables that describe the state of the system or medium. Examples of these variables are the pressure, temperature, and density. For a traveling, sinusoidal plane wave propagating in the positive direction of the x axis (when no attenuation of the waves occurs because absorption of energy by the medium is absent), the changes in the physical variables can each be expressed in the form of Eq. (1), provided that the medium responds linearly to the stresses imposed upon it.

$$q = Q \cos \omega\left(t - \frac{x}{v}\right) \quad \text{or} \quad q = \text{Re}\,(Qe^{j\omega(t-x/v)}) \tag{1}$$

In this equation q designates any one of the variables that undergoes sinusoidal change owing to the presence of the disturbance in the medium, and Q designates the amplitude of the cyclic changes in that variable; t and x are the time and space coordinates, ω is the angular frequency ($\omega = 2\pi f$), f is the frequency, and v is the free-field velocity, i.e., the propagation velocity of a plane wave traveling through a liquid medium of infinite extent. Equation (1) is one solution, namely, that representing a wave traveling in the positive x direction, of the one-dimensional elastic wave equation as it applies to an ideal, linear, homogeneous, perfectly elastic (dissipationless), liquid medium:

$$\frac{\partial^2 \xi}{\partial t^2} = \frac{1}{\rho_0 \beta_S} \frac{\partial^2 \xi}{\partial x^2} \tag{2}$$

In this equation ξ is the instantaneous displacement of an element of volume of the medium, β_S is the adiabatic compressibility of the medium, and ρ_0 is the mean density of the medium. This approximation to the more general hydrodynamical equation is valid under conditions that permit linearization, that is, when the velocity amplitude, $\dot{\Xi} = (\partial \xi / \partial t)_{\max}$, of the elementary volume element is small in comparison with the velocity of sound propagation, and when the adiabatic compressibility, which is the reciprocal of the adiabatic elastic bulk modulus K, is not significantly dependent upon pressure over the range of pressure variations present in the acoustic field. Since sound propagation is very close to an adiabatic process at all frequencies of interest, the adiabatic compressibility is a significant parameter in the description of sound propagation. It is related to the free-field sound propagation velocity for compressional waves as follows:

$$v^2 = v_i^2 = \frac{1}{\rho_0 \beta_S} = \frac{\gamma}{\rho_0 \beta_T} = \frac{C_p / C_v}{\rho_0 \beta_T} \tag{3}$$

The velocity of propagation can be expressed, as indicated in Eq. (3), in terms of the isothermal compressibility β_T by introducing the ratio of specific heats. Clearly a measurement of the velocity of propagation of a plane compressional wave can be interpreted immediately to yield the adiabatic compressibility of the medium if the density is known; and if the value of γ is also known, the isothermal compressibility can be determined.

Equation (2) is a special case of the more general wave equation which is applicable to three-dimensional propagation:

$$\frac{\partial^2 \xi}{\partial t^2} = \frac{1}{\rho_0 \beta_S} \nabla^2 \xi \tag{4}$$

Solutions of Eq. (4) include not only waves propagating in the positive r direction, away from the origin, but also those propagating in the negative

r direction, i.e., toward the origin. All are represented when the $\pm$ sign is placed in the exponent for one-dimensional propagation, e.g.,

$$\xi = \Xi_{\pm}(r)e^{j(\omega t \pm \mathbf{k}\cdot\mathbf{r})} \tag{5}$$

The wave vector $\mathbf{k}$ which appears in the solution is related to the angular frequency and the propagation velocity as follows:

$$\mathbf{k} = k\mathbf{n} \qquad k = \frac{\omega}{v} = \frac{2\pi}{\lambda} \qquad v = f\lambda \tag{6}$$

Equation (4) is itself a specialization, applicable to fluids of the type indicated, of the following wave equation describing propagation of disturbances in a dissipationless, isotropic, elastic solid:

$$\frac{\partial^2 \xi}{\partial t^2} = \frac{K + \frac{4}{3}G}{\rho_0} \nabla\nabla \cdot \xi - G\nabla \times \nabla \times \xi \tag{7}$$

The specialization for fluids is obtained when the modulus of shear rigidity G is set equal to zero which is true for lossless fluids, since the latter are characterized by an inability to support an elastic shear strain.

It is possible to express the displacement vector as the sum of terms involving a scalar potential ϕ and a vector potential $\boldsymbol{\phi}$:

$$\xi = \nabla\phi + \nabla \times \boldsymbol{\phi} \tag{8}$$

For irrotational motion, such as in a plane compressional wave of infinite lateral extent, the vector potential $\boldsymbol{\phi} = 0$, and only the scalar displacement potential ϕ remains; that is,

$$\xi = \nabla\phi \tag{9a}$$

The time derivative of the displacement potential is obviously the velocity potential ψ, i.e.,

$$\frac{\partial \phi}{\partial t} = \psi \tag{9b}$$

These potentials are fundamental functions (analogous to electric field potentials) in terms of which acoustic field parameters may be expressed.

Returning to a consideration of the simple plane wave propagating in an ideal isotropic elastic medium in the positive x direction, we can express the sinusoidally varying acoustic parameters in terms of the displacement potential or velocity potential and in terms of one another.

$$p = -\rho_0 \frac{\partial \psi}{\partial t} \qquad \dot{\xi}_x = (\nabla\psi)_x \tag{10}$$

$$s = \frac{\rho - \rho_0}{\rho_0} = \beta_S p \tag{11}$$

$$\vartheta = \frac{T\theta}{\rho_0 C_v'} p = (\gamma - 1)\frac{\beta_S}{\theta} p \tag{12}$$

TABLE 1. RELATIONS BETWEEN AMPLITUDES

Parameter	*Parameter symbol, q*	*Amplitude symbol, Q*	*P* (dyn/cm²)	*S*
Pressure	P	p	—	$-\rho v^2$
Condensation	S	s	$\begin{matrix}+\ 1\\ -\rho_0 v^2\end{matrix}$	—
Particle displacement	ξ	Ξ	$\begin{matrix}+\ 1\\ -j\omega\rho_0 v\end{matrix}$	$\begin{matrix}+\ v\\ +j\omega\end{matrix}$
Particle velocity	$\dot{\xi}$	$\dot{\Xi}$	$\begin{matrix}+\ 1\\ -\rho_0 v\end{matrix}$	$\begin{matrix}+\\ +\end{matrix} v$
Particle acceleration	$\ddot{\xi}$	$\ddot{\Xi}$	$\begin{matrix}+\ j\omega\\ -\rho_0 v\end{matrix}$	$\begin{matrix}+\\ +\end{matrix} j\omega v$
Temperature	ϑ	Θ	$\begin{matrix}+1\\ +\theta\end{matrix}\left(\beta_T - \dfrac{1}{\rho_0 v^2}\right)$	$\begin{matrix}+\rho_0 v^2\\ -\ \theta\end{matrix}\left(\beta_T - \dfrac{1}{\rho_0 v^2}\right)$

† Multiply expression in table by column heading to obtain relations equal to the relations given apply to plane waves traveling in either direction. The upper sign applies to negative direction (see Eq. 5). The amplitude of the change in any one physical parameter value of the appropriate quantity in the table. One self-consistent set of units is used in

where s is the condensation or the fractional change in density, ρ is the instantaneous density, ϑ is the instantaneous temperature increment resulting from adiabatic compression of the medium, θ is the isobaric thermal expansion coefficient, and C_p' is the heat capacity at constant pressure per gram. The interrelation of the acoustic field parameters is shown in Table 1. The method of detection and description of the field, in any specific case, may depend on the measurement of one or several of these parameters. The quantity $\rho_0 v$, the product of density and sound velocity, which appears in many relations in the table, is known as the characteristic acoustic impedance of the medium, Z_0; that is,

$$Z_0 = \rho_0 v \tag{13}$$

For plane traveling waves it is numerically equal to the specific acoustic impedance, which is defined as the ratio of the pressure p to the particle velocity v at any point in the field. For other field configurations, including

OF THE VARIOUS PHYSICAL PARAMETERS†

Ξ (cm)	$\dot{\Xi}$ (cm/s)	$\ddot{\Xi}$ (cm/s²)	Θ (°C)
$\begin{matrix}+\\-\end{matrix} j\omega\rho_0 v$	$\begin{matrix}+\\-\end{matrix} \rho_0 v$	$\begin{matrix}+\\-\end{matrix} \dfrac{\rho_0 v}{j\omega}$	$+\dfrac{\theta}{+\beta_T - \dfrac{1}{\rho_0 v^2}}$
$\begin{matrix}+j\omega\\+v\end{matrix}$	$\begin{matrix}+1\\+v\end{matrix}$	$\begin{matrix}+\\+\end{matrix} \dfrac{1}{j\omega v}$	$+\dfrac{\theta}{-\beta v^2\left(\beta_T - \dfrac{1}{\rho_0 v^2}\right)}$
—	$\begin{matrix}+1\\+j\omega\end{matrix}$	$\begin{matrix}-1\\-\omega^2\end{matrix}$	$+\dfrac{\theta}{-j\omega\rho_0 v\left(\beta_T - \dfrac{1}{\rho_0 v^2}\right)}$
$\begin{matrix}+\\+\end{matrix} j\omega$	—	$\begin{matrix}+1\\+j\omega\end{matrix}$	$+\dfrac{\theta}{-\rho_0 v\left(\beta_T - \dfrac{1}{\rho_0 v^2}\right)}$
$\begin{matrix}-\\-\end{matrix} \omega^2$	$\begin{matrix}+\\+\end{matrix} j\omega$	—	$+\dfrac{j\omega\theta}{-\rho_0 v\left(\beta_T - \dfrac{1}{\rho_0 v^2}\right)}$
$\begin{matrix}+j\omega\rho_0 v\\-\theta\end{matrix}\left(\beta_T - \dfrac{1}{\rho_0 v^2}\right)$	$\begin{matrix}+\rho_0 v\\-\theta\end{matrix}\left(\beta_T - \dfrac{1}{\rho_0 v^2}\right)$	$\begin{matrix}+\rho_0 v\\-j\omega\theta\end{matrix}\left(\beta_T - \dfrac{1}{\rho_0 v^2}\right)$	—

amplitude quantities tabulated in the Amplitude Symbol column. *Note:* $j = \sqrt{-1}$. The waves traveling in the positive direction and the lower sign applies to waves traveling in the is simply equal to the amplitude of the change in any other parameter times the absolute the table.

plane standing waves, the specific acoustic impedance differs numerically from $\rho_0 v$ and is, in general, a function of position. It should be noted also that the characteristic acoustic impedance is dependent on the type of wave that is propagating, since the velocity of shear waves is different from that of compressional waves.

The intensity I of the sound wave is defined as the time average of the rate of propagation of energy through unit area normal to the direction of propagation, and it is related to field-parameter amplitudes as follows for plane traveling waves

$$I = \frac{P^2}{2Z_0} = \frac{P\dot{\Xi}}{2} = \frac{Z_0\dot{\Xi}^2}{2} \tag{14}$$

The energy density of the wave motion at a specific position in the field is the sum of the kinetic energy, per unit volume, of the moving volume

TABLE 2. NUMERICAL EXAMPLES OF PHYSICAL PARAMETERS FOR WATER

Material	f (MHz)	T (°C)	P_0 (atm)	I (W/cm²)	P (atm)	S	Ξ (cm)	$\dot{\Xi}$ (cm/s)	$\ddot{\Xi}$ (cm/s²)	Θ (°C)	$\frac{\dot{\Xi}}{v}$
Multiply figures in table by	1	1	1	1	1	10^{-5}	10^{-6}	1	10^{6}	10^{-4}	10^{-5}
Water, degassed, distilled	1	30	1	0.01	0.171	0.762	0.183	1.15	7.22	3.82	0.762
				1	1.71	7.62	1.83	11.5	72.2	38.2	7.62
				100	17.1	76.2	18.3	115	722	382	76.2

element and the potential energy, per unit volume, of compression (or expansion) of the element. For plane traveling waves it is equal to the ratio of the intensity to the velocity of propagation, i.e.,

$$E_0 = \frac{\rho_0 \dot{\Xi}^2}{2} = \frac{I}{v} \tag{15}$$

It may be remarked that rms quantities are not employed in the majority of publications in acoustics, and consequently the symbols in Eqs. (14) and (15) are the amplitudes of the acoustic field parameters. If rms values had been used, the factors 2 would have been eliminated from the equations.

As stated previously, linearizing of the hydrodynamical equations depends upon two assumptions which can now be expressed symbolically:

$$\frac{\dot{\Xi}}{v} \ll 1 \qquad \frac{(\beta_S)_{P_0+P} - (\beta_S)_{P_0-P}}{(\beta_S)_{P_0}} \ll 1 \tag{16}$$

where P_0 represents the ambient pressure in the absence of a sound wave. Nonlinear or second-order effects still may be of importance for values of $\dot{\Xi}/v$ smaller, for example, than 0.01, but the linearized equations constitute a good first approximation for calculating values of the physical parameters when this numerical limit is placed on the interpretation of the symbol $\ll 1$.

Table 2 shows values of the numerical magnitudes of the acoustic field parameters for a plane traveling wave, when the propagation medium is water, for representative intensity values of the wave spanning four orders of magnitude. It may be noted particularly that the temperature excursion in water is small, and that this parameter is entirely unrelated to the monotonic rise in temperature of the specimen, which occurs only when energy is absorbed by the specimen. However, even for low-amplitude ultrasonic waves which may be used as a probe to measure the response of a system to an extremely small perturbation, the pressure amplitude may be comparable to one atmosphere, and the amplitude of the particle acceleration can be exceedingly high.

Table 3 lists values for the various characteristic constants of a number of materials of general utility or otherwise important in biological investigations employing ultrasound. These data may be used in connection with the relations appearing in Table 1 to obtain numerical values of field parameters such as those listed in Table 2. It is usually convenient to express the intensity in watts per square centimeter and the acoustic pressure amplitude in atmospheres. However, for calculations using the expressions of Table 1 the intensity should be expressed in ergs per square centimeter per second and the pressure amplitude in dynes per square centimeter if the other parameters are expressed in the indicated units.

TABLE 3A. PHYSICAL CONSTANTS OF VARIOUS MATERIALS

Material	T (°C)	P (atm)	ρ_0 (g/cm³)	v (cm/s)	$\rho_0 v$ [g/(cm²)(s)]	C_p/C_v	β_T (cm/d²)	θ [(°C)⁻¹]	α (cm⁻¹)
Multiply figures in table by	1	1	1	10^5	10^5	1	10^{-12}	10^{-5}	1
Water									
Degassed, distilled	0	1	0.999841	1.4027	1.4025	1.000583	50.86	−5.89	
α proportional to f^2[a]	10	1	0.999701	1.4476	1.4472	1.001085	47.79	+9.45	
	20	1	0.998207	1.4827	1.4800	1.00656	45.86	21.19	25×10^{-5}
	30	1	0.995651	1.5094	1.5028	1.01526	44.76	30.75	
	40	1	0.992220	1.5292	1.5173	1.02575	44.20	38.93	
	0	136	0.9941	1.4245	1.4161	1.00012	49.58	2.01	
	10	136	0.9946	1.4700	1.4621	1.00356	46.69	15.09	
	20	136	0.9961	1.5057	1.4998	1.01041	44.74	25.10	
	30	136	0.9986	1.5329	1.5308	1.01827	43.40	34.05	
	40	136	1.0019	1.5531	1.5560	1.02672	42.48	40.92	
Water solutions									
0.9% normal saline[b]	0	1	1.00668	1.4134	1.4228			1.98	
	10	1	1.00631	1.4582	1.4674			8.46	
	20	1	1.00460	1.4932	1.5001			23.89	
	30	1	1.00189	1.5198	1.5268			29.94	
	40	1	0.99837	1.5394	1.5369			40.07	
Oils									
Castor. At 30°C, α proportional to $f^{5/3}$[a,c]	0	1	0.972	1.580	1.536				0.26
	10	1	0.960	1.536	1.474				0.16
	20	1	0.952	1.494	1.422				0.096
	30	1	0.946	1.452	1.374				0.057
	40	1	0.941	1.411	1.328				0.037
Phenylated silicone, Dow-Corning no.	0	1	1.124	1.446	1.625				
710, α proportional to f^2, to approx.	10	1	1.112	1.409	1.567				0.135
20 MHz[a,d]	20	1	1.102	1.378	1.518				0.070
	30	1	1.095	1.349	1.477				0.040
	40	1	1.089	1.321	1.438				0.024
Aluminum (rolled)			2.70	6.42	17.3				
Ceramics									
(approximate range)			2.5 to 3.4	4.6 to 6.8	12 to 18				
Glasses									
Borate crown (light)			2.24	5.10	11.4				
Pyrex (702)			2.32	5.64	13.1				
Silicate flint (heavy)			3.88	3.98	15.4				
Silica (fused)			2.2	5.97	13.1				
Steels									
Stainless (347)			7.91	5.79	45.8				

TABLE 3B. PHYSICAL CONSTANTS OF BIOLOGICAL MEDIA†

Material	T (°C)	P (atm)	ρ_0 (g/cm³)	v (cm/s)	$\rho_0 v$ [g/(cm²)(s)]		α (cm⁻¹)
Multiply figures in table by	1	1	1	10^5	10^5		1
Central nervous system[a,e,f,g]							

	40	1	1.089	1.321	1.438				0.024
Aluminum (rolled)			2.70	6.42	17.3				
Ceramics									
(approximate range)			2.5 3.4	4.6 6.8	12 18				
Glasses									
Borate crown (light)			2.24	5.10	11.4				
Pyrex (702)			2.32	5.64	13.1				
Silicate flint (heavy)			3.88	3.98	15.4				
Silica (fused)			2.2	5.97	13.1				
Steels									
Stainless (347)			7.91	5.79	45.8				

TABLE 3B. PHYSICAL CONSTANTS OF BIOLOGICAL MEDIA†

Material	T (°C)	P (atm)	ρ_0 (g/cm³)	v (cm/s)	$\rho_0 v$ [g/(cm²)(s)]		α (cm⁻¹)
Multiply figures in table by	1	1	1	10^5	10^5		1
Central nervous system[a,e,f,g]							
Average for brain	37	1	1.03	1.51	1.56		0.11
Cortical gray matter (cat)	37	1	1.03				0.08
Cortical white matter (cat)	37	1	1.03				0.14
Spinal cord (mouse 24 h after birth)	2						0.017
	10						0.050
	28						0.095
	40						0.115
	45						0.125
Muscle (skeletal)[a,e,f]	37	1	1.07	1.57	1.68		0.13
Fat[a,f]	37	1	0.97	1.44	1.40		0.05
Bone							
Skull (human)[h]	37	1	1.7	3.36	6.0		
Frequency, MHz 0.6		1					0.4
0.8		1					0.9
1.2		1					1.7
1.6		1					3.2
1.8		1					4.2
2.25		1					5.3
3.5		1					7.8

† Further numerical data are given by Goldman and Hueter [1956, 1957].

[a] Values of α for 1 MHz.

[b] Measurements of W. D. Wilson, U.S. Naval Ordnance Laboratory.

[c] Power dependence indicated holds over entire range at measurements from 400 kHz to 500 MHz at 30°C.

[d] Measurements at 26°C over the frequency range 1 to 2000 MHz indicate (assuming negligible velocity dispersion) the presence of a single relaxation process centered at 40 MHz.

[e] Varies with direction of sound propagation relative to fiber orientation.

[f] α proportional to frequency.

[g] The young mouse cord is virtually unmyelinated and displays a value of α, at 37°C, equal to the average value for the adult animal.

[h] Absorption coefficient listed for bone includes effects of reflections at interfaces within the bone structure.

Reflection and Refraction

Reflection and refraction of acoustic waves occur in a manner analogous to that for electromagnetic waves, and many of the concepts that arise in the theory of transmission lines are applicable in "one-dimensional" situations. The formulas listed in Table 4 are for media within which no acoustic absorption occurs and for which the normals to the planar wave fronts and the normals to the interfaces lie in the same plane.

Case 1. Reflection and transmission occur at a single interface between two media. The reflection coefficient $\mathscr{R}_a$, the transmission coefficient $\mathscr{T}_a$, and the standing-wave ratio (SWR), for waves incident on the interface from

TABLE 4. PRESSURE AMPLITUDE OF REFLECTED AND TRANSMITTED WAVES FOR VARIOUS COMBINATIONS OF MEDIA†

Case 1. Wave in medium 1 at normal incidence on boundary between medium 1 and medium 2. No energy returned to interface in medium 2. No absorption within media.

Configuration	*Definition*	*Formulas*
$\rho_1 v_1$ | $\rho_2 v_2$ $\rightarrow$ $\rightarrow$ P_{1+} P_{2+} $\leftarrow$ $\leftarrow$ P_{1-} P_{2-} $\longrightarrow +$	$r_{2/1} = \dfrac{\rho_2 v_2}{\rho_1 v_1}$	$\mathscr{R}_a = \left\lvert \dfrac{P_{1-}}{P_{1+}} \right\rvert = \left\lvert \dfrac{1 - r_{2/1}}{1 + r_{2/1}} \right\rvert$ $\mathscr{T}_a = \left\lvert \dfrac{P_{2+}}{P_{1+}} \right\rvert = \left\lvert \dfrac{2r_{2/1}}{1 + r_{2/1}} \right\rvert$ $(\mathrm{SWR})_1 = \begin{cases} r_{2/1} \text{ when } r_{2/1} > 1 \\ 1/r_{2/1} \text{ when } r_{2/1} < 1 \end{cases}$

Case 2. Wave in medium 1 at normal incidence. Slab of medium 3 interposed between medium 1 and medium 2. No energy returned to interface in medium 2. No absorption within media.

Configuration	*Definitions*	*Formulas*
$\rho_1 v_1$ | $\rho_3 v_3$ | $\rho_2 v_2$ P_{1+} P_{2+} P_{1-} $P_{2-} = 0$ $\leftarrow x_3 \rightarrow$ $\longrightarrow +$	$r_{2/1} = \dfrac{\rho_2 v_2}{\rho_1 v_1}$ $r_{3/1} = \dfrac{\rho_3 v_3}{\rho_1 v_1}$ $r_{2/3} = \dfrac{\rho_2 v_2}{\rho_3 v_3}$	$\mathscr{R}_a = \left\lvert \dfrac{P_{1-}}{P_{1+}} \right\rvert = \left[1 - \dfrac{4r_{2/1}}{(r_{2/1}+1)^2 \cos^2 \dfrac{\omega x_3}{v_3} + (r_{3/1}+r_{2/3})^2 \sin^2 \dfrac{\omega x_3}{v_3}} \right]^{1/2}$ $\mathscr{T}_a = \left\lvert \dfrac{P_{2+}}{P_{1+}} \right\rvert = \left[\dfrac{4r_{2/1}^2}{(r_{2/1}+1)^2 \cos^2 \dfrac{\omega x_3}{v_3} + (r_{3/1}+r_{2/3})^2 \sin^2 \dfrac{\omega x_3}{v_3}} \right]^{1/2}$

TABLE 4 (*continued*)

Case 3. Wave in medium 1 incident at angle θ_1 with respect to normal on boundary between medium 1 and medium 2. No energy returned to interface in medium 2. No absorption within media.

Configuration	*Definition*	*Formulas*
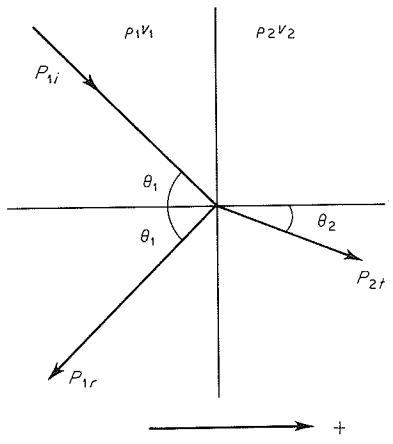	$r_{2/1} = \dfrac{\rho_2 v_2}{\rho_1 v_1}$	$\mathscr{R}_a = \left\lvert \dfrac{P_{1r}}{P_{1i}} \right\rvert = \left\lvert \dfrac{\dfrac{\cos\theta_2}{\cos\theta_1} - r_{2/1}}{\dfrac{\cos\theta_2}{\cos\theta_1} + r_{2/1}} \right\rvert$ $\mathscr{T}_a = \left\lvert \dfrac{P_{2t}}{P_{1i}} \right\rvert = \left\lvert \dfrac{2r_{2/1}\cos\theta_1}{\cos\theta_2 + r_{2/1}} \right\rvert$ $\dfrac{\sin\theta_1}{\sin\theta_2} = \dfrac{v_1}{v_2}$

Case 4. Longitudinal or shear wave in medium 1 incident at angle θ_1. Solid or viscoelastic media. Mode conversion with generation of shear waves in media 1 and 2. No energy returned to interface in medium 2. Absorption within media sufficiently small for impedance to be approximated by real parts.

Configuration	*Definitions*	*Formulas*
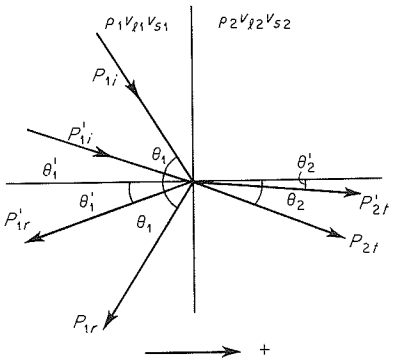	$r_{2/1} = \dfrac{\rho_2 v_{l2}}{\rho_1 v_{l1}}$ $r'_{2/1} = \dfrac{\rho_2 v_{s2}}{\rho_1 v_{l2}}$ $r'_{1/1} = \dfrac{\rho_1 v_{s1}}{\rho_1 v_{l1}}$	$\dfrac{\sin\theta_1}{\sin\theta_2} = \dfrac{v_{l1}}{v_{l2}}$ $\dfrac{\sin\theta_1}{\sin\theta'_2} = \dfrac{v_{l1}}{v_{s2}}$ $\dfrac{\sin\theta_1}{\sin\theta'_1} = \dfrac{v_{l1}}{v_{s1}}$

† *Note:* Only the ratios of the magnitudes of the pressure amplitudes are listed; i.e., the phase factors are not included.

medium 1 are functions only of the ratio of the characteristic acoustic impedances of the two media, $r_{2/1} = \rho_2 v_2/\rho_1 v_1$. For partial reflection at normal incidence, the complete expression for the pressure variation for a sinusoidal disturbance of infinite extent can be represented by the summation of two waves, one traveling in the positive and the second in the negative x direction:

$$p = P_+ e^{j\omega(t-x/v)} + P_- e^{j\omega(t+x/v)} \tag{17}$$

where P_+ is the amplitude of the pressure wave traveling in the positive direction, and P_- is the amplitude of a similar wave traveling in the negative direction. The standing-wave ratio in either medium may be defined as

$$\text{SWR} = \frac{|P_{\max}|}{|P_{\min}|} = \frac{1 + |P_-/P_+|}{1 - |P_-/P_+|} \tag{18}$$

where $P_{\max}$ is the maximum value of the pressure amplitude in the field of interference of the incident and reflected waves, and $P_{\min}$ is the minimum value of the pressure amplitude. A distinction is required between reflection and transmission coefficients referring to the amplitude of the disturbance and those referring to the power carried by the acoustic waves. The coefficients are defined respectively as the ratios of the amplitudes or the intensities of the reflected and transmitted waves to the amplitude or intensity of the incident wave, i.e.,

$$\mathscr{R}_a = \frac{P_{1-}}{P_{1+}} = \frac{Z_2 - Z_1}{Z_2 + Z_1} \qquad \mathscr{T}_a = \frac{P_{2+}}{P_{1+}} = \frac{2Z_2}{Z_2 + Z_1} \tag{19}$$

$$\mathscr{R}_I = \frac{I_{1-}}{I_{1+}} = \left(\frac{P_{1-}}{P_{1+}}\right)^2 = \mathscr{R}_a^2 \qquad \mathscr{T}_I = \frac{I_{2+}}{I_{1+}} = \frac{Z_1}{Z_2}\,\mathscr{T}_a^2 \tag{20}$$

In these expressions subscript a designates amplitude coefficients and subscript I designates power or intensity coefficients. Conservation of energy requires that the sum of the power reflection and transmission coefficients should always equal unity whereas the sum of the amplitude coefficients is not in general equal to unity.

$$\mathscr{R}_I + \mathscr{T}_I = 1 \tag{21}$$

The coefficients described here as transmission coefficients are frequently described as absorption coefficients in experiments involving irradiation of a specimen. This difference in viewpoint arises from the fact that in irradiation experiments, interest is confined to measuring the standing-wave ratio in the medium situated in front of the specimen. Any energy transmitted into the specimen is therefore effectively lost or appears to be absorbed. From the point of view of the properties of the interface between two media, this "lost" energy is merely transmitted into the second medium. The term absorption coefficient will be reserved for later use when a study is made of the attenuation of the transmitted wave-amplitude mechanisms which are operative within the second medium.

Case 2. A slab of a third medium of thickness x_3 is interposed between two media. The reflection coefficient $\mathscr{R}_a$ and the transmission coefficient $\mathscr{T}_a$ are functions of the ratios of the characteristic impedances and of the quantity $\omega x_3/v_3$ (equal to $2\pi x_3/\lambda_3$), which is determined by the ratio of the thickness of medium 3 and the wavelength in it. If the characteristic impedance of medium 3 is intermediate between those of media 1 and 2, then the transmission coefficient can be maximized by choosing the thickness x_3 to satisfy the relation

$$\frac{x_3}{\lambda_3} = \frac{2n-1}{4} \qquad n = 1, 2, 3, \ldots \tag{22}$$

The amplitude transmission coefficient then becomes

$$\mathscr{T}_a = \left| \frac{2r_{3/1}}{r_{3/1} + r_{2/3}} \right| \tag{23}$$

That is, the best choice of thickness that can be made for any interposed material (if its characteristic acoustic impedance is any value between those of the other media) is one-quarter wave or odd multiples thereof. In addition, if one is free to choose the interposed material so that its characteristic acoustic impedance is optimum for transmitting the acoustic energy, then the reflected wave in medium 1 can be completely eliminated by choosing the intermediate material so that

$$(\rho_3 v_3)^2 = (\rho_1 v_1)(\rho_2 v_2) \tag{24}$$

If the characteristic acoustic impedance of medium 3 is not between those of the other two media, then the optimum choice of thickness for the slab to obtain the maximum value of the transmission coefficient is an integral multiple of a half-wavelength, i.e.,

$$x_3/\lambda_3 = n(1/2) \qquad n = 1, 2, 3, \ldots \tag{25}$$

The transmission coefficient then becomes identical with Eq. (19). If media 1 and 2 have nearly equal characteristic acoustic impedances less than that of medium 3, and if the thickness of the interposed slab satisfies the relation $r_{3/1}(\omega x_3/v_3) \leq 1/10$, then the transmission coefficient does not differ from that of case 1 by more than 1 percent. If the characteristic acoustic impedance of medium 3 is less than that of media 1 and 2, then $r_{2/3}$ should be used in place of $r_{3/1}$ in the foregoing inequality.

Case 3. A plane wave is incident at any angle θ_1 on the plane interface between two fluid media. The angle of refraction θ_2 is a function of the angle of incidence and the ratio of the velocities of sound in the two media. The pressure transmission and reflection coefficients also involve the ratio of characteristic impedances. If $\sin\theta_1 > v_1/v_2$, then the incident wave is totally reflected, and there is no propagation of a refracted wave in medium 2. It should also be observed from the form of the reflection coefficient that there is no reflected wave if the ratio of velocities satisfies either of the

relations $\rho_2/\rho_1 > v_1/v_2 > 1$ or $\rho_2/\rho_1 < v_1/v_2 < 1$, and if the angle of incidence satisfies the relation

$$\sin\theta_1 = \frac{r_{21}^2 - 1}{r_{21}^2 - (v_2/v_1)^2} \tag{26}$$

Case 4. When the waves are incident obliquely and both media are solids or viscoelastic, the effects of shear rigidity are exhibited. The boundary conditions to be satisfied are continuity of pressure and of the normal and parallel components of particle displacement. The condition on the parallel component is satisfied by the occurrence of shear waves in one or both media. In the configuration of Table 4, the direction of polarization of the shear waves is in the plane of the diagram. An obliquely incident longitudinal wave generates reflected and refracted longitudinal waves, and in addition reflected and refracted shear waves. An incident shear wave polarized in the plane of the diagram generates a similar set of four waves. A shear wave obliquely incident as indicated and polarized perpendicularly to the diagram, that is, parallel to the interface, will generate only refracted and reflected shear waves of the same polarization since there is no component of motion perpendicular to the interface (Redwood, 1960). If either medium behaves as an ideal fluid, then it does not support shear-wave propagation (Mayer, 1964). Muskat and Meres [1940] derived expressions for the ratios of the *components* of displacements perpendicular to an interface between two perfectly elastic solids; their results are given below, and they may be used not only for perfectly elastic solids but also, with caution, for those viscoelastic solids exhibiting small absorption of energy. Absorption will be regarded then as the result of independent processes influencing the wave amplitudes during propagation toward and away from the interface. The following definitions apply in this paragraph only:

$$a \equiv \frac{v_{s_2}}{v_{s_1}}\left[1 - 2\left(1 - \frac{G_2}{G_1}\right)\sin^2\theta_1'\right]$$

$$b \equiv \frac{G_2}{G_1}\frac{v_{s_1}}{v_{s_2}} - a$$

$$d^{\pm} \equiv \frac{G_2}{G_1}\left(\frac{v_{l_2}}{v_{s_2}}\cos\theta_1\cos\theta_2' \pm \frac{v_{l_1}}{v_{s_2}}\cos\theta_2\cos\theta_1'\right)$$

$$e^{\pm} \equiv b^2\sin\theta_1\sin\theta_2 \pm \frac{v_{l_2}}{v_{s_1}}\left(b + \frac{v_{s_2}}{v_{s_1}}\right)^2\cos\theta_1\cos\theta_1'$$

$$f^{\pm} \equiv \frac{v_{l_1}}{v_{s_2}}\cos\theta_2\cos\theta_2'\left[a^2 \pm \frac{4v_{s_2}^2}{v_{s_1}v_{l_1}}\left(\frac{G_2}{G_1} - 1\right)^2\sin^2\theta_1'\cos\theta_1\cos\theta_1'\right]$$

$$g \equiv (d^+ + e^+ + f^+)^{-1}$$

The ratios of the perpendicular components of the displacements are as follows. Ratios of total displacement amplitudes are obtained by multiplying by appropriate trigonometric functions of the angles $\theta_{1,2}$ and $\theta_{1,2}'$.

1. For reflection of a longitudinal wave:

$$\left(\frac{\xi_{1r}}{\xi_{1i}}\right)_{\perp} = g(d^{-} - e^{-} - f^{-})$$

2. For conversion of an incident longitudinal wave into a reflected shear wave:

$$\left(\frac{\xi'_{1r}}{\xi_{1i}}\right)_{\perp} = -2g \sin\theta_1 \sin\theta_2 \left[b\left(b + \frac{v_{s_2}}{v_{s_1}}\right) + 2a\frac{v_{s_1}}{v_{l_2}}\left(\frac{G_2}{G_1} - 1\right)\cos\theta_2 \cos\theta'_2\right]$$

3. For reflection of a shear wave:

$$\left(\frac{\xi'_{1r}}{\xi'_{1i}}\right)_{\perp} = -g(d^{-} - e^{-} - f^{-})$$

4. For conversion of an incident shear wave into a reflected longitudinal wave:

$$\left(\frac{\xi_{1r}}{\xi'_{1i}}\right)_{\perp} = \cot\theta'_1 \cot\theta_1 \left(\frac{\xi'_{1r}}{\xi_{1i}}\right)_{\perp}$$

5. For refraction of a longitudinal wave:

$$\left(\frac{\xi_{2t}}{\xi_{1i}}\right)_{\perp} = 2g\frac{v_{l_1}}{v_{s_1}}\cos\theta_2\left[\left(b + \frac{v_{s_2}}{v_{s_1}}\right)\frac{v_{s_2}}{v_{s_1}}\cos\theta'_1 + a\cos\theta'_2\right]$$

6. For conversion of an incident longitudinal wave into a refracted shear wave:

$$\left(\frac{\xi'_{2t}}{\xi_{1i}}\right)_{\perp} = 2g\frac{v_{s_2}}{v_{s_1}}\sin\theta_1 \sin\theta_2\left[2\frac{v_{s_2}}{v_{l_2}}\left(\frac{G_2}{G_1} - 1\right)\cos\theta_2 \cos\theta'_1 - b\right]$$

7. For refraction of a shear wave:

$$\left(\frac{\xi'_{2t}}{\xi'_{1i}}\right)_{\perp} = 2g\frac{v_{s_2}v_{l_2}}{v_{s_1}^{2}}\cos\theta'_1\left[\frac{v_{l_1}}{v_{l_2}}a\cos\theta_2 + \left(b + \frac{v_{s_2}}{v_{s_1}}\right)\cos\theta_1\right]$$

8. For conversion of an incident shear wave into a refracted longitudinal wave:

$$\left(\frac{\xi_{2t}}{\xi'_{1i}}\right)_{\perp} = 2g\frac{v_{l_1}}{v_{s_1}}\cot\theta'_1 \sin\theta'_2 \cos\theta_2\left[b - 2\frac{v_{s_1}}{v_{l_1}}\left(\frac{G_2}{G_1} - 1\right)\cos\theta_1 \cos\theta'_2\right]$$

The formulas given in this section (cases 1 to 4) are important, for example, in calculating, at least approximately, the amplitude of the waves reflected at tissue interfaces, the accuracy of geometric placement or localization of a beam focus deep in tissue, the acoustic velocity values from standing-wave data, the magnitude of the effect of the reflected acoustic energy on driving transducers, etc. The formulas are also useful in the design of ultrasonic

instruments where considerations of energy transfer from the transducer to the material of interest arise. More complicated configurations of materials and interfaces may arise in practice. The effects on the field of absorption within a medium will be considered in the section dealing with the physical mechanisms of absorption.

Absorption

When an ultrasonic wave propagates through any real liquid, energy is absorbed from the wave and converted into heat. The rate of heat production in a selected volume of a medium in which such a field exists is determined by the amplitude, frequency, and spatial distribution of the field parameters. A variety of different mechanisms may play a role in the conversion of sonic energy into heat, and these will be discussed.

The occurrence of absorption modifies the phenomenological description of lossless plane-wave propagation by the introduction of an absorption coefficient, i.e.,

$$q = Qe^{-\alpha x} \operatorname{Re}\left(e^{j\omega(t-x/v)}\right) \tag{27}$$

where α is the amplitude absorption coefficient per unit distance. The intensity absorption coefficient per unit distance, μ, is equal to 2α. The fractional energy loss per unit volume per cycle is

$$\frac{\delta E_0}{E_0} = \frac{1}{E_0}\int_0^{1/f} (P_0 + p)\, dV = 2\alpha\lambda \tag{28}$$

where E_0 is the energy stored per unit volume. This quantity may also be expressed in terms of a quality factor Q_m or the logarithmic decrement Δ' of a field parameter per cycle, defined by Eq. (29), both of which are commonly used to describe the behavior of acoustic or electrical resonators.

$$\frac{\delta E_0}{2\pi E_0} = \frac{1}{Q_m} = \frac{\Delta'}{\pi} = \tan\varphi = \frac{1}{\pi f t_D} \simeq \frac{\alpha\lambda}{\pi} \text{ for } \alpha \ll \frac{\omega}{v} \tag{29}$$

where φ is the angle of lag between a perturbation applied to the medium and an appropriate response parameter, and t_D is the decay constant of a field-amplitude parameter. Absorption occurs in a homogeneous liquid when the changes in density are not in time phase with the changes in pressure, i.e., when the time at which the maximum pressure occurs differs from the time at which maximum density occurs. This type of behavior is produced by a variety of mechanisms classified under two general categories, relaxation and hysteresis.

Relaxation processes

It will be convenient to discuss relaxation phenomena first of all in terms of a specific example. The relaxation mechanism which is related to the shear viscosity of the medium is chosen for this purpose. If viscosity is the only mechanism responsible for absorption of a traveling, plane compressional wave, then the absorption coefficient is given by

$$\alpha_v = \frac{2\pi^2 f^2}{\rho_0 v_l^3} \cdot \frac{4}{3}\eta \equiv Bf^2 \qquad \text{for } \frac{\alpha_v \lambda}{2\pi} \ll 1 \tag{30}$$

where η is the shear-viscosity coefficient of the medium, and $B = 8\pi^2\eta/3\rho_0 v_l^3$ is the classical absorption parameter related to viscosity. In many nonmetallic liquids, particularly those which are associated and which exhibit appreciable viscosity, it is found that the measured absorption coefficient is approximately described by the classical absorption expression (30) within a factor of about 3. In other cases the classical and measured absorption-coefficient values differ by orders of magnitude. Consider first a hypothetical liquid for which Eq. (30) accurately describes the measured absorption coefficient at lower frequencies. At higher frequencies it appears that the absorption coefficient should increase in proportion to the square of the frequency, assuming that the viscosity remains constant while the frequency is allowed to increase. This prediction is approximately true over only a limited frequency range for which the "effective value" of the viscosity coefficient is the same as the value at low frequencies, that is, under "static" conditions. As the frequency increases, the effective viscosity decreases monotonically toward zero, owing to the finite time required for the transfer of momentum between adjacent regions of the liquid.

Under nonequilibrium conditions the shear stress across a planar element at any position in a medium is not equal to the static value given by the product of the shear-viscosity coefficient and the space gradient of the particle velocity, but this product constitutes the value toward which it tends. The simplest hypothesis to make regarding the approach to the "static" value is to assume that its rate is proportional to the difference between the instantaneous value and the "static" value; i.e.,

$$\frac{\partial \mathbf{T}}{\partial t} = \frac{1}{\tau_1}\left(\eta^0 \frac{\partial \xi}{\partial x} - \mathbf{T}\right) \tag{31}$$

where τ_1 is the proportionality constant which is in the nature of a time constant, the relaxation time, and η^0 is the low-frequency viscosity coefficient.

Consider the situation shown in Fig. 1, where a viscous incompressible liquid is in dynamic equilibrium at time $t < 0$. A state of laminar flow is imposed by an applied small velocity $\dot{u}_i(x_0)$ at the plane $x = x_0$ while the plane at $x = 0$ is fixed. The velocity present in the viscous liquid will

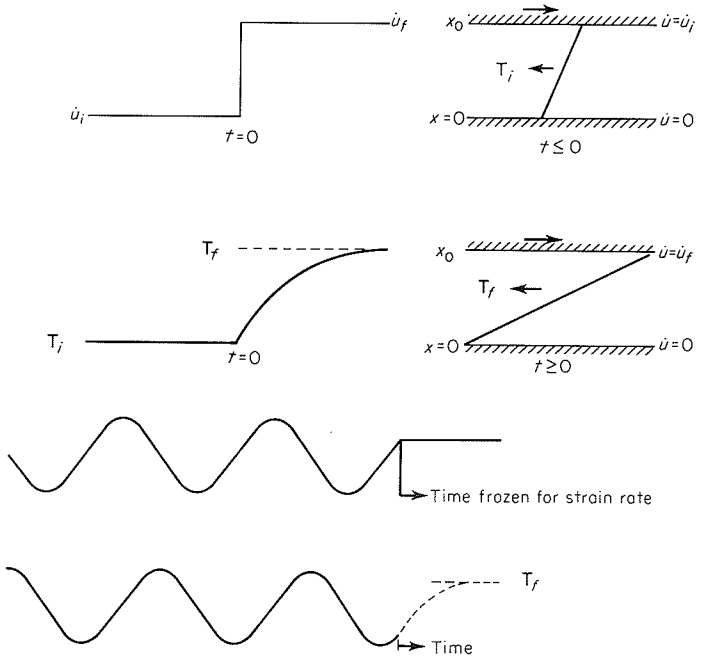

FIG. 1. Viscous fluid medium subjected to step-function and sinusoidal strain rates.

depend linearly upon x, and the shear stress $\mathbf{T}_i = -\eta^0 \dot{u}_i/x_0$ will be independent of x and t. Let the velocity at the plane $x = x_0$ be increased instantaneously to the value $\dot{u}_f(x_0)$ so that a small step-function perturbation is applied to the system. There will be a tendency for the shear stress at any value of x to increase toward a new value $\mathbf{T}_f$, where $\mathbf{T}_f = -\eta^0 \dot{u}_f/x_0$. Since transfer of momentum in the x direction is necessary to achieve this increase, the shear stress $\mathbf{T}(t)$ will not rise to $\mathbf{T}_f$ immediately but will tend asymptotically to this limit. An approximate solution to Eq. (31) is obtained by supposing that the kinematic viscosity coefficient is large enough so that inertial forces can be neglected, and by regarding $\eta^0 \partial\dot{\xi}/\partial x$ as the time-independent stress $\mathbf{T}^0$ to which the instantaneous stress $\mathbf{T}$ tends; Eq. (31) becomes

$$\frac{\partial \mathbf{T}}{\partial t} = \frac{1}{\tau_1}(\mathbf{T}^0 - \mathbf{T}) \tag{32}$$

yielding the solution

$$\mathbf{T} = \mathbf{T}^0 - (\mathbf{T}^0 - \mathbf{T}_i)e^{-t/\tau_1} \qquad \text{since } \mathbf{T} = \mathbf{T}_i \text{ at } t = 0$$

Since also $\mathbf{T} = \mathbf{T}_f$ as $t \to \infty$, $\mathbf{T}^0$ must be identified with $\mathbf{T}_f$. Consequently the shear stress in this hypothetical experiment increases approximately exponentially toward $\mathbf{T}_f$ with time constant τ_1. A time delay is exhibited

in the response of the liquid, where "response" refers to the changes in the time-dependent stress $\mathbf{T}(t)$, after imposition of the step function $\dot{u}_i \rightarrow \dot{u}_f$. It should be noted that there is no "time delay" in our ability to *define* $\mathbf{T}_f$ in an incompressible medium since it is equal to $-\eta^0\, d\dot{u}_f/dx$ which is constant for all $t \geq 0$. The concept of $\mathbf{T}_f$ as a stress toward which the instantaneous stress in the liquid tends, even though it may never reach it, can be helpful in visualizing the response of a viscous liquid to a *sinusoidal* change in the imposed strain rate. In this case it is evident that a time delay in the response of the liquid will result in a phase delay between stress and imposed strain rate. Such a phase delay is characteristic of relaxing systems subjected to sinusoidal perturbation.

When the ultrasonic perturbation is a sinusoidal change in the rate of strain, one should make the following substitutions in Eq. (31):

$$\mathbf{T} = \mathbf{T}_0(x)e^{j(\omega t+\varphi)} \qquad \dot{\xi} = \dot{\xi}_0(x)e^{j\omega t} \tag{33}$$

where φ is the phase delay between stress and particle velocity. The substitution of these expressions leads to a description of the response of the system in terms of a frequency-dependent effective viscosity:

$$\frac{\mathbf{T}}{\partial\dot{\xi}/\partial x} = \frac{\mathbf{T}_0 e^{j\varphi}}{\partial\dot{\xi}_0/\partial x} = \frac{\eta^0}{1+j\omega\tau_1} \equiv \eta^*(\omega) \tag{34}$$

The effective viscosity obtained here is a complex number and contains a contribution [the imaginary part of $\eta^*(\omega)$] which implies that such a medium has the property of a dynamic shear modulus, $G^* = G' + jG''$, with a nonzero real part. The real part of the complex viscosity coefficient at any frequency decreases uniformly from the low-frequency value η^0 to zero as the frequency increases

$$\eta(\omega) = \frac{\eta^0}{1+(\omega\tau_1)^2} \tag{35}$$

It is appropriate to define the equivalent complex shear modulus $G^* \equiv G' + jG''$ by

$$G^*(\omega) = \frac{\mathbf{T}_0 e^{j\varphi}}{\partial\xi_0/\partial x} = \frac{j\omega\eta^0}{1+j\omega\tau_1} = \frac{G^\infty(\omega\tau_1)^2}{1+(\omega\tau_1)^2} + j\frac{G^\infty\omega\tau_1}{1+(\omega\tau_1)^2} \tag{36}$$

where $G^\infty \equiv \eta^0/\tau_1$. The real part of the complex shear modulus shown in Fig. 2 varies from zero at zero frequency to an asymptotic value G^∞ at frequencies very much greater than $f_1 = 1/2\pi\tau_1$. The frequency f_1 is thus called the relaxation frequency for the viscous mechanism. The imaginary part of the complex shear modulus increases from zero at zero frequency to a maximum at the relaxation frequency and falls again to zero at indefinitely high frequencies. As the frequency increases, the liquid exhibits an effective nonzero real part of the shear modulus, and this property allows

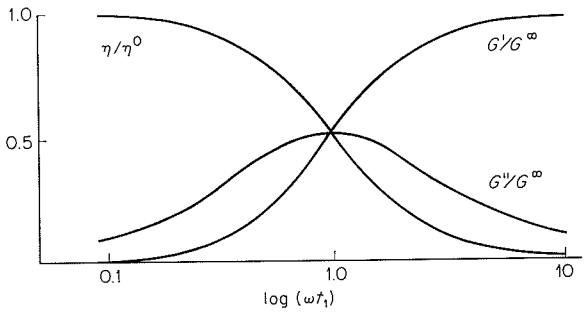

FIG. 2. Variation of the normalized shear modulus and dynamic viscosity with frequency for a single relaxation process. (*After Barlow and Lamb*, 1959.)

the propagation of heavily damped shear waves to occur. The propagation velocity as well as the absorption coefficient will be strongly dependent upon frequency:

$$\alpha_s = \frac{2\pi f}{v_{s0}} = \frac{\sin (G''/2G')}{[1 + (G''/G')^2]^{1/4}}$$
$$v_s = v_{s0} \frac{[1 + (G''/G')^2]^{1/4}}{\cos (G''/2G')} \tag{37}$$

where $v_{s0} = \sqrt{G'/\rho_0}$, the shear-wave velocity limit as the frequency approaches zero. We therefore observe a drastic change in the behavior of a liquid medium of moderate viscosity as the frequency of an applied acoustic perturbation is varied. At low frequencies it behaves like a viscous liquid which does not allow the propagation of shear waves. At frequencies considerably higher than the relaxation frequency, the equations predict that the absorption coefficient due to viscosity should approach a constant nonzero value, and that the velocity of propagation of such waves should approach a constant value which is determined by G^∞. It is found in the case of some hydrocarbon oils (Barlow and Lamb, 1959) that G^∞ is of the order of magnitude 10^{10} dyn/cm^2, i.e., within two orders of magnitude of the values characteristic of metals. In other words, the liquid is behaving much like a glass. The first known example of materials exhibiting behavior that is determined predominately by a single viscous relaxation mechanism of the type just described is molten zinc chloride, studied by Gruber and Litovitz [1964].

The behavior described is characteristic of the simplest form of relaxation phenomena that can be characterized by a single relaxation time. The necessary physical features are the existence of a disequilibrium between two molecular states, and activation energies of appropriate magnitude

which relate to the transition between these states. In the case of shear viscosity the initial and final states correspond to different local arrangements of molecules relative to one another and to vacant lattice sites in the pseudo-crystalline model of liquids. A transition constitutes the passage of a molecule from one site to an adjacent vacant site under the influence of shear stresses in the liquid. The potential barriers that impede transitions between the states must be low enough so that an appreciable fraction of the population in either state can achieve a transition to the other state within a half period of the sound wave. The presence of the potential barriers results in the phase lag, φ, between the applied perturbation and the resulting response of the system if the barriers are not too low. If the barriers are too low, the phase lag is negligible since the response takes place in a time small compared with the period of the wave and a negligible fraction of the sound energy density is converted to heat per cycle. The statements of the preceding two sentences are the phenomenological equivalent of the conditions that apply at zero frequency and infinite frequency, respectively.

In terms of absolute reaction-rate theory (Fig. 3) the free energies of activation for a simple two-state transition scheme can be related to the transition rate constants as follows:

$$k_f = \frac{\Psi_t k_B T}{h} e^{-\Delta G^+/RT}$$
$$k_b = \frac{\Psi_t k_B T}{h} e^{-\Delta G^-/RT} \tag{38}$$

where ΔG^+ is the free energy of activation for the forward transition, and ΔG^- is that for a backward transition, Ψ_t is a transition probability constant, and k_B and h are Boltzmann's and Planck's constants, respectively. The relaxation time τ_1 is a function of the transition rate constants k_f and k_b, the concentrations of reacting species, and the stoichiometry of the reaction

FIG. 3. Energy-level diagram for a system with two stable states, e.g., $X_1 \rightleftharpoons X_2$.

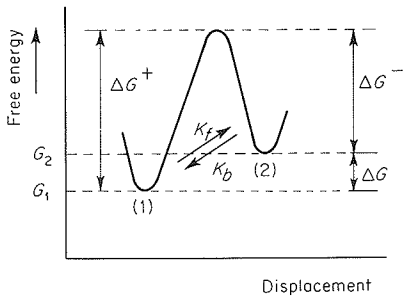

(Eigen and de Maeyer, 1963). Consequently, a measurement of the relaxation frequency of a process as a function of temperature is a potential means of determining energies of activation and rate constants.

As one might expect, the observed behavior of most materials, including those of biological interest, is by no means so simple that it can be described adequately by a single relaxation time. It is found that sonic parameter magnitudes generally vary less drastically with frequency than the predictions of a single relaxation process require. Such behavior can be encompassed within the theory of relaxation processes by supposing that a discrete number of such processes are operative at the same frequency (each process may be described by a different value of the relaxation time), or alternatively by supposing that a continuous distribution of relaxation times exists. Since the latter possibility is more general, attention here will be confined to it. For the viscosity relaxation mechanism, Eq. (36) would be replaced by

$$G^*(\omega) = G^\infty \int_{\tau_a}^{\tau_b} g_1(\tau) \frac{(\omega\tau)^2\, d\tau}{1 + (\omega\tau)^2} + jG^\infty \int_{\tau_a}^{\tau_b} g_1(\tau) \frac{\omega\tau\, d\tau}{1 + (\omega\tau)^2} \tag{39}$$

where τ_a and τ_b are the bounds of the distribution of relaxation times. The distribution function $g_1(\tau)$ bounded by the values zero and one, expresses the contribution to the complex shear modulus which is derived from processes having relaxation times between τ and $\tau + d\tau$. An objective of the experimenter is the determination of the distribution function which then provides at least an approximate indication of the range of values of the free energies of activation $\Delta G^{\pm}$.

As previously stated, the viscosity mechanism as it relates to shear waves has been discussed in detail as a specific example of the general class of relaxation mechanisms. The analysis may be extended readily to predict a frequency dependence of the bulk modulus and the associated bulk viscosity. The argument follows similar lines and will not be developed in detail here. The results for the bulk modulus are (Litovitz and Davis, 1965)

$$K^*(\omega) = K^0 + \frac{\Delta K^\infty (\omega\tau_2)^2}{1 + (\omega\tau_2)^2} + j\Delta K^\infty \frac{\omega\tau_2}{1 + (\omega\tau_2)^2} \tag{40}$$

for a single relaxation process and

$$K^*(\omega) = K^0 + \Delta K^\infty \int_{\tau_c}^{\tau_d} g_2(\tau) \frac{(\omega\tau)^2\, d\tau}{1 + (\omega\tau)^2} + j\Delta K^\infty \int_{\tau_c}^{\tau_d} g_2(\tau) \frac{\omega\tau\, d\tau}{1 + (\omega\tau)^2} \tag{41}$$

for a multiple process. In these expressions K^0 is the value of the zero-frequency bulk modulus and ΔK^∞ is the increment in the value of the bulk modulus as the frequency is changed from zero to infinity. The bulk viscosity coefficient is given in either case by

$$\eta_v(\omega) = \frac{\text{Im } K^*}{\omega} \tag{42}$$

The results (36) and (40) may be combined to show the frequency dependence of the absorption coefficient (per wavelength) and the propagation velocity of plane, longitudinal (compressional) waves for which the appropriate modulus is $K^* + \frac{4}{3}G^*$ from Eq. (7) (Litovitz and Davis, 1965):

$$\alpha_l\lambda = \pi \frac{\dfrac{\Delta K^\infty \omega\tau_2}{1+(\omega\tau_2)^2} + \dfrac{(4G^\infty/3)\omega\tau_1}{1+(\omega\tau_1)^2}}{K^0 + \dfrac{\Delta K^\infty(\omega\tau_2)^2}{1+(\omega\tau_2)^2} + \dfrac{(4G^\infty/3)(\omega\tau_1)^2}{1+(\omega\tau_1)^2}} \tag{43}$$

$$v_l^2 = \frac{1}{\rho_0}\left[K^0 + \frac{\Delta K^\infty(\omega\tau_2)^2}{1+(\omega\tau_2)^2} + \frac{(4G^\infty/3)(\omega\tau_1)^2}{1+(\omega\tau_1)^2}\right] \tag{44}$$

Equations (39) and (41) may be combined similarly in the case of a multiple process. Litovitz and coworkers have found that for a wide variety of materials ranging from molten metals to associated organic liquids the ratio $\eta_v/\eta = \Delta K^\infty\tau_2/G^\infty\tau_1$ remains substantially constant and near unity. Consequently, the intermolecular forces that are responsible for both shear and bulk viscosity appear to have the same origin.

The fundamental process that underlies the phenomenon of viscosity is the transfer of momentum. This process is governed by the diffusion equation,

$$\frac{\partial y}{\partial t} = \mathscr{D}\nabla^2 y \tag{45}$$

which also governs the diffusion of thermal energy and of mass. It is appropriate to inquire whether these processes are also subject to relaxational behavior.

The process of thermal diffusion or heat conduction makes a small, usually negligible, contribution to the absorption of ultrasonic waves in nonmetallic liquids and liquidlike media. Molten metals are exceptions for which the contribution from thermal conduction, given quantitatively by the following relation, is comparable to the contribution from viscosity:

$$\alpha_t = \frac{2\pi^2 f^2}{\rho_0 v_l^3}(\gamma - 1)\frac{\varkappa}{C_p} \tag{46}$$

where $\varkappa$ is the thermal conductivity coefficient (Kirchhoff, 1868). According to theory and experiment, relaxation of the thermal conductivity mechanism occurs in the frequency range well above that presently accessible to experiments except in the case of rarefied gases.

The effect of mass diffusion in liquid mixtures through which an ultrasonic wave is propagating is even smaller than that of thermal diffusion. In principle, a contribution to the absorption coefficient arises from the diffusion of mass in response to concentration gradients created by the sound wave, but the magnitude of such a contribution is entirely negligible.

The situation is drastically modified if the "diffusion path length" is considered to be of molecular dimensions instead of being comparable with the sonic wavelength. Although the concepts of continuum mechanics are invalid over distances as small as inter- or intramolecular dimensions, analogies between the processes of thermal and mass diffusion and the processes of molecular rearrangement which result in a change of molar internal energy and molar volume, respectively, may be at least suggested. However poor such analogies are, the processes of molecular rearrangement in response to a perturbing ultrasonic field can result in substantial contributions to the absorption coefficient and in behavior that is described in terms of relaxation processes known as thermal and structural relaxation, respectively.

Inter- or intramolecular reorganization can be expected to involve a change in the free energy. The elementary two-state concepts of Fig. 3 may be invoked again—the molar free-energy difference between the two equilibrium states is ΔG. Now for a process occurring at virtually constant ambient pressure and temperature,

$$\Delta G = \Delta H - T\,\Delta S = \Delta U + P_0\,\Delta V - T\,\Delta S \tag{47}$$

where ΔH, ΔS, ΔU, and ΔV are the associated changes in molar enthalpy, entropy, internal energy, and volume, respectively. The longitudinal wave ultrasonic absorption coefficient which is associated with such a transition can be obtained by lengthy thermodynamic analysis (Lamb, 1965):

$$\alpha_r\lambda = \pi\frac{v_l^0}{v_l^\infty}\left\{\left[\frac{\Delta\beta_T}{\beta_S{}^0}\right]^{1/2} - \left[(\gamma^0 - 1)\frac{\Delta C_p}{C_p{}^0}\right]^{1/2}\right\}^2 \frac{\omega\tau_3}{1 + (\omega\tau_3)^2} \tag{48}$$

where v_l^0 and v_l^∞ are the phase velocities at zero and infinite frequency, respectively. This particular form of the equation, obtained by the method of Andreae and Lamb [1956], is particularly convenient for showing the contributions from structural and thermal relaxation processes. However, since any two of the incremental thermodynamic quantities may be chosen independently, the general expression is too intractable for analysis of the experimental results. Successful analyses have been performed in cases where it has been possible to make either of the two following assumptions:

1. The "structural" relaxation condition: $\Delta V \neq 0$, $\Delta H = 0$.
2. The "thermal" relaxation condition: $\Delta H \neq 0$, $\Delta V = 0$.

In either of these cases, one of the terms in brackets in Eq. (48) is eliminated. In structural relaxation, the second term is eliminated since the perturbation by the sound field is assumed to proceed isothermally, so that $\gamma^0 = 1$; in thermal relaxation the incremental isothermal compressibility $\Delta\beta_T$ is zero.

Structural relaxation may be visualized as a process of molecular reorganization which occurs in response to the pressure fluctuations in an ultrasonic field. The reorganization involves a change in the molar volume of the

reacting system with a probable change in the molar entropy, and it proceeds isothermally. Thermal relaxation may be imagined as a process responding to the temperature fluctuations in the ultrasonic wave. The process involves molecular reorganization in such a way that the molar volume change is zero or essentially zero, but both the internal energy and entropy may change. The absorption coefficients are then

1. $$\frac{\alpha_r\lambda}{\pi} \approx \frac{\Delta\beta_T}{\beta_S}\frac{\omega\tau_4}{1+(\omega\tau_4)^2} \qquad \text{structural process} \qquad (49)$$

2. $$\frac{\alpha_r\lambda}{\pi} \approx (\gamma^0-1)\frac{\Delta C_p}{C_p{}^0}\frac{\omega\tau_5}{1+(\omega\tau_5)^2} \qquad \text{thermal process} \qquad (50)$$

where the velocity dispersion factor, $v_l{}^0/v_l{}^\infty$, in Eq. (48) has been approximated by equating it to unity, since the velocity dispersion $\Delta v_l/v_l{}^0 = v_l{}^\infty/v_l{}^0 - 1$ is normally less than 1 percent.

An example of a process that undergoes structural relaxation is the intermolecular rearrangement of molecules of an associated liquid, which gives rise to the frequency-dependent shear and volume viscosities discussed previously. An example of a process that undergoes thermal relaxation is the intramolecular rearrangement known as rotational isomerism. Also the transfer of energy between translational degrees of freedom and internal vibrational modes of a molecule is characterized by thermal relaxation. The majority of processes that undergo thermal relaxation require only a single relaxation time for the description whereas structural relaxation processes require, in general, a distribution of relaxation times. Thermal relaxation processes in liquids have been reviewed by Lamb [1965], and structural relaxation processes by Litovitz and Davis [1965].

Each equation, (49) and (50), may be represented by

$$\frac{\alpha_r v}{f} = \alpha_r\lambda = 2(\alpha_r\lambda)_{\max}\frac{\omega\tau}{1+(\omega\tau)^2} \qquad (51)$$

where $(\alpha_r\lambda)_{\max}$ is the maximum value of the relaxational absorption per wavelength, attained at the relaxation frequency $f_r = 1/2\pi\tau$, i.e., when $\omega\tau = 1$ (Fig. 4*a*). An alternative formulation of Eq. (51) is

$$\frac{\alpha_r}{f^2} = \frac{A}{1+(f/f_r)^2} \qquad (52)$$

where $A = 2(\alpha_r\lambda)_{\max}/vf_r$. The advantage of using Eq. (52) is seen in Fig. 4*c*, where the relaxational contribution to the absorption is shown added to the contribution due to viscosity, the latter being given by Eq. (30). The sum is the measured value of the absorption parameter,

$$\left(\frac{\alpha}{f^2}\right)_{\text{measured}} = \frac{A}{1+(f/f_r)^2} + B \qquad (53)$$

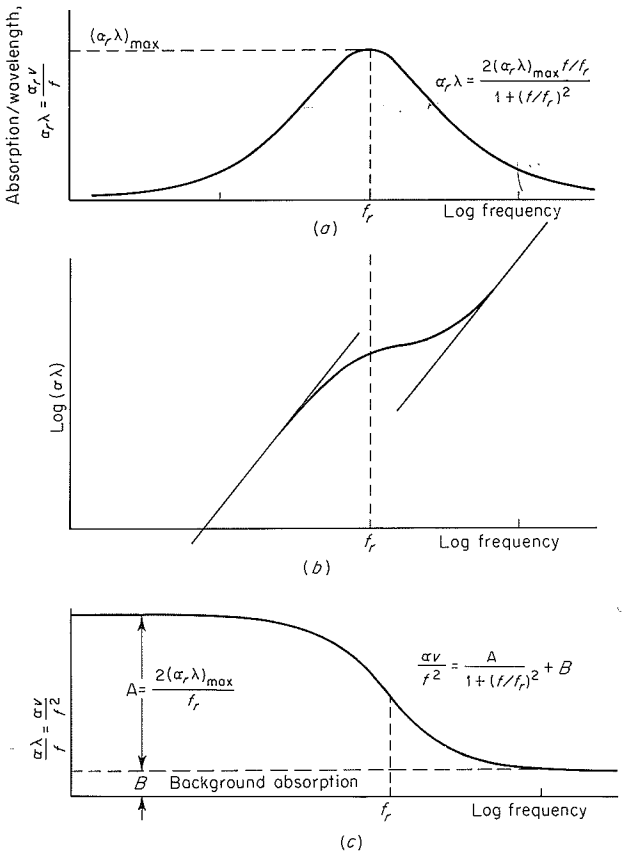

FIG. 4. (*a*) Relaxational contribution to the ultrasonic absorption per wavelength, $\alpha_r\lambda$, for a single relaxation process. (*b*) Absorption per wavelength, $\alpha_r\lambda$, for a single relaxation process added to absorption due to viscosity, $\alpha_v \propto f^2$. (*c*) Absorption parameter, α_r/f^2, for a single relaxation process and background absorption due to viscosity.

The occurrence of relaxation is shown by the sigmoid form of α/f^2 plotted against frequency. Two measurements of α/f^2 (for example, at the highest and lowest frequencies available) are sufficient to show whether at least one relaxation region lies between the frequencies employed.

The occurrence of relaxation is not only associated with a peak in the relation between the absorption per wavelength and the frequency, but it is also accompanied by dispersion of the velocity of sound in the same frequency range, i.e.,

$$v^2 = (v^0)^2 + 2v^0\,\Delta v\,\frac{\omega\tau}{1+(\omega\tau)^2} \qquad (53a)$$

The amplitude of the absorption peak and the increment of sound dispersion Δv are related as follows:

$$\frac{\Delta v}{v} \approx \frac{(\alpha_r \lambda)_{\max}}{\pi} \tag{54}$$

provided $(\alpha_r \lambda)_{\max}/\pi \ll 1$, which is the case for compressional waves in most materials of interest.

Since the magnitude of the velocity dispersion is very small (usually less than 1 percent), very accurate measurement of velocity is required if quantitative deductions are to be made. Carstensen's technique [1954] yields adequate precision, but simple interferometers do not. Observation of velocity dispersion in connection with an absorption maximum provides valuable confirmation that relaxational behavior is being observed. If only part of the relaxational spectrum is accessible experimentally, the following equation provides a useful relationship between $\alpha_r \lambda$ and the slope of the velocity dispersion curve at the same frequency:

$$\frac{\alpha_r \lambda}{dv/df} = \frac{1}{2v\tau}(1 + \omega\tau)$$

Liquids have been subdivided into various classes on the basis of their ultrasonic absorption characteristics (Pinkerton, 1949; Markham et al., 1951; Herzfeld and Litovitz, 1959). The first group has ultrasonic absorption-coefficient values close (within 10 to 20 percent) to those calculated on the basis of shear viscosity losses. Monatomic liquids such as argon and mercury are in this group, as well as some diatomic liquids such as oxygen and nitrogen. At the present time no biologically interesting material is known to be in this class.

The second group is characterized by a positive temperature coefficient of absorption and by values of the absorption coefficient from one to three orders of magnitude times the values calculated on the basis of a shear-viscosity mechanism alone. Polyatomic, unassociated liquids such as benzene, carbon tetrachloride, and carbon disulfide are in this group. The excess absorption of these liquids arises from exchange of energy between the external and internal degrees of freedom. To the authors' knowledge, the only biological materials for which ultrasonic absorption coefficients have been determined as a function of temperature are nerve tissue and blood proteins. The nerve-tissue measurements were made on spinal cords of one-day-old mice at a frequency of 0.98 MHz. The temperature coefficient of the absorption coefficient for sonic *intensity* is positive; the latter increases from 0.034 Np/cm at 2°C to 0.25 Np/cm at 45°C (Dunn, 1965). These values for spinal cord are comparable in magnitude to the values for the more highly absorbing liquids of this type, e.g., carbon disulfide. At present,

it is unwarranted to assume that the absorption mechanisms operative under the circumstances indicated in tissue are predominately of the thermal relaxation type. Various relaxation mechanisms may be equally important.

The blood proteins exhibit a negative temperature coefficient of absorption (Carstensen et al., 1953). The acoustic absorption properties of blood appear to be largely determined by the protein content, and there is no apparent connection with the third class of liquids for which a negative temperature coefficient is characteristic—the associated, polyatomic ones. Liquids studied of this type, which include water and alcohols, exhibit values of the absorption coefficient between one and three times that calculated from the shear viscosity.

From the meager amount of precise data available on the ultrasonic absorption properties of biological materials, and from the widely different values reported for presumably the same materials (Goldman and Hueter, 1957), it is apparent that determination of these properties is in an early stage.

The equilibria of chemical reactions may also be perturbed by an ultrasonic field through either the influence of the pressure or the temperature oscillation (Stuehr and Yeager, 1965). In these cases it is more likely that both ΔH and ΔV would be nonzero, so that neither of the simplifying assumptions would apply. However, if the reaction takes place in aqueous solution, then isothermal conditions may be assumed to apply at low concentrations since $\gamma = 1$ for water at 4°C and γ is not greatly different from unity at somewhat higher temperatures.

An ultrasonic field can also interact with liquid media by inducing incipient phase changes. An extremely high rate of absorption of energy from the field occurs if it is present in a binary liquid mixture which is maintained close to a critical solution temperature (Fixman, 1962; Anantaraman et al., 1966). The state of aggregation of the molecules in the mixture is strongly influenced by the temperature oscillation. A distribution of relaxation times is required to explain the behavior that is similarly observed for media in the vicinity of a phase change involving the transition from an isotropic liquid state to a mesomorphic state or liquid-crystalline structure (Hoyer and Nolle, 1956; Edmonds and Orr, 1966).

All the relaxation processes just discussed may occur simultaneously under appropriate circumstances, and the relative importance of each is determined by the structure and the composition of the medium. One type of relaxation process may predominate over a certain frequency range whereas another type may constitute the important mechanism in a different portion of the acoustic spectrum, thus giving rise to the concept of "ultrasonic spectroscopy" (Clark and Litovitz, 1960). Quantitative knowledge of relaxation effects provides a method of considerable potential for deriving valuable information on the dynamic aspects of structure and energy-transfer processes of molecular species in biological systems.

Hysteresis

It has been observed for highly viscous liquids and gases that at frequencies greater than the viscous relaxation frequencies, the absorption per wavelength (or per cycle) is at a level greater than the calculated viscous absorption and is separated from the latter by a constant amount (Mason and McSkimin, 1947; Litovitz and Lyon, 1954). Such constancy of the energy loss per cycle is characteristic of a hysteresis mechanism, but as yet there is no adequate explanation for the origin of such a mechanism.

Relative motion

Relative motion produced by an acoustic field between structured elements and an embedding fluid results in absorption of energy from the field. This mechanism has been shown to constitute a significant fraction of the absorption in suspensions of erythrocytes in saline solution (Carstensen and Schwan, 1959). Whether it is important at the molecular level has not yet been established, although relative motion has been suggested as the mechanism responsible for the degradation of DNA in solution by intense, noncavitating ultrasound (Hawley et al., 1963).

Relative motion results because of differences in density between suspended structures and embedding fluid. Consequently, frictionlike forces are produced between the structures and the fluid, which result in loss of energy from the acoustic field. Rotational motion can occur even if the mass of the suspended element is equal to that of the displaced fluid since the density of the suspended element may not be uniform over its volume.

An approximation analysis employing the concepts of frictional force constants and equivalent masses yields a relaxation-type expression for the absorption coefficient, Eq. (55) below, with the modification that the "relaxation frequency" and the amplitude factor are frequency-dependent (Brandt et al., 1937; Angerer et al., 1954; Fry, 1952). A general analysis of this type of system is that of Epstein [1941], who considers the problem of absorption of sound in a medium containing spherical particles with diameters small compared to the acoustic wavelength. The absorption coefficient calculated from this treatment yields, to a first approximation, the same expression as that obtained from the approximation analysis which assumes that the structural elements are stiff in shear compared with the embedding medium. The latter analysis indicates that the same form of expression applies in the case of nonspherical elements, that is, in general,

$$\alpha = \frac{c}{2v} \frac{(1 - \rho_0/\rho_e)^2}{\rho_0/\rho_e} \omega_0 \frac{(\omega/\omega_0)^2}{1 + (\omega/\omega_0)^2} \frac{M}{M_e} \tag{55}$$

where $\omega_0 = R_f/M_e$, $\omega = 2\pi f$, v is the acoustic phase velocity, ρ_0 and ρ_e are the densities of the embedding medium and the structured elements, respectively, and c is the volume concentration of structured elements, i.e., the volume of fluid displaced by the elements per unit volume of suspension. The symbols R_f and M_e designate the frictional force constant and the effective mass of an element, respectively, and are given by the following relations for spherical particles (Lamb, 1945):

$$R_f = 6\pi a_s \eta \left[1 + \left(\frac{\rho_0}{2\eta}\right)^{1/2} a_s \omega^{1/2}\right] \tag{56}$$

$$M_e = M + m\left[\frac{1}{2} + \frac{9}{4(\rho_0/2\eta)^{1/2} a_s \omega^{1/2}}\right] \tag{57}$$

where η is the shear viscosity of the embedding fluid, a_s is the radius and M the mass of an element, and m is the mass of fluid displaced per particle. Values for R_f and M_e for nonspherical elements can be estimated from Eqs. (56) and (57) by inserting an average value for the radius if the element does not deviate greatly from a spherical shape. The ratio $\omega_0 = R_f/M_e$ has the dimension of an attenuation factor.

The frequency dependence of the absorption coefficient due to relative motion as described by Eq. (55), (56), and (57) and that due to relaxation as described by Eq. (51) are compared in Fig. 5*a* where the absorption coefficient per wavelength is shown as a function of frequency. It is seen that, compared with a single relaxation process, a marked broadening of the absorption curve occurs when relative motion is present. Experimental results obtained on suspensions of bovine erythrocytes in saline, after correction for absorption by protein components, and values calculated from Eq. (55), are shown in Fig. 5*b* (Carstensen and Schwan, 1959).

FIG. 5. (*a*) Comparison of the frequency dependence of $\alpha\lambda$ due to relative motion and relaxational absorption. (*b*) Comparison of experimentally determined nonprotein absorption in bovine erythrocytes in saline (points) with absorption computed for relative motion (lines) using $\rho_e = 1.084$ g/cm³, $\eta = 0.01$ poise, and $a_s = 2.3$ μm. (*After Carstensen and Schwan*, 1959*a*.)

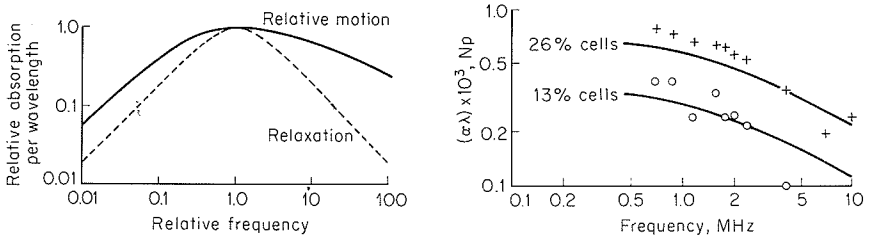

Bubble mechanisms

Gas bubbles present in a liquid exert a marked influence on the propagation characteristics of ultrasound in the medium. Since some biological components normally contain gas "bubbles," e.g., lung, and since bubbles can be introduced either by design of the investigator or inadvertently, it is necessary to consider quantitatively the effects of gaseous inclusions on the propagation of ultrasound (see Sec. 4 under "Tissues"). When the bubble dimensions are small compared with the acoustic wavelength, several physical processes become important in contributing to the dissipation of acoustic energy (Devin, 1959; Fry and Dunn, 1962). The time rate of dissipation of acoustic energy by a bubble is greatest when the resonant frequency of the acoustic field is equal to that of the bubble. The radius of a resonant bubble R_R is given by

$$R_R = \frac{1}{\omega_R}\left[\left(\frac{3\gamma_g P_0}{\rho_0}\right)\left(\frac{g_R}{\epsilon}\right)\right]^{1/2} \tag{58}$$

where

$$g_R = 1 + \frac{2\sigma}{P_0 R_R}\left(1 - \frac{1}{3h_1}\right) \tag{59}$$

$$\epsilon = 1 + \frac{3(\gamma_g - 1)}{2\Phi R_R}\left[1 + \frac{3(\gamma_g - 1)}{2\Phi R_R}\right] \tag{60}$$

$$\Phi = \left(\frac{\omega_R \rho_g c_p}{\varkappa_g}\right)^{1/2} \tag{61}$$

and ω_R is the resonant angular frequency of the bubble, γ_g is the ratio of the specific heats of the gas in the bubble ($\gamma_g = 1.4$ for O_2, N_2, air), P_0 is the static pressure, R_R is the mean radius of the bubble, ρ_0 is the density of the liquid, ρ_g is the density of the gas, σ is the surface tension, $h_1 = \gamma_g/\epsilon$, c_p is the heat capacity of the gas at constant pressure, and $\varkappa$ is the thermal conductivity coefficient of the gas. The quantity h_1 lies between unity (isothermal case) and γ_g (adiabatic case); consequently g_R is always positive. As an example of the magnitudes of the quantities involved, a resonant frequency of 1 MHz for an air bubble in water corresponds to a bubble radius of approximately 3 μm.

The total dissipation parameter b is equal to the sum of the thermal, radiation, and viscous dissipation parameters, respectively, b_t, b_r, and b_v, and when a population of bubbles of uniform size is present, the acoustic pressure-absorption coefficient α per unit path length is related to b as follows:

$$\alpha = \frac{bn_R v}{4} \frac{3\gamma_g P_0/R_R^2 + \omega^2 \rho_0}{\left[\frac{1}{4\pi R_R}\left(\rho_0 \omega^2 - \frac{3g_R \gamma_g P_0}{\epsilon R_R^2}\right)\right]^2 + b^2\omega^2} \tag{62}$$

where n_R is the number of bubbles of radius R_R per unit volume. At the resonant frequency, Eq. (62) becomes

$$\alpha = \frac{n_R v}{4b\omega_R{}^2}\left(\frac{3\gamma_g P_0}{R_R{}^2} + \omega_R{}^2\rho_0\right) \tag{63}$$

The radiation dissipation parameter is given by

$$b_r = \frac{\rho_0\omega_R{}^2}{4\pi v} \tag{64}$$

and the viscous dissipation parameter by

$$b_v = \frac{\eta}{\pi R_R{}^3} \tag{65}$$

where η is the coefficient of shear viscosity of the liquid. The complete expression for the thermal dissipation parameter is quite complex. However, when $2\Phi R_R \leq 2$,

$$b_t \simeq B_t \frac{\gamma_g - 1}{\gamma_g}\frac{(2\Phi R_R{}^2)^2}{30} \tag{66}$$

where

$$B_t = \frac{3\gamma_g P_0 g_R}{4\pi R_R{}^3\omega_R\epsilon} \tag{67}$$

Further, when $2\Phi R_R \geq 5$,

$$b_t \simeq B_t\left[\frac{1 - 1/\Phi R_R}{1 + 2\Phi R_R/3(\gamma_g - 1)}\right] \tag{68}$$

Equations (62) and (63) apply to the case where all bubbles are of equal radius. When this is not so, a summation over all radii is necessary and can be accomplished by numerical integration of the right-hand side of Eq. (62) over the appropriate range of R_R.

Large-amplitude Effects

The previous sections have been concerned with acoustic fields which can be quantitatively described in terms of a "linear" analysis. That is, it is assumed that the change in the density of the medium is linearly proportional to the change in the pressure (waves are of infinitesimal amplitude). For waves of finite amplitude, the linear analysis is not adequate to describe the acoustic field when appreciable deviation occurs from the linear approximation to the relation between the incremental changes in density and pressure determined by the equation of state for the medium. The interest here is in the intermediate range between waves of infinitesimally small amplitude and strong shock waves. A number of distinct phenomena, not readily

observed for low-amplitude acoustic waves, become apparent as the wave amplitude is increased. Some of the more important phenomena are discussed briefly, and quantitative relations are presented which are useful for determining their importance in experimental situations.

Radiation pressure

If structures possessing acoustic properties different from that of an embedding medium are subjected to high-level acoustic radiation, steady or unidirectional forces exerted on them are readily observed. Such a force results when the acoustic energy density changes abruptly with position in the medium, e.g., at an interface between media of different acoustic properties; such a force also results when acoustic energy is absorbed within a homogeneous medium.

Radiation pressure at interfaces. Radiation pressure can exert steady forces on interfaces between media having different values of acoustic velocity and/or density. The force of radiation pressure at a plane interface is dependent on the relative amounts of incident energy reflected and transmitted or absorbed and is quantitatively equal to the difference in the energy densities in the two media. The energy density, or average energy per unit volume, E_0, of a plane traveling wave is given by Eq. (15). The radiation pressure P_r or force per unit area F_r/A exerted at an interface can be expressed as

$$P_r = \frac{F_r}{A} = DE_0 = D\frac{I}{v_1} \tag{69}$$

where D is given in Table 5 for a variety of physical configurations (Hueter and Bolt, 1955; Fry and Dunn, 1962), I is the acoustic intensity, and v_1 is the acoustic velocity in the medium from which the sound waves are incident. It is possible to compute the total acoustic power or average intensity of a sound beam using relations (15) and (69) by measuring the force exerted by an ultrasonic beam on a reflector or absorber of large size. In order to accomplish this, it is essential, if a reflector is used, that none of the energy reflected at the interface be allowed to return to the source to modify its acoustic output. This condition can be realized by using a deflecting reflector and absorbing the reflected energy (Hueter and Bolt, 1955). It should be noted that in some cases the direction of the radiation force is opposite to the direction of propagation, for example, at the nonreflecting interface between two media of equal characteristic impedances where the acoustic velocity of medium 1 is greater than that of medium 2.

Radiation pressure on spheres. The radiation force exerted on a "soft" sphere (i.e., one such that the pressure amplitude is zero over its surface) suspended in a traveling-wave ultrasonic field is a function of the ratio of

TABLE 5. THE CONSTANT D OF EQ. (69) FOR VARIOUS PHYSICAL CONFIGURATIONS

Physical configuration	D
Perfect absorber, normal incidence, $r_{2/1} = 1$	1
Perfect reflector, normal incidence, $r_{2/1} = 0$ or $r_{2/1} = \infty$	2
Perfect reflector, incidence at angle θ_1 to sound beam, $r_{2/1} = 0$ or $r_{2/1} = \infty$	2
Nonreflecting interface, normal incidence, $r_{2/1} = 1$ $v_1 \neq v_2$ For $v_1 < v_2$, force in direction of propagation For $v_1 > v_2$, force opposite to direction of propagation	$1 - \frac{v_1}{v_2}$
Partially reflecting interface, normal incidence, $r_{2/1} \neq 1$	$2\,\frac{(r_{2/1} - 1)^2 + 2r_{2/1}(1 - v_1/v_2)}{(r_{2/1} + 1)^2}$
Note: $r_{2/1} = \frac{\rho_2 v_2}{\rho_1 v_1}$	

the diameter of the sphere to the wavelength of the sound. For a "rigid" sphere, i.e., one whose surface does not deform, the radiation force is dependent, in addition, upon the relative densities of the sphere and the embedding medium. Both types of spheres are useful in the calibration of ultrasonic fields. In order to obtain precise values for the acoustic field variables at a specific location in a beam, it is desirable to employ a method of radiation-pressure measurement in which the volume of the region is small enough so that the variation in the values of the variables is small. Thus radiation force measured with spheres of appropriate size permits accurate determinations of acoustic field parameters at specific sites in a field. One radiation-pressure method utilizes a small stainless steel sphere (½ to 1 wavelength in diameter) suspended by a bifilar arrangement in the sound field (Fox and Griffing, 1949). The radiation force F_r deflects the sphere, and the magnitude of this deflection d_s (measured by a cathetometer) permits accurate evaluation of the force exerted by the radiation field. For small angular deflections of the suspension from the vertical,

$$F_r = \frac{d_s(m_s - m)g}{L_w} \tag{70}$$

where L_w is the length of the suspension, m_s is the mass of the sphere, m is the mass of the displaced liquid, and g is the gravitational constant. In practice, the sound level is varied, for example, by changing the voltage across the transducer, and the deflection of the sphere is plotted as a function

of the square of the driving voltage since the latter is proportional to the intensity and consequently directly proportional to the energy density.

The radiation force is expressed in terms of the energy density and radius of the "rigid" sphere as

$$F_r = \left[f\left(ka_s, \frac{\rho_s}{\rho_0}\right) + d\left(ka_s, \frac{\rho_s}{\rho_0}\right) \right] \pi a_s^2 E_0 \tag{71}$$

where $k = 2\pi/\lambda$ is the wave number, a_s is the radius of the sphere, ρ_s is the density of the sphere, and ρ_0 is the undisturbed density of the liquid medium. For the "soft" sphere case, the radiation force can be expressed as

$$F_r = f(ka_s)\pi a_s^2 E_0 \tag{72}$$

Numerical values for the functions $d(ka_s,\rho_s/\rho_0)$, $f(ka_s,\rho_s/\rho_0)$ and $f(ka_s)$ are tabulated and plotted elsewhere (Maidanik, 1957; Maidanik and Westervelt, 1957; Fry and Dunn, 1962). Measurements with "soft" spheres have not been extensively employed except in a preliminary fashion for the absolute calibration of ultrasonic fields. The use of soft spheres has the advantage that the force exerted on the sphere in the sound field is a monotonic function of ka, and thus a higher degree of absolute accuracy might conceivably be attained in this case.

Stokes and Oseen forces

The "average Stokes force" on a structure suspended in a high-intensity ultrasonic field arises from the temperature dependence of the viscosity of the medium. The viscosity is greater during a rarefaction (lower temperature) than during a compression (higher temperature), and, consequently, the time average of the product of the viscosity and particle velocity is not zero. The force exerted on a stationary sphere of radius a_s in a fluid medium having a shear viscosity η and moving with a velocity $\dot{\xi}$ is

$$F = 6\pi a_s \eta \dot{\xi} \tag{73}$$

which results in a unidirectional force exerted on the structure. In the case of a liquid, since the viscosity is decreased during compression and increased during rarefaction, the average force is oriented in a direction opposite to the direction of propagation of the acoustic field (Hueter and Bolt, 1955; Westervelt, 1951).

The Oseen steady force, which is independent of the temperature variations of the sound field, arises as the result of wave distortion and can be derived by extending Eq. (73) to include a term of second order in the velocity (Westervelt, 1951), i.e.,

$$F = 6\pi a_s \eta \dot{\xi}(1 + h_2\dot{\xi}) \tag{74}$$

where h_2 is an appropriate coefficient. If the ratio of the amplitude of the second harmonic to that of the fundamental is designated by $s_{2/1}$ and the phase angle by $\varphi_{2/1}$, then

$$\dot{\xi} = \dot{\Xi} [\sin \omega t + s_{2/1} \sin (2\omega t + \varphi_{2/1})] \tag{75}$$

and if h_2 is approximated as $3\rho_0 a_s/8\eta$, the steady force exerted on the sphere is given approximately by

$$F \simeq -3a_s^2 \rho_0 s_{2/1} \dot{\xi}^2 \sin \varphi_{2/1} \tag{76}$$

It is seen from Eq. (76) that the direction of the force can be either toward or away from the source, depending on the magnitude of the phase angle $\varphi_{2/1}$. The average Stokes and Oseen forces will not be considered further in this chapter since, in liquids subjected to ultrasonic fields, other steady forces are of greater importance over the range of values of the field parameters of interest here.

Streaming

In the case of an absorbing medium the space gradient of the radiation pressure P_r is related to the absorption coefficient as follows:

$$\frac{dP_r}{dx} = -2\alpha E_0 \tag{77}$$

where E_0 is the energy density. In general, this pressure gradient produces streaming of the medium.

It is desirable to present an expression for approximately estimating streaming speeds from a knowledge of the values of the pressure-absorption coefficient per unit path length, the beam and vessel diameter, the shear-viscosity coefficient, and the sound level (Nyborg, 1953 and 1965; Liebermann, 1949; Eckart, 1948). Although a well-founded basic theory exists from which acoustic streaming values for specific cases can be calculated in principle, the computations to obtain flow-velocity relations involve approximations to realize tractability. Calculations by different investigators indicate that computed values are in the range of the experimentally measured values. The following formula for obtaining at least an order-of-magnitude estimate of the streaming speed is useful when the magnitude of the absorption coefficient is such that $2\alpha L_b \leq 3$, where α is the amplitude absorption coefficient per unit path length, and L_b is the "length" of the beam. If the streaming speed is designated by v_f, then (Nyborg, 1953)

$$v_f \simeq \frac{\alpha \rho_0 a^2 \dot{\Xi}^2}{2\eta} \tag{78}$$

where $\dot{\Xi}$ is the acoustic particle velocity amplitude, a is the beam radius, and ρ_0 and η are the density and the shear-viscosity coefficient of the medium, respectively. As a specific example consider a 1-MHz beam in water at room temperature. If $a = 0.2$ cm, $\rho_0 = 1.0$ g/cm^3, $\alpha = 2 \times 10^{-4}$ Np/cm, $\eta = 0.01$ poise, and $\dot{\Xi} = 300$ cm/s, then $v_f = 36$ cm/s. The reader is referred to the review by Nyborg [1965] for details on acoustic streaming phenomena.

Finite-amplitude waves

An acoustic wave of finite amplitude, initially monochromatic, becomes distorted as it propagates. That is, harmonics are generated by transfer of energy from the fundamental. As the original monochromatic form of the wave takes on a spectral character, the waveform becomes stabilized at that distance from the source where the time rate of energy transfer to the harmonics equals the time rate of energy dissipated through absorption. A region of stabilization exists for each harmonic—defined for the second harmonic, for example, as that region in which the ratio of the amplitude of the second harmonic to that of the fundamental is "maximum." Near a sound source that radiates monochromatic waves, the absorption coefficient is nearly that for waves of infinitesimal amplitude. In the region of stabilization, the absorption coefficient is maximal, and at great distances from the source, where the wave returns to the original sinusoidal form, the absorption coefficient again approaches that for waves of small amplitude. Thus, the absorption coefficient of finite-amplitude waves leads to nonexponential attenuation. The amount of energy transferred to the harmonics per unit path length is a function of the nonlinearity of the equation of state of the medium and the pressure amplitude of the acoustic disturbance. The reader is referred to the review by Beyer [1965] for details on nonlinear acoustics.

Interacting particles

The hydrodynamic flow pattern produced by an acoustic field in a region containing closely neighboring suspended particles results in a Bernouilli attraction (Hueter and Bolt, 1955). This situation obtains if the amplitude of the periodic displacement of the particles is only a small fraction of the amplitude of the periodic displacement of the fluid. It is assumed here that laminar flow obtains. This is ensured in the case of a liquid if the Reynolds number ($\mathrm{Re} = 2a_1 v_f \rho_0/\eta$) is less than 1,000. In this expression v_f is the flow velocity in the constriction between the particles, a_1 the particle radius, ρ_0 the density of the embedding liquid, and η the shear-viscosity coefficient. The force of attraction between the particles can be expressed in terms of the acoustic intensity and a factor that depends on the geometry of the flow

pattern. For two spherical particles of radii a_1 and a_2 spaced a distance d_1 between centers in a medium of acoustic velocity v, the force of attraction is

$$F = \frac{3\pi a_1^3 a_2^3}{d_1^4} \frac{I}{v} \tag{79}$$

If the particles are free to move, the speed of coalescence is determined by the viscous forces acting upon them, in addition to the Bernouilli attraction. If the particles are elastically fastened to other structures, a stretching of these elastic bonds occurs.

Cavitation

The term *cavitation* refers to the phenomena associated with the growth and collapse of bubbles or vapor-filled cavities in liquid media. Such phenomena are produced in a liquid subjected to an ultrasonic disturbance when the acoustic pressure amplitude during rarefaction reduces the hydrostatic pressure to some "threshold" value, which depends upon the physical parameters describing the state of the medium. The destructive forces attending cavitation produce physical, chemical, and biological effects (El'piner, 1964) which alter the medium being irradiated and can lead to erroneous results for acoustic velocity and absorption measurements. A comprehensive review of the physics of cavitation has been prepared by Flynn [1964]. Brief remarks on the way cavitation threshold depends on frequency, temperature, pressure, pulse length, and viscosity follow.

It is first noted that the types of cavitation phenomena observed can be classified into two categories: (1) quiet degassing of a liquid containing dissolved or entrained gas; and (2) catastrophic collapse of cavities accompanied by a broadband noise spectrum. The following discussion considers the latter phenomenon only, which is initiated only if the medium experiences a tensile stress greater than a threshold value during a portion of the rarefaction phase of the ultrasonic disturbance. No single investigator has studied all aspects of ultrasonically induced cavitation, and considerably more information is available on water than on any other material. The method of preparation of the liquid is most important, and, since many techniques have been employed in cavitation studies, the results on cavitation thresholds by different investigators do not always agree. The frequency dependence of the minimum acoustic pressure amplitude required for the production of cavitation (detected by the broadband noise spectrum produced) for both degassed and air-saturated water at room temperature, is constant at approximately 2 atm and approximately ½ atm, respectively, from approximately 10^2 to 10^4 Hz and increases rapidly in the range from 10^2 kHz to 1 MHz, where the threshold at the latter frequency is greater than 50 atm (Esche, 1952; Flynn, 1964; Fry and Dunn, 1962). In the

temperature range 10 to 50°C, at 60 kHz, it has been shown that the threshold value of the acoustic pressure amplitude required for the production of cavitation in water increases monotonically with increasing hydrostatic pressure (Blake, 1949; Fry and Dunn, 1962). The same data can be interpreted to show that for water, at 60 kHz, the cavitation threshold, at constant pressure, decreases linearly with increasing temperature. Strasberg [1959] has shown that the acoustic pressure amplitude required for the initiation of cavitation decreases with increasing gas content, at 25 kHz and 20 to 24°C. The minimum acoustic pressure amplitude for the production of cavitation increases with decreasing pulse length of the acoustic disturbance (Hueter and Bolt, 1955), and the particular range of pulse-length values over which this increase becomes marked is a function of frequency. For example, for air-saturated water, this marked increase occurs for pulse lengths in the range of 300 to 500 ms at a frequency of about 400 kHz. For degassed castor oil, the sharp trend to higher threshold values occurs in the range of pulse lengths 30 to 40 ms at a frequency of 25 kHz. High-viscosity liquids such as oils and solutions of high polymers impede the growth of bubbles, and thereby possess relatively high cavitation thresholds (Hueter and Bolt, 1955).

Since there are many techniques available for the determination of acoustic velocity and absorption in liquid media, requiring different acoustical conditions, it is essential in such work that the investigator choose those experimental conditions which ensure that cavitation is not present in order that the resulting data may be meaningful.

3. MEASUREMENT METHODS

The utilization of ultrasonic energy for biomedical or biophysical purposes requires, in general, a knowledge of the acoustic velocity and absorption of the biological media under all conditions of interest. These parameters, together with the density or compressibility, are sufficient and necessary to characterize the propagation of low-amplitude plane unreflected ultrasonic waves represented by Eq. (27). The velocity and absorption-coefficient values are functions of the frequency and the ambient temperature; they are also functions of the ambient pressure, but this dependence will not be considered further since atmospheric pressure is usually applicable. Under nonlinear conditions of moderate or high amplitudes, it is also necessary to consider the amplitude dependence of velocity and absorption, and therefore the absolute intensity of the sound wave must be measured. In Table 6 a brief summary is given of various techniques applicable in different frequency ranges for measurement of the velocities and absorption coefficients of compressional and shear waves and also the sonic intensity in liquids and in viscoelastic solids. No attempt will be made to give an exhaustive description of all the listed techniques, but a few will be selected for further comment.

TABLE 6. LIST OF EXPERIMENTAL METHODS

Medium	*Compressional-wave velocity*	*Compressional-wave absorption*	*Shear-wave velocity*	*Shear-wave absorption*	*Intensity*
Liquid:					
Low frequencies (<0.1 MHz)	Resonance[a]	Resonance-reverberation[b]	Resonance of torsional transducer[c]	Bandwidth of torsional transducer[c]	Radiation pressure[j]
Moderate frequencies (0.1–50 MHz)	Continuous-wave interferometer[d] "Sing-around" system[e]	Pulse transmission (fixed path[f] or variable path[g])	Complex reflection coefficient[i]		Transient thermoelectric method[h]
		Transient thermoelectric method[h]			
High frequencies (50 MHz–1 GHz)	Pulse and continuous-wave interferometer[e]	Pulse transmission[k]	Resonant cavity transducers[s]		
Very high frequencies (1–10 GHz)	Brillouin scattering[m]	Cavity transducers[l] Brillouin scattering[m]			
Viscoelastic solids:					
Low frequencies (<0.1 MHz)	Transducer input impedance[n]		Transducer input impedance[n]		
Moderate frequencies (0.1–50 MHz)	Pulse travel time or phase shift[q]	Pulse transmission (immersion[q] or buffer[p])	Pulse travel time or phase shift[q]	Pulse transmission (mode conversion[q] or buffer[p])	
High frequencies (>50 MHz)	2-pulse interferometer[r]	Transient thermoelectric method[h] Pulse transmission[p]			

[a] McSkimin [1964]
[b] Leonard [1948]; Tamm and Kurtze [1951]
[c] Mason [1948]
[d] Hubbard [1931]; Del Grosso, Smura, and Fougere [1954]
[e] Greenspan and Tschiegg [1957]
[f] Carstensen [1954]; Siegert [1963]
[g] Pellam and Galt [1946]; Andreae, Bass, Heasell, and Lamb [1958]
[h] Dunn and Fry [1957]
[i] Mason, Baker, McSkimin, and Heiss [1949]
[j] Fox and Griffing [1949]
[k] Tamm, Kurtze, and Kaiser [1954]; Hunter and Dardy [1964]
[l] Dunn and Hawley [1965]
[m] Fleury and Chiao [1966]; Benedek and Greytak [1966]
[n] Oestreicher [1951]
[p] McSkimin [1951]
[q] Nolle and Mifsud [1953]; Schneider and Burton [1949]
[r] Litovitz, Lyon, and Peselnick [1954]
[s] Lamb and Richter [1966]

It is notable that no single technique is universally applicable, and, in fact, the majority are restricted to a frequency range of about two decades. Such limitation on the applicability of a single technique is primarily due to the strong frequency dependence of the absorption coefficient, as shown in Eq. (30).

An additional limitation relates to the size of available specimens in comparison with the wavelengths. Fairly large volumes of liquid, typically 10 to 1,000 ml, are required by many of the techniques. In the case of biological materials this quantity is frequently not available. The development of experimental techniques requiring only small volumes of liquid is extremely desirable for further progress. A review of measurement techniques has been given by McSkimin [1964], and references to other papers are included in reference *a* of Table 6.

Velocity Measuring Methods

Interferometric method

The most convenient instrument for measuring the propagation velocity of compressional waves in nonviscous liquids at frequencies around 1 MHz is the continuous-wave interferometer. Hubbard [1931] has given a detailed account of the theory of operation, and Del Grosso et al. [1954] have reviewed numerous considerations in design and use. The attainable accuracy without undue complication is approximately 0.1 percent. For comparison with this accuracy figure, variations in velocity with frequency and temperature over the ranges of interest may be at most as great as 1 percent. In the interferometer, which is illustrated schematically in Fig. 6, a transducer generates plane compressional waves in the liquid specimen. These propagate until they are reflected from a plane-parallel movable reflector. A standing-wave pattern is set up between the parallel faces of the transducer and reflector, and this standing-wave field reacts on the transducer and influences the electrical impedance which is presented to the electronic driving circuit. With neglect of absorption, equivalent states of reinforcement of the standing-wave pattern occur when the reflector is moved coaxially relative to the transducer, and these positions are separated by distances equal to one half-wavelength of the sound in the liquid at the frequency of operation. If the transducer is connected in a parallel resonant circuit, then the voltage developed across this circuit exhibits sharp minima at successive half-wavelength positions. In practice, to achieve the desired accuracy, the reflector is displaced through a measured distance equal to at least 100 half-wavelengths, and the average measured wavelength is calculated. The velocity of propagation is immediately obtained as the product of the wavelength and the frequency of oscillation of the transducer. The

[a] McSkimin [1964]
[b] Leonard [1948]; Tamm and Kurtze [1951]
[c] Mason [1948]
[d] Hubbard [1931]; Del Grosso, Smura, and Fougere [1954]
[e] Greenspan and Tschiegg [1957]
[f] Carstensen [1954]; Siegert [1963]
[g] Pellam and Galt [1946]; Andreae, Bass, Heasell, and Lamb [1958]
[h] Dunn and Fry [1957]
[i] Mason, Baker, McSkimin, and Heiss [1949]
[j] Fox and Griffing [1949]
[k] Tamm, Kurtze, and Kaiser [1954]; Hunter and Dardy [1964]
[l] Dunn and Hawley [1965]
[m] Fleury and Chiao [1966]; Benedek and Greytak [1966]
[n] Oestreicher [1951]
[p] McSkimin [1951]
[q] Nolle and Mifsud [1953]; Schneider and Burton [1949]
[r] Litovitz, Lyon, and Peselnick [1954]
[s] Lamb and Richter [1966]

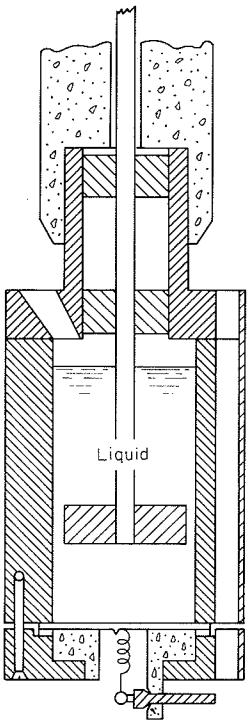

FIG. 6. Schematic diagram of an ultrasonic interferometer. (*After Andreae and Edmonds*, 1961.)

latter can be measured with appropriate accuracy by a crystal-controlled frequency calibrator.

A particularly simple method of operation, which permits measurements with an accuracy of 0.5 percent, has been described (Andreae and Edmonds, 1961). In this instrument the oscillator driving the transducer is over-coupled so that its frequency of operation is sensitive to the radiation resistance of the transducer. An audio-frequency beat note between the driving oscillator and a crystal-controlled oscillator in a frequency meter is monitored by the observer. Successive half-wavelength positions of the reflector are identified as positions of minimum or zero beat.

For appropriate operation of an interferometer it is particularly important that the reflector and transducer be accurately parallel, preferably within $\frac{1}{100}$ wavelength at the highest frequency of operation. Control of the temperature in the sample is essential and should be maintained to better than 0.1°C. It should be noted that undesired modes of propagation,

associated with reflection of ultrasonic waves from the sides of the container, have been a cause for erroneous results in some cases (Del Grosso et al., 1954).

At high frequencies when absorption in the specimen is high, it is not practicable to set up a standing-wave field. Under these circumstances it is possible to observe electrical interference between the electric signal from an ultrasonic pulse which has been transmitted once through the liquid sample and a continuous-wave signal which is introduced into the receiving amplifier and which is derived from the oscillator driving the transducer (McSkimin, 1964). In this case it is necessary to replace the reflector by a receiving transducer which can pick up the ultrasonic signal passing once through the specimen. The continuous-wave signal provides a reference phase with which the phase of the signal transmitted through the specimen can be compared. Successive positions of destructive interference serve to identify positions of the receiving transducer which are separated by one wavelength. Both types of pulse equipment described on pages 252–255 may be used in this manner.

Sing-around method

This system, which was originated by Hiedemann [1947] and developed to a point of practical utility by Greenspan and Tschiegg [1957], makes use of pulse propagation in the liquid specimen. A simplified diagram is shown in Fig. 7. To initiate operation, the transmitting transducer is shock-excited, and it generates an ultrasonic pulse. Arrival of the ultrasonic pulse at the receiving transducer initiates a new cycle of events by providing a trigger for the driver which excites the transmitting transducer. Consequently the transmitting transducer is excited at regular intervals equal to the time of travel for signals around the entire circuit comprising the ultrasonic path and the return path in the electric circuitry. The delay time in the electric system is very small in comparison with the travel time along the ultrasonic path, and consequently the repetition rate of the pulses is a measure of the velocity of propagation in the liquid sample. The frequency of recycling can be measured by a digital counter. The method is capable of extreme accuracy in measurement of velocity if extensive precautions are taken to ensure that the electric delay time is constant in operation. These precautions involve wave shaping and control of the amplitude of signals at numerous locations in the circuit. The instrument developed by Forgacs [1960], which is more suitable for the measurement of relative than absolute velocity, is capable of detecting a velocity change of one part in 10^7. This performance was obtained by using 10 MHz resonant-frequency transducers and crystal-controlled electronic counters to measure the elapsed time for the occurrence of between 10^3 and 10^6 cycles of the sing-around system.

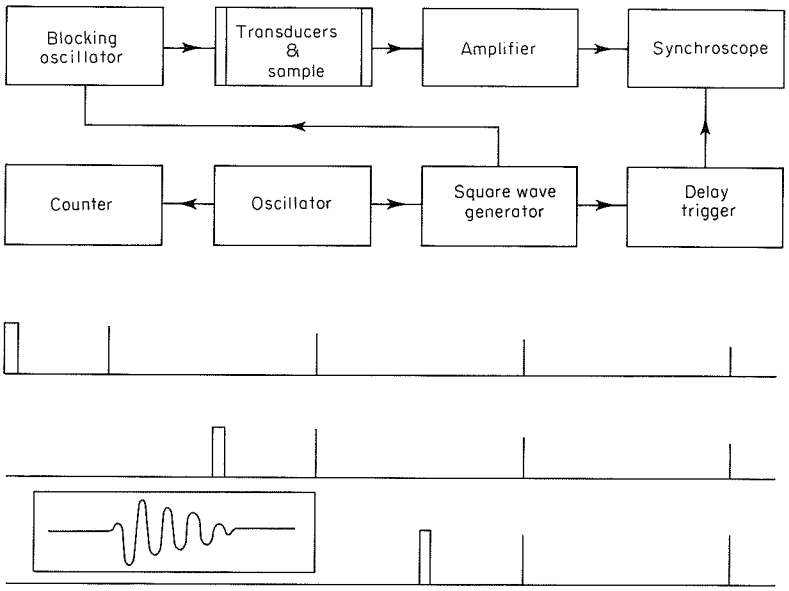

FIG. 7. Schematic diagram of the "sing-around" system for velocity measurements. (*After Greenspan and Tschiegg*, 1957.)

A simplified version of the sing-around system was described by Ficken and Hiedemann in 1956. They were not concerned at that time with attempts to control the shape or amplitude of the electric signals, but they claimed an accuracy of better than 1 percent for their measurements of velocity.

Blackstock [1966] has suggested that inaccurate results may be obtained with the sing-around method if it is used with viscous liquids. His analysis of the transient solution of the viscous wave equation shows the possible occurrence of transient signals of greater amplitude than the steady-state signals. In these circumstances the transient signal would be effective in triggering the electric system, and the measured velocity would refer to the transient rather than to the steady-state solution.

Velocity difference method

A method of making comparative measurements of velocity has been described by Carstensen [1954]. This instrument, illustrated in Fig. 8, incorporates a sample chamber which is divided into two parts separated by a thin, acoustically transparent diaphragm. A reference liquid of acoustic impedance similar to that of the sample is placed on one side of the diaphragm, and the unknown sample on the other. One of a pair of transducers, matched in frequency and mounted with fixed separation on the carriage, dips into each liquid. Motion of the carriage causes a given path

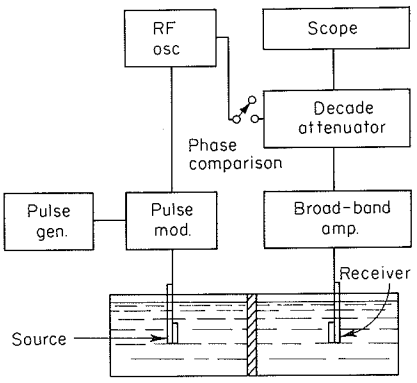

FIG. 8. Schematic diagram of a fixed-path apparatus for velocity and absorption measurements. (*After Schwan and Carstensen*, 1952.)

length of the reference liquid to be replaced in the path of propagation of an ultrasonic pulse between the transducers by the same path length of the liquid to be measured. The phase of the continuous-wave signal arriving at the receiving transducer depends on the difference of the sound velocities in the two liquids. This difference can be measured with an accuracy of 1 part in 10^4, and so the method is preferred for the detection of velocity dispersion in the sample. Since the absolute velocity in water, the most common reference liquid, is known with an accuracy of only 1 part in 3,000 (McSkimin, 1965), the final accuracy of measurement of the velocity in the sample is limited to this figure also.

Optical method

Debye and Sears [1932] and Lucas and Biquard [1932] showed that the alternating compressions and rarefactions of a sound wave, propagating in a liquid medium, correspond to an optical diffraction grating and thereby make possible the determination of the speed of sound and the absorption coefficient in transparent media by several methods. The most commonly employed experimental method utilizes the arrangement shown in Fig. 9. A plane traveling sound beam is produced by a transducer, usually quartz, at one end of the sound chamber, and provision for absorbing all incident acoustic energy is present at the distant end of the cell (to ensure that no standing waves are produced). Collimated monochromatic light is made to pass through the ultrasonic cell normal to the direction of sound propagation. The image of the slit is then focused on a photographic plate, along with the various diffracted orders. The diffraction angle θ, for order n, is

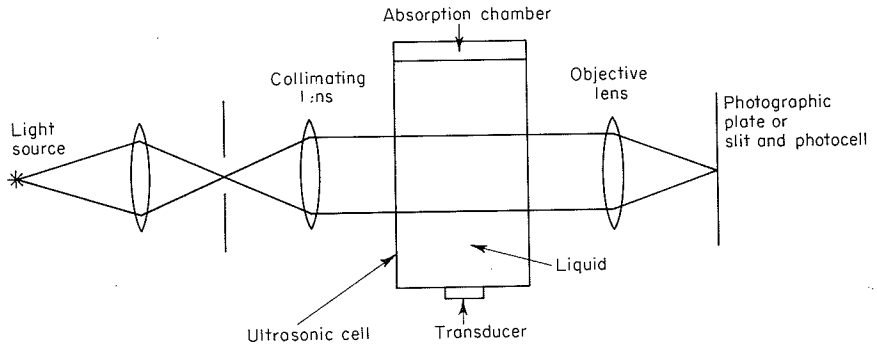

FIG. 9. Schematic diagram of an optical technique.

given by the Raman and Nath [1935] theory as

$$\sin \theta = n \frac{\lambda_l}{\lambda_s} \tag{80}$$

where λ_l is the wavelength of the incident light, and λ_s is the wavelength of the propagating sound wave, from which the speed of sound is readily computed.

The acoustic absorption coefficient in the liquid is determined by employing a photodetector (in place of the photographic plate) and measuring the intensity of one of the diffracted orders as a function of the distance from the sound source.

The reader is urged to examine Willard's publication of 1941 for further details of the optical method. However, it is appropriate to mention here a major disadvantage of the optical method, i.e., the uncertainty of the length of the light path through the sound beam.

Absorption Measuring Methods

Pulse transmission methods

Pulse transmissions systems for the measurement of absorption coefficient and velocity in the same apparatus may be divided into two classes: those using a fixed path and those using a variable path. The *variable-path* instrument, illustrated schematically in Fig. 10, was originated by Pellam and Galt [1946] and further developed by Litovitz and coworkers [1954] and by Lamb and collaborators [1958].† The method is particularly suitable for absolute measurements of absorption coefficient in the 5 to 500 MHz frequency range. The amplitude of a short ultrasonic pulse transmitted

† See Andreae et al. [1958].

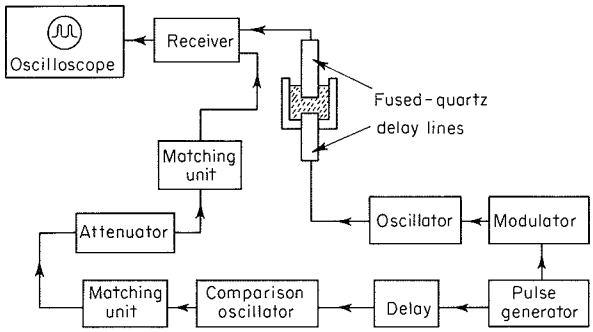

FIG. 10. Schematic diagram of a variable-path pulse apparatus for absorption measurements. (*After Heasell and Lamb*, 1956*a*.)

through the liquid sample is compared with the amplitude of a pulse derived from a reference oscillator and passed through the same amplifying system. Alteration of the amplitude of the received signal, which is caused by alteration in the ultrasonic path length, is matched by a corresponding alteration in the amplitude of the comparison signal, produced by adjusting an electrical attenuator in the comparison channel. This attenuator provides the reference for the attenuation measurement and should be either a highly accurate resistive attenuator or a piston attenuator consisting of a waveguide operating below cutoff. In the latter case the standard of attenuation depends only on the geometry of the waveguide and the mode of propagation within it, and these can be accurately determined. This technique has been used to measure the absorption coefficient of a large number of liquids in the frequency range from 0.5 to 500 MHz (Lamb, 1965; Litovitz and Davis, 1965; Hunter and Dardy, 1964; Edmonds, Pearce, and Andreae, 1962; Andreae and Joyce, 1962; Heasell and Lamb, 1956; Tamm, Kurtze, and Kaiser, 1954). Three different instruments operating on the same principle are generally needed to cover this range of frequency. The range of absorption-coefficient values which may be thus measured extends from 0.1 to 120,000 dB/cm. Extensive precautions must be taken to ensure parallelism of the surfaces of sending and receiving transducers and accurate displacement along the direction of pulse propagation, if absolute measurements are required. Relative measurements are not so critical. It is assumed in interpreting the measurements that plane waves are propagated in the liquid sample. This is unlikely to be strictly true, however, since it is known that transducers having a diameter that is only a small multiple of the wavelength of sound in the transducer materials (which is usually the case especially at the lower frequencies) vibrate in a number of different modes involving nonuniform displacement of the faces in contact with a liquid sample. This possible source of difficulty appears to be of no great practical significance

because the receiving transducer integrates over the cross-sectional area of the beam. However, the diffraction pattern of a piston source must be taken into account at lower frequencies (Carome and Witting, 1961), e.g., at less than 10 MHz when the absorption coefficient is small. Divergence of the beam causes an apparent increase in the absorption coefficient, for which correction must be made. At the far boundary of the Fresnel region, $x = r_c^2/2\lambda$, this correction can amount to 1.5 dB relative to the amplitude at the source (Bass, 1958). A given pair of transducers, which are matched in their fundamental frequencies for thickness vibration, can be operated at a number of different frequencies which are odd harmonics of the fundamental. In this system accuracy of temperature control is also essential and should be maintained within ± 0.1°C (Andreae et al., 1958; Edmonds, 1966).

The transmission technique that utilizes a *fixed path length* was developed by Carstensen [1954] and is shown in Fig. 8. Under pulsed conditions, it is particularly suitable for making comparative measurements of absorption coefficients and, under continuous-wave conditions, for measuring velocity of propagation as described on pages 250–251. The changes in the received pulse height resulting from motion of the carriage can be measured by the comparison technique described above and interpreted as relative absorption. Siegert [1963] has developed this technique further to permit more accurate control of temperature and concentration of the sample.

This type of instrument is particularly suitable for measurements in the lower megahertz frequency range, and it has been used to make absorption measurements down to 0.3 MHz. The method has the disadvantage of requiring comparatively large sample volumes—typically one-half liter. However, it has the important advantage of requiring no correction for diffraction effects which result in apparent absorption. If the reference liquid is chosen to have nearly the same velocity of propagation as the sample, then the diffraction pattern of the sending transducer is not changed significantly when the carriage is moved relative to the diaphragm, and the receiving transducer remains in the same position in the field. This is not true of the variable-path instrument described above where at low frequencies it is necessary to make a correction for diffraction effects which can account for as much as 30 percent of the measured "absorption." (Under the latter circumstances the accuracy of determination of the absorption-coefficient value can be as poor as ± 50 percent.) With the fixed-path apparatus it is estimated that the absorption coefficient can be determined to better than 0.05 dB/cm and in favorable circumstances to 0.02 dB/cm. Errors in absorption are reported to be less than 5 percent in the frequency range above 1 MHz and to reach 10 percent only at the lowest frequencies.

The method of pulse transmission listed in Table 6 as suitable for measurement of the acoustic velocity and absorption coefficient of viscoelastic solids

bears close similarity to the phase comparison and pulse transmission techniques just described. It differs insofar as samples of viscoelastic media have fixed boundaries, and it is not convenient to change the dimensions of the sample, or the ultrasonic path length, as it is with a liquid. Under such circumstances the sample is held between transmission media, which may be either liquid or solid, but which are characterized by low values of the absorption coefficient. It is necessary to know the velocities and the attenuation coefficients of the transmission media, and also their acoustic impedances, in order that an analysis of the phases and amplitudes of the pulses received may yield the desired information on the absorption and velocity parameters of the sample.

Transient thermoelectric method

The methods discussed in the previous sections have in common the requirement that the sample to be measured be a homogeneous medium (excised heterogeneous samples of biological material of simple geometry, e.g., slabs having plane-parallel sides, are also appropriate if an "average value" for the absorption coefficient is desired). Thus, these methods are not suitable for *in situ* measurements. The transient thermoelectric method provides a technique wherein a very small thermocouple is embedded in the tissue of a living organism and the absorption coefficient determined in the small volume of tissue immediately surrounding the junction (W. J. Fry and R. B. Fry, 1953; Dunn, 1962). This method is also suitable in those cases where absorption coefficients of relatively small volumes of liquid media are to be considered, in particular, at ultrahigh frequencies (Dunn and Breyer, 1962). The following is a brief description of the transient thermal electric measuring method (W. J. Fry and R. B. Fry, 1954*a*, 1954*b*; Dunn and W. J. Fry, 1957; W. J. Fry and Dunn, 1962). A small calibrated thermocouple probe (usually uninsulated) is embedded in the tissue to be studied, and the specimen is exposed to rectangular acoustic pulses of known intensities. The transient thermoelectric output produced in response to an acoustic pulse of known amplitude is recorded on a magnetic oscillograph employing a galvanometer having a time constant of the order of 10^{-2} s. The rise time of the pulse is of the order of 10^{-3} s. The transient temperature change detected by the thermocouple embedded in the tissue possesses two distinct phases (see Fig. 11). The first phase, which reaches an equilibrium value rapidly (in about 10^{-1} s), results from the conversion of acoustic energy into heat by the viscous forces acting between the wires of the thermocouple and the immediately surrounding medium. This phase is, of course, not present in the tissue when the thermocouple is absent. The second phase exhibits an almost linear characteristic (for pulse durations of the order of 1 s) and results from acoustic energy converted into heat by

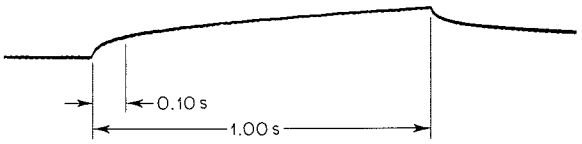

FIG. 11. Thermoelectric emf produced at the probe terminals in response to a 1.0 s pulse of ultrasound.

absorption in the tissue surrounding the thermocouple junction. If the thermocouple wires are sufficiently small in diameter, the initial time rate of change of temperature of the second phase is related to the acoustic amplitude absorption coefficient per unit path length by the following relation:

$$\alpha = \frac{\rho_t c_p' J}{2I}\left(\frac{dT}{dt}\right)_0 \tag{81}$$

where $\rho_t c_p'$ is the heat capacity per unit volume of the tissue in calories per cubic centimeter per degree Celsius, I is the acoustic intensity in watts per square centimeter, and J is the mechanical equivalent of heat in joules per calorie. The acoustic intensity of the plane traveling wave field to which the tissue sample is exposed must be known and can be determined by a thermoelectric probe which has been calibrated previously against a radiation-pressure detector (Dunn and W. J. Fry, 1957). The heat capacity per unit volume must also be known. The evaluation of the quantity $(dT/dt)_0$ follows from the experimentally determined temperature-time relation utilizing the second phase of the recording only, if certain criteria are satisfied (W. J. Fry and R. B. Fry, 1954*a*, 1954*b*). Let it suffice here to indicate that for a copper-constantan thermocouple junction 0.0005 in. in diameter, embedded in a material having absorption properties similar to castor oil and irradiated with a pulse duration of 1 s by a 1 MHz sound beam having a width at half-intensity of 4 mm and an intensity level such that the total temperature rise is not greater than 1°C, the total error introduced by assuming that the time rate of rise of the slow phase of the thermocouple response is identical with $(dT/dt)_0$ in the above equation is not more than 1 percent.

In employing this method, it is necessary to recognize that the known sound intensity used in exposing the sample will be diminished upon propagating from the surface of the sample to the position of the thermocouple junction. Thus it is necessary to make an appropriate correction in the computation of the absorption coefficient. In many cases this correction is relatively small and can be accomplished by using a value of α obtained by inserting the value of the incident intensity in Eq. (81) (Dunn, 1962).

Knowledge of the anatomic position of the thermocouple junction is essential since it is generally desired to make a measurement within a specific

tissue structure. Further, since the acoustic exposing beam is generally not planar over a very large area, it is essential that a known part of the beam (i.e., for which the intensity is known) irradiate the region occupied by a thermocouple junction. The techniques for determining the precise position of the thermocouple junction within the tissue include optical methods and even acoustical means during the experiment. There are, however, situations for which one must delay determining the anatomic position of the junction until after the experimental animal has been sacrificed when dissection and histological techniques can be employed (Dunn, 1962).

The transient thermoelectric method also provides a procedure for determining acoustic absorption-coefficient values of dielectric liquids in the ultrahigh-frequency region. In this case the piezoelectric sound source, in contact with the liquid under investigation, is excited electrically, at an odd harmonic of the fundamental thickness mode, to produce a single acoustic pulse with rectangular envelope of, for example, 0.1 s duration. As a result of this relatively short acoustic pulse, the heating action of the viscous forces, already described, produces a transient temperature rise in the immediate neighborhood of the thermocouple junction. The transient thermal emf produced in the thermocouple circuit, which can be amplified and displayed by an oscilloscope (see Fig. 12), is a measure of the acoustic intensity in a plane-wave field in the neighborhood of the junction. The thermocouple response, which is directly proportional to the acoustic intensity in the neighborhood of the junction, is observed as the deflection of the electron beam spot from its initial equilibrium position for varying distances between the sound source and probe. The acoustic intensity absorption coefficient per unit path length is then readily computed. This method has been employed to determine acoustic absorption-coefficient values for selected oils in the frequency range from approximately 10 to 1,000 MHz (Dunn and Breyer, 1962).

Thermocouples are fabricated readily from 0.003-in.-diameter commercially available wires, which are then etched in acid to reduce the diameter to approximately 0.0005 in. in the vicinity of the junction. Assembly of the thermocouple can be accomplished by either soldering or welding. Both lap and butt joints can be used without observed differences in the ensuing results. A welding technique has been developed especially for fabrication of miniature junctions by Hawley et al. [1962].

In addition to the advantage already indicated in using the transient thermoelectric method, i.e., that it enables *in situ* determinations of acoustic absorption to be made, it also has the advantage that highly stable measurements can be made, i.e., the thermoelectric probe is insensitive to stray or r-f fields, it has a low electrical input impedance, and it can be used as a primary standard for accurately determining absolute sound levels at ultrasonic frequencies [see Eq. (81)]. However, the transient thermoelectric

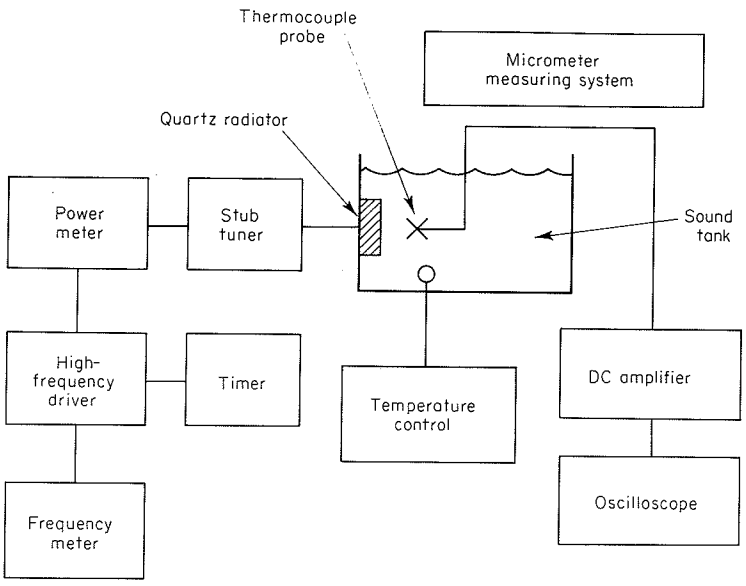

FIG. 12. Block diagram of instrumentation for generating and detecting uhf sound in liquids.

method does suffer the following disadvantages: (1) in the low-megahertz frequency range it is relatively insensitive, requiring acoustic intensities of the order of 1 W/cm² to obtain a suitable output; (2) it cannot be used to determine the temporal waveform of the acoustic disturbance.

Interferometric method

Musa [1958] has considered the conditions under which an interferometer may yield valid measurements of absorption coefficient. Direct measurements can be made when α is very small or very large, but an iterative procedure is required for intermediate values. Cerf [1963] has generalized this analysis to include the case of operation at frequencies other than harmonics of the transducer's fundamental frequency and has concluded that Musa's results remain valid. Subsequent developments have led to the use of this technique at fixed frequencies close to the harmonics. It has been found preferable to multiplicate the entire apparatus for operation at each frequency, instead of attempting to change frequency with a single interferometer. When $\alpha\lambda/2\pi < 10^{-2}$, an absorption coefficient is obtained from a plot of the relation

$$\tanh^{-1}\frac{U_m}{U_M} = \alpha_2 l + \beta_2 \tag{82}$$

where U_m and U_M designate respectively any successive minimum and maximum in the relation between the voltage at the receiving transducer and the liquid path length, and l designates the median value of path length for the minimum-maximum pair; β_2 is a function of the frequency and the acoustic impedances of the transducers and the liquid sample, and α_2 is an attenuation coefficient to be related to the absorption coefficient α of the liquid. In operation, α_2 may be as much as 15 percent less than α, owing to diffraction effects. Therefore, measurement of relative absorption is obtained initially. However, conditions can be controlled such that for two liquid samples, X and Y,

$$\frac{\alpha_{2,X}}{\alpha_X} = \frac{\alpha_{2,Y}}{\alpha_Y} \tag{83}$$

Hence, if α_Y for a standard liquid is known, and $\alpha_{2,X}$ and $\alpha_{2,Y}$ are measured at the same frequency, α_X can be calculated. Adequate control of the apparatus and experimental conditions calls for selection of the transducer and mounting so that the graph of the experimental data followed the linear form of Eq. (82), and also for readjustment of the transducer alignment for each reading of the maximum received voltage, U_M.

Early results obtained by using this technique are subject to greater error than was then realized (see p. 287). Reliable data were first published in 1968. In particular, sudden changes of absorption with change of frequency were not confirmed.

Transducers

Ultrasound above approximately 100 kHz is most conveniently and practically produced by using piezoelectric materials as elements to convert electric to acoustical energy (see, for example, Hueter and Bolt, 1955, for a review). These elements can also be used to transform energy in the inverse direction, i.e., acoustical to electric. Such elements are cut with proper orientation from crystals that possess the piezoelectric property to a sufficiently marked degree or from suitably prepared ceramic materials (Mason, 1950). The problem of choosing the proper orientation is not discussed here; rather, information concerning particular elements suitable for ultrasonic transducers is presented.

Transmitters

The suitability of a material for use in transducers for producing ultrasound is dependent on a number of factors, the relative importance of which is determined by the application. These factors include the magnitude of the piezoelectric coefficients, stability, dielectric properties, electrical breakdown

TABLE 7. PHYSICAL CONSTANTS OF PIEZOELECTRIC MATERIALS

Material	ρ_c (kg/m³)	v_c (m/s)	$\rho_c v_c$ [kg/(m²)(s)]	e (C/m²)	d (m/V)	$\epsilon_c\epsilon_0$ (F/m)	κ (Ω-m)
Multiply figures in table by	10^3	10^3	10^6	1	10^{-12}	10^{-12}	10^9
Quartz, X-cut	2.65	5.72	15.16	0.176	2.04	40.6	>1000
95% $BaTiO_3$; 5% $CaTiO_3$, plate	5.55	5.64	31.1	16.4	149	10,800	>10
PZT-4	7.5	4.60	34.5	18.6	289	10,600	>10
PZT-5A	7.75	4.35	33.7	19.9	374	15,300	>100
Lithium sulfate, Y-cut	2.06				13	91.5	>10
Tourmaline, Z-cut	3.1				2.16	66.5	>100

strength, and tensile
is the one used for th
strength, but it requi
power outputs. On
much higher dielectr
strengths for equal p
have the disadvantag
and electrical input i
at the present time,
essential to a study,
However, if accurate
may be used.

It is necessary to
as a function of driv
ultrasonic studies.
impedance of the tra
tronic power amplif
the appropriate cons
in Table 7, and simp
It should be noted th
(which is equal to th
between the electrod
at its boundary in co
velocity produced in
of the acoustic prope
and acoustic proper
is, these media cons
example, the magni
by the element on
situation.

Consider the situ
thickness L_c is elect
radiate acoustic ene
impedance $\rho_0 v$, whi
faces. It is assume
an extremely low im
face, i.e., for this
equal to zero. It is
purposes if the med
element is supported
for the purpose of
paratively no losses
unrestrained as far

strength, and tensile strength of the material. Quartz (the X-cut orientation is the one used for the plate mode) has high stability, high electric and tensile strength, but it requires relatively high electric field strengths to obtain high-power outputs. On the other hand, the polycrystalline ceramics possess much higher dielectric-constant values and require much lower electric field strengths for equal power outputs from the same-size radiating area. They have the disadvantages of lesser stability than quartz, higher internal losses and electrical input impedances too low at high frequencies. Consequently, at the present time, if accurate reproducibility of irradiation conditions is essential to a study, then quartz is the material of choice for the transducers. However, if accurate reproducibility is not important, the ceramic materials may be used.

It is necessary to estimate the acoustic output from transducer elements as a function of driving voltage in order to assess the feasibility of proposed ultrasonic studies. Further, it is important to estimate the input electrical impedance of the transducers so that they can be driven by appropriate electronic power amplifiers and coupling circuits. Accordingly, the values of the appropriate constants of a number of transducer materials are presented in Table 7, and simplified formulas and graphs are included in this discussion. It should be noted that the relation between the voltage applied to an element (which is equal to the product of the electric field strength and the distance between the electroded faces) and the pressure or particle velocity produced at its boundary in contact with a medium is linear. The pressure or particle velocity produced in the medium in contact with the element is also a function of the acoustic properties of that medium, and the configuration, dimensions, and acoustic properties of other media to which it in turn is coupled. That is, these media constitute the load on the element, and they determine, for example, the magnitude of the acoustic pressure amplitude which is exerted by the element on the bounding medium under a given electrical driving situation.

Consider the situation in which a piezoelectric element of radius r_e and thickness L_e is electrically excited to vibrate in a plate-thickness mode to radiate acoustic energy in the z direction into a medium of characteristic impedance $\rho_0 v$, which is in contact with the element over one of the large faces. It is assumed that the medium in contact with the opposite face has an extremely low impedance so that virtually no radiation occurs from this face, i.e., for this medium the terminating impedance may be considered equal to zero. It is possible to approximate this situation for all practical purposes if the medium into which the sound is radiated is a liquid and the element is supported near its periphery and is air-backed. It is also assumed, for the purpose of obtaining the simplified relations given here, that comparatively no losses occur in the holder and that the element is essentially unrestrained as far as its vibration is concerned, except by the medium into

which it radiates. Under these conditions the "average" intensity produced at the face of the crystal operating at the lowest resonant frequency is given by

$$I = \frac{4}{10^4} e^2 \left(\frac{E}{L_c}\right)^2 \frac{1}{\rho_0 v} \tag{84}$$

where E designates the applied voltage, and e is a constant determined by the type and orientation of the material from which the piezoelectric element is made (see, for example, Hueter and Bolt, 1955). If, from the formula, one wishes to obtain the intensity in watts per square centimeter, the value of e should be expressed as coulombs per square meter, as listed in Table 7. The units of $\rho_0 v$ should be kilograms per square meter per second, and that of L_c should be the meter. The value of the intensity given by Eq. (84) is constant over the area of the vibrating element at the surface of the element. Owing to Fresnel and Fraunhofer diffraction of the waves in the regions $x \leq r_c^2/2\lambda$ and $x \geq 2r_c^2/\lambda$ distant from the sound source, the distribution of the acoustic field variables (pressure, particle velocity, etc.) is not constant over a plane parallel to the vibrating surface (Fry and Dunn, 1962). Consequently, the transverse intensity distribution may exhibit one or more maxima and minima, depending on the axial coordinate position.

The lowest resonant frequency of the element is given by the relation

$$f_R = \frac{v_c}{2L_c} \tag{85}$$

where L_c designates the thickness of the element, and v_c is the plate velocity (the speed of sound in the thickness direction). Table 7 lists values of the constants e, v_c, and $\rho_c v_c$ for the different materials used as elements for thickness mode operation. In order for Eq. (84) to apply approximately, it is necessary that essentially no acoustic energy be reflected back to the radiating face and that the diameter of the vibrating element be greater than about one wavelength. This implies that the input acoustic impedance $P/\dot{\Xi}$ into the contacting medium approximates a pure resistance (equal to $\rho_0 v$ in this case). As an example of the use of these formulas, consider a quartz plate of thickness 0.286 cm (1 MHz fundamental resonant frequency) excited with 50 V and radiating into water at 30°C. Calculation indicates that the developed acoustic intensity is 25 W/cm². The maximum intensity obtainable in water, using X-cut quartz transducers radiating directly into the medium as limited by mechanical failure, is 2,000 W/cm². The corresponding value for barium titanate is 800 W/cm². Since the ceramic materials are prepolarized by an applied unidirectional field during manufacture, and since during each half-cycle of operation, the applied electric field is opposite to the original polarizing field, if the latter is sufficiently great it may cause partial depolarization, which thus reduces the piezoelectric activity of the

element. Therefore, under some conditions of operation, the threshold for electric breakdown of the surfaces between the electrodes rather than the breaking stress of the piezoelectric unit determines the maximum intensity obtainable with these materials (Hueter and Bolt, 1955).

The variation of the radiated intensity as one moves off resonant operation (at constant driving voltage across the element) is illustrated by the graph of Fig. 13. This figure can be used to compute the output intensity for the type of system just discussed for a range of values of the ratio $\rho_c v_c/\rho_0 v$ of the characteristic impedances of the crystal and the medium, and for a wide range of values of the frequency. The quantity γ_c is given by the relation

$$\gamma_c = 180 \frac{f}{f_R} \tag{86}$$

FIG. 13. Relative acoustic intensity radiated by piezoelectric element versus frequency, at constant driving voltage. The parameter varying from curve to curve is the ratio of the characteristic acoustic impedance of the piezoelectric element to that of the medium.

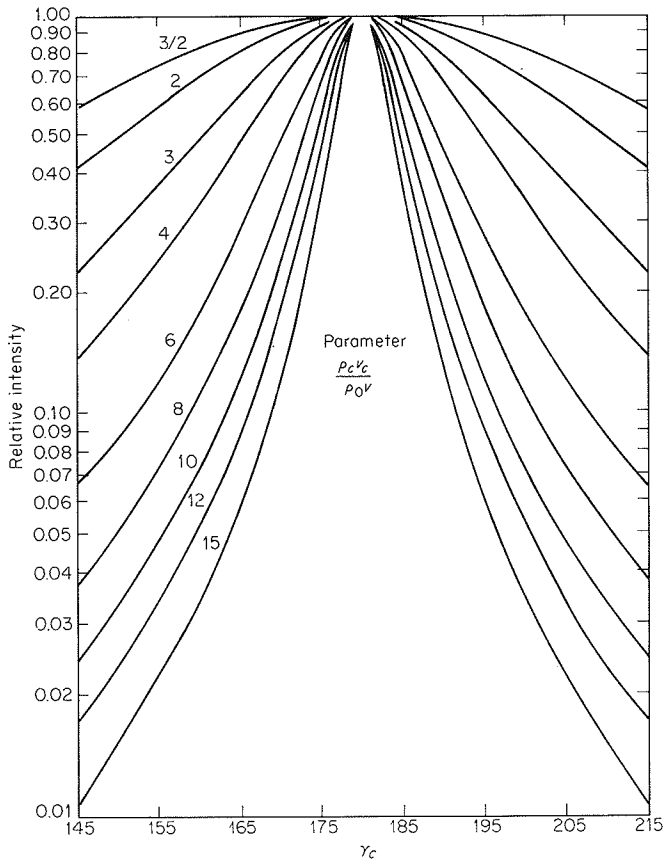

where f is the operating frequency, f_R is the first resonant frequency, and γ_c is expressed in degrees. It should be noted that relative intensity is plotted along the vertical axis of the graph. The figure thus illustrates the relative sharpness of resonant operation under different loading conditions, i.e., for media of different characteristic impedances. The intensity at any off-resonant frequency is obtained by calculating the product of the result of Eq. (84) and the value of the relative intensity for the value of γ_c corresponding to the frequency of interest and for the value of the parameter $\rho_c v_c/\rho_0 v$ for the materials under consideration. Since the input electrical impedance of the element changes with frequency, some adjustment of the driving generator may be necessary to maintain the constant-voltage condition.

It is necessary to know, at least approximately, the electrical input impedance of the piezoelectric elements in order to be able to specify the characteristics of the electronic generators required to furnish the power. For elements loaded as just discussed, i.e., no load on one face and terminated in the characteristic impedance of the bounding medium on the other large face, the electrical input impedance relation takes the following form at resonance (see, for example, Fry et al., 1948):

$$Z_e = \frac{1}{j\omega C_0 + (4e^2/\rho_0 v)(A_c/L_c^2)} \tag{87}$$

where

$$C_0 = \frac{\epsilon_c \epsilon_0 A_c}{L_c} \tag{88}$$

in mks units. The first term in the denominator of Eq. (87) arises as a result of the "static" capacitance of the element and can be calculated from Eq. (88), where ϵ_c designates the dielectric constant relative to free space, ϵ_0 designates the dielectric permittivity of free space, A_c is the radiating area of the element, and all other symbols have been defined previously. The product $\epsilon_c \epsilon_0$ is listed in Table 7 for various piezoelectric materials. The term $\rho_0 v$ designates the characteristic impedance of the bounding medium as in Eq. (84). Equation (87) can be represented as an equivalent electric circuit of two branches, as illustrated in Fig. 14. One branch of this parallel circuit represents the static capacitance of the piezoelectric element, and the other branch represents the "motional" impedance, i.e., the part of the electrical input impedance which results from the fact that mechanical motion of the element and bounding medium modify the electric field between the electrodes. Since Eq. (87) applies to resonant operation, the electrical impedance of the motional branch is a pure "resistance" and is thus represented as a real number. For off-resonant operation, the motional branch would contain both a real and an imaginary part. Equation (87) is derived by neglecting all losses except radiation losses into the bounding medium

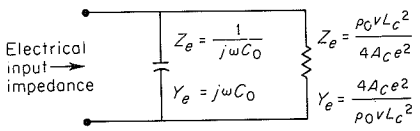

FIG. 14. Equivalent parallel electric circuit of piezoelectric plate element operating at resonance and radiating from one face only. Impedances and admittances shown. See Eq. (87).

and by assuming that the piezoelectric element holder does not affect appreciably the operation of the element (Fry et al., 1948). These assumptions are reasonable for calculating approximate values of the electrical input impedance if the element is radiating into a liquid medium and if the opposite face is bounded by a gas or by a material of comparatively low characteristic impedance. If the electric power to the element is supplied by a cable of capacitance C_x, then the quantity C_0 of Eq. (87) is replaced by $C_0 + C_x$ in calculating the electrical input impedance at the cable terminals.

Receivers

Piezoelectric elements are also used to measure ultrasonic field characteristics. Employed in this way, an element responds by producing an electric field between two electrodes, placed on appropriate faces, when certain specific faces (or the entire element if a hydrostatic response unit is employed) are subjected to the changing pressure of the sound field. Several different types of elements are useful. The plate type can be employed when the energy to be detected is in the form of plane wavefronts of constant phase, and when it is not necessary to observe amplitude variations in the field, which occur over areas small compared to the area of the detector. Obviously such plate detectors interfere drastically with the field.

Piezoelectric probes other than the plate forms can be employed. The desired type may be one in which the maximum dimension of the probe is small compared to one wavelength of the sound in the medium. This goal is easily attained at frequencies below 100 kHz, but it cannot be achieved as a practical device at a few hundred kilohertz and higher. Two major difficulties arise. First, the input impedance becomes so high that it is difficult to realize a reasonable sensitivity. Second, construction of the device and the associated electric connections raise major technical problems. Consequently, in the neighborhood of 1 MHz, the smallest probes of the piezoelectric types are not less than ½ to one wavelength in maximum dimension. In general, they are sensitive to the direction of orientation in the field, and with them precise measurements of sound level are not possible in the megahertz frequency range. However, such probes are

necessarily employed in this frequency range for the determination of field characteristics in which the relative time phase at different positions in the field is desired. Precision measurements of sound levels in the megahertz frequency range, combined with the capability of resolving the fine structure of the fields, can be realized with the thermocouple probes discussed on page 256.

Consider receivers for which the "maximum diameter" is small compared to a wavelength of sound in the medium. One such configuration is that of a rectangular solid element. As already indicated, the usual difficulty that arises at ultrasonic frequencies, even below 1 MHz, is the realization of small size. Hence, it is most convenient to use a piezoelectric element that provides an electric response when it experiences a pressure over all faces simultaneously. Elements such as lithium sulfate and tourmaline possess this property, and with these materials it is not necessary to design a holder that decouples some of the faces from the medium in which the sound field exists.

When such an element is subjected to an acoustic pressure amplitude P, a voltage of amplitude E will appear across a load. The relation between the magnitudes of these quantities is

$$\left|\frac{E}{P}\right| = \frac{\omega A_e d}{\sqrt{(1/R_p^2) + (\omega C)^2}} \tag{89}$$

where C is the shunt capacitance of the electric load C_L, combined with that, C_0, of the crystal (i.e., $C = C_0 + C_L$); R_p is the resistance of the parallel combination of the shunt resistance, R_e, of the piezoelectric element and that, R_L, of the load [i.e., $R = R_e R_L/(R_e + R_L)$]; A_e is the area of an appropriate electroded face; and d is the piezoelectric coupling parameter listed in Table 7. If R_p and $1/\omega C$ are expressed in ohms, d in meters per volt, A_e in square meters, and P in newtons per square meter, then E is in volts. From Eq. (89) it is clear that an increase in the shunt capacitance across the element results in a decrease in sensitivity. In addition, it is apparent that, as the frequency decreases from high values for any given element, the sensitivity begins to decrease when the magnitude of the capacitive reactance $1/\omega C$ becomes comparable to and larger than the shunt resistance R_p. This is illustrated in Fig. 15, where the voltage output per unit pressure is shown as a function of the nondimensional quantity $\omega R_p C$. The sensitivity is independent of the frequency (as long as the maximum diameter of the element is much smaller than the wavelength) when $R_p \gg 1/\omega C$ and is given by

$$\left|\frac{E}{P}\right|_\infty = \frac{A_e d}{C_0 + C_L} \tag{90}$$

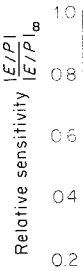

FIG. 15. Re

The sensitivity drops
the relation

The frequency is in
clear that the flat p
frequencies by incre
correspondingly dec
It is important, the
required, to use fo
resistivity. Specific
flat response range
which can be estima
ing Eq. (85) and va

The hollow tubula
for plotting acousti
radially oriented el
over the entire oute
The interior of the c
tion of gas pockets.
tional in response,
compared to a wave
dimensions as smal
(Ackerman and Hc
to about 100 kHz (
sound levels quantit
some idea of acous

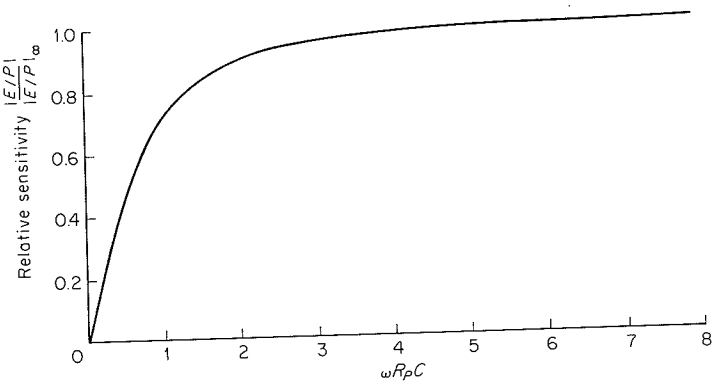

FIG. 15. Relative sensitivity of probe versus $\omega R_p C$. See Eq. (89).

The sensitivity drops to one-half this value for a frequency $f_{1/2}$ which satisfies the relation

$$f_{1/2} = \frac{1}{2\pi\sqrt{3}} \frac{1}{R_p(C_0 + C_L)} \tag{91}$$

The frequency is in hertz if R_p is in ohms and $C_0 + C_L$ is in farads. It is clear that the flat portion of the sensitivity curve can be extended to lower frequencies by increasing the capacitance of the load, but the sensitivity is correspondingly decreased over the flat portion of the frequency range. It is important, therefore, if low-frequency operation at high sensitivity is required, to use for the piezoelectric element a material of high volume resistivity. Specific examples are shown in Table 8. The upper end of the flat response range of sensitivity is limited by the resonant frequency f_R, which can be estimated, for probes of such shape, by a computation employing Eq. (85) and values of v_c from Table 7.

The hollow tubular piezoelectric ceramic probe is also employed extensively for plotting acoustic field patterns. This receiver is designed so that a radially oriented electric field appears in response to a pressure exerted over the entire outer surface of the cylinder including the end terminations. The interior of the cylindrical tube can be made compliant by the incorporation of gas pockets. In order for such a probe to be completely nondirectional in response, it is necessary that its maximum diameter be small compared to a wavelength. Probes of this type have been constructed with dimensions as small as $\frac{1}{16}$ in. in length and $\frac{1}{16}$ in. in outside diameter (Ackerman and Holak, 1954). They are nondirectional at frequencies up to about 100 kHz ($\lambda = 1.5$ cm in saline). They cannot be used to determine sound levels quantitatively above about 100 kHz, but are useful in obtaining some idea of acoustic field configurations at frequencies up to the 1-MHz

TABLE 8. NUMERICAL EXAMPLES OF NONRESONANT PIEZOELECTRIC PROBES

Material	d (m/V)	A_e (m²)	C (F)	R_o (Ω)	E/P [(V/N)(m²)]	E/P (V/atm)	$f_{\frac{1}{2}}$ (Hz)	f_R (kHz)
Multiply figures in table by	10^{-12}	10^{-6}	10^{-14}	10^{12}	10^{-4}	1	1	1
Lithium sulfate (Y-cut)	13	4	18.3	5	2.84	28.8	0.1	1380
Tourmaline (X-cut)	2.16	4	18.3	50	0.65	6.6	0.014	1800

TABLE 9. NUMERICAL EXAMPLES OF RESONANT PIEZOELECTRIC PROBES

Material	d (m/V)	A_e (m²)	f_R (MHz)	C_L (F)	$\rho_0 v$ [(kg/m²)(s)]	E/P [(V/N)(m²)]	E/P (V/atm)	$R_L \gg$ (Ω)
Multiply figures in table by	1	10^{-4}	1	1	10^6	10^{-3}	10^{-10}	10^3
Quartz (X-cut)	100	1	1	0	1.5	16	16	1000
Barium titanate (plate)	100	1	1	0	1.5	0.15	0.15	0.1

range ($\lambda = 1.5$ mm). A
of 0.012 in. has an "op
(V/N)(m²).

A very important co
the decoupling of the
which may also be exci
field. If sufficient sound
structure, then the prob
which is related more n
structure rather than th

Consider now receiv
element, in many cases
one megahertz or above
is chosen to result in r
field. In this case the "
across, and, in fact, i
transmitter and receiver

The relation between
by Eq. (85) when the vib
air for example. The v
from noncapacitive and
in parallel with the eleme
in parallel resonance at
If, at resonant angular
inductance, is equal to o
circuit is equal to $Q_e L$ a
piezoelectric element a
R_c, and the resistance of
the sensitivity of the rec

$$\frac{E}{P} = 0.0$$

where P is the pressure
and E is the voltage pro
priate piezoelectric coup
and $\rho_0 v$ is the characteri
receiver is placed. If
in kilograms per square
e in coulombs per squar
is in volts. The form of
tion in terms of electri

range ($\lambda = 1.5$ mm). A probe of the size just indicated with a wall thickness of 0.012 in. has an "open-circuit" pressure sensitivity of the order of 10^{-6} (V/N)(m²).

A very important consideration in the design of piezoelectric probes is the decoupling of the piezoelectric element from the supporting structure which may also be excited to vibrate by virtue of its presence in the sound field. If sufficient sound energy is conducted to the element by the supporting structure, then the probe can exhibit a voltage across its output terminals which is related more nearly to the sound distribution along the supporting structure rather than that at the piezoelectric element.

Consider now receivers that operate at resonance. The piezoelectric element, in many cases in which the operating frequency is of the order of one megahertz or above, takes the form of a plate for which the thickness is chosen to result in resonant operation at the frequency of the acoustic field. In this case the "diameter" of the plate face may be many wavelengths across, and, in fact, in some applications the same element may act as transmitter and receiver.

The relation between element thickness and resonant frequency is given by Eq. (85) when the vibrating element is backed by a low acoustic impedance, air for example. The voltage sensitivity can be increased over that obtained from noncapacitive and/or resistive loading by employing an inductance L in parallel with the element, and an associated cable of such value as to result in parallel resonance at the mechanical resonant frequency of the element. If, at resonant angular frequency ($\omega = \omega_{cR}$), Q_e, the electrical Q of this inductance, is equal to or greater than 10, then the impedance of the parallel circuit is equal to $Q_e L$ and is resistive. Then, if the shunt resistance of the piezoelectric element and associated loss components are designated by R_c, and the resistance of the load is R_L (the input impedance into an amplifier), the sensitivity of the receiver is

$$\frac{E}{P} = 0.04 \frac{\left(\frac{eA_c/L_c}{\rho_0 v}\right)}{\frac{1}{R_L} + \frac{1}{R_c} + \frac{1}{Q_e \omega_{cR} L} + \frac{4(eA_c/L_c)^2}{A_c \rho_0 v}} \tag{92}$$

where P is the pressure amplitude of the acoustic field without the receiver, and E is the voltage produced across the load. The quantity e is the appropriate piezoelectric coupling parameter for the element, as given in Table 7, and $\rho_0 v$ is the characteristic acoustic impedance of the medium in which the receiver is placed. If A_c is expressed in square meters, L_c in meters, $\rho_0 v$ in kilograms per square meter per second, R_L and R_c in ohms, L in henrys, e in coulombs per square meter, and P in newtons per square meter, then E is in volts. The form of the denominator of Eq. (92) permits the representation in terms of electric circuit elements as illustrated in Fig. 16, i.e., a

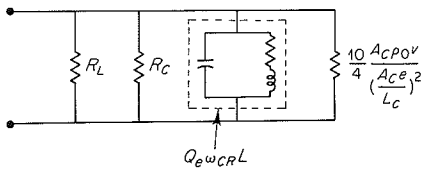

FIG. 16. Equivalent electric circuit of resonant, plate-type piezoelectric receiver and associated circuitry. See Eq. (92).

parallel arrangement of the four elements, the reciprocal of the input impedance being equal to the denominator expression.

If the quantity $1/R_L$ is much smaller than the combination of other terms in the denominator of Eq. (92) and $C_L = 0$, then it is possible to rewrite Eq. (92) as

$$\frac{E}{P} = 0.04\,\frac{e/\rho_0 v}{1/\kappa + \omega_{cR}(\epsilon_0\epsilon_c/Q_e + 0.04\pi e^2/v_c\rho_0 v)} \tag{93}$$

where the same units as used for Eq. (92) apply, $\kappa \equiv A_c R_c/L_c$, and v_c is in units of meters per second. Values for the quantities e, ϵ_0, ϵ_c, κ, and v_c are given in Table 7. Several numerical examples illustrating the magnitudes of the quantities involved for various types of piezoelectric elements are shown in Table 9.

4. ULTRASONIC VELOCITY AND ABSORPTION DATA FOR BIOLOGICALLY SIGNIFICANT MEDIA

Solvents

Water

The absorption-coefficient value for distilled water is greater than one would expect from consideration of the viscosity and thermal conductivity losses [see Eqs. (30) and (46)]. This excess absorption above the "classical" value has been attributed by Hall [1948] to a structural relaxation mechanism involving the transition of water molecules from a bonded, "icelike," structure to another "crystalline" structure of smaller specific volume. The relaxation frequency for the transition is presumably far above the accessible experimental frequency range for ultrasonic techniques, i.e., above 10^9 Hz, and only the contribution to the absorption coefficient at "low" frequencies ($f \ll f_r$) is observed directly. Litovitz and Carnevale [1955], investigating the pressure dependence of the ultrasonic absorption, obtained data that lend support to the model of a two-state structure for water. Although Hall's model was based on the concept of a transition between two possible crystalline structures of water (following the suggestion of Bernal and Fowler [1933],

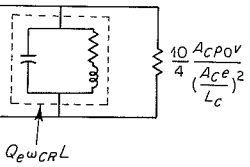

valent electric circuit of type piezoelectric receiver ircuitry. See Eq. (92).

ciprocal of the input

ination of other terms is possible to rewrite

(93)

$^2/v_c\rho_0 v)$

$\equiv A_c R_c/L_c$, and v_c is in es e, ϵ_0, ϵ_c, κ, and v_c trating the magnitudes oelectric elements are

DATA FOR

r is greater than one l thermal conductivity n above the "classical" relaxation mechanism ed, "icelike," structure lume. The relaxation the accessible experi-., above 10^9 Hz, and at "low" frequencies e [1955], investigating n, obtained data that ater. Although Hall's n two possible crystal-nal and Fowler [1933],

which is no longer favored because of the implied rigidity of the structures), calculations based on it are equally applicable to more recent models for water, wherein one of the possible molecular states is an unbonded state, permitting the water molecule to engage in more or less free rotation. These models include the flickering cluster model of Frank and Wen [1957] and Némethy and Scheraga [1962], the "significant structure" theory of Marchi and Eyring [1964], the clathrate model of Claussen [1951*a*, 1951*b*, 1951*c*], and Pauling and Marsh [1952], and the vacant-lattice point model of Samoilov [1946, 1957*a*, 1957*b*] and Forslind [1952, 1954]. These theories treat specific molecular arrangements for which certain water molecules participate in fewer than four hydrogen bonds. Discrete changes of energy associated with the formation or rupture of hydrogen bonds are envisaged. In contrast to this view, Lennard-Jones and Pople [1951] proposed a diffuse-continuum model in which hydrogen bonds are not broken but are distorted by increases in the total energy of a lattice of water molecules. Increase of temperature is considered to destroy the icelike lattice and to establish an irregular arrangement of molecules at distances greater than a few molecular diameters. This model conforms particularly well with the results of spectroscopic experiments which distinctly favor a continuum of energetic states to describe the structure of water. Spectroscopic data have been used by Stevenson [1965] to show that the concentration of monomeric water (having all hydrogen bonds broken) is much smaller than the value predicted by Némethy and Scheraga. No current theory of the structure of water is able to account satisfactorily for all available experimental data, and a likely compromise appears to be a model comprising several "smeared-out" energy levels, i.e., a continuum exhibiting several maxima in populations at certain energies. A review of theories of the structure of ice, liquid water, and ionic solutions has been published by Kavanau [1964].

Increasing the temperature of water from 0°C causes breakdown of the open, higher-energy, icelike structure to form a greater concentration of more favored, lower-energy, close-packed water structures. Both structures are, of course, subject to normal thermal expansion with increasing temperature. The ultrasonic absorption resulting from the perturbation of the distribution of water molecules between the allowed structures is shown in Fig. 17 as a function of temperature. The temperature dependence of the absorption coefficient is due to a combination of two effects, the relative importance of which is unknown: firstly, the response by varying the concentration of water molecules in the different structural states, which is greater at low temperatures as compared with higher temperatures; and, secondly, the temperature dependence of the relaxation time for the structural reorganization. Dielectric-constant measurements indicate that the relaxation time of the cluster-forming and dissolution process of the model due to Frank and Wen would have a mean value of 10^{-10} to 10^{-11} s (Collie, Hasted, and Ritson,

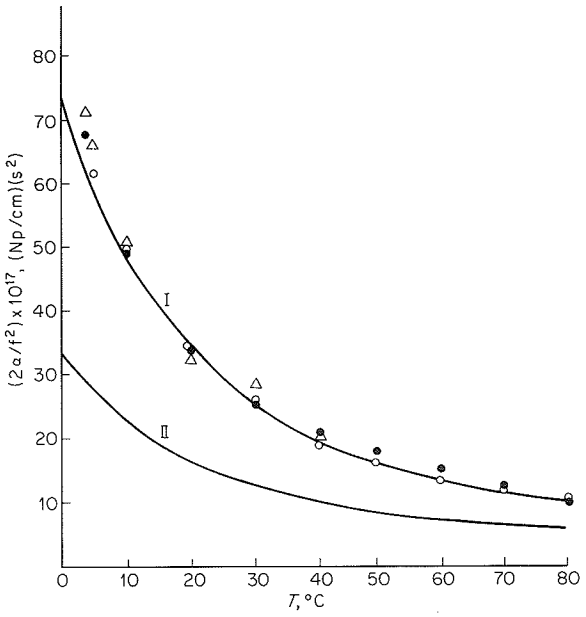

FIG. 17. Absorption parameter $2\alpha/f^2$ for water as a function of temperature. Curve I: Hall's theory for structural absorption. Curve II: contribution B due to shear viscosity. Points are experimental absorption values less the magnitude B due to shear viscosity. (*After Hall*, 1948.)

1948). This is at least consistent with the observation that the relaxation frequency is much higher than the ultrasonic range presently accessible to measurement.

One consequence of the competing processes of structural change and thermal expansion is the minimum in the specific volume of water at 4°C. Since change of temperature is not accompanied by change of volume at this temperature, it follows conversely that change of pressure will not be accompanied by change of temperature, and therefore that sound waves propagate isothermally in water at 4°C (also, $\gamma = 1$ and $\beta_T = \beta_S$). At higher temperatures isothermal conditions will be maintained approximately in water and dilute aqueous solutions up to normal room temperatures and beyond, the usefulness of this simplification depending on the degree of approximation that is acceptable in specific cases. Consequently, the interpretation of ultrasonic absorption data on aqueous solutions may frequently be restricted to consideration of structural relaxation processes responding to the pressure perturbation only. However Andreae et al. [1965] have argued that this simplification is not always permissible.

Another feature of the properties of water is the existence of a minimum in the product of density and adiabatic compressibility at approximately

74°C. The velocity
a maximum at thi
exhibited by dilute a
velocity may be redu
in the structural brea
and comparable data
of amino acids in w
precisely by McSki
Grosso et al. [1954].

Organic Solvents

Although solution
macromolecules in s
represent those part
which tend to assum
their immediate en
groups would be a n
therefore be made o
solvents in ultrasoni
as carbon tetrachlo

FIG. 18. Propagation v
as a function of tempera

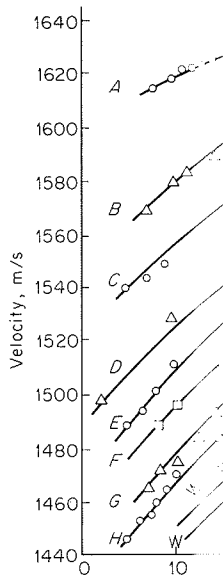

74°C. The velocity of sound propagation in pure water therefore exhibits a maximum at this temperature (Willard, 1947). Similar behavior is exhibited by dilute aqueous solutions although the temperature of maximum velocity may be reduced by the presence of the solutes, since the latter assist in the structural breakdown of water. Figure 18 shows the data of Willard and comparable data obtained by Barrett [1966] on water and eight solutions of amino acids in water. The velocity in water has been measured most precisely by McSkimin [1965], Greenspan and Tshiegg [1957], and Del Grosso et al. [1954].

Organic Solvents

Although solutions in water or saline will serve as models for biological macromolecules in some physiological situations, they are not adequate to represent those parts of the macromolecules which are hydrophobic and which tend to assume conformations permitting the exclusion of water from their immediate environment. A model solvent for such hydrophobic groups would be a nonpolar organic solvent such as hexane. Mention must therefore be made of the behavior to be expected from the use of organic solvents in ultrasonic absorption experiments. Unassociated liquids, such as carbon tetrachloride, benzene, the halogen derivatives of these two

FIG. 18. Propagation velocity in water and aqueous solutions of amino acids at 45 MHz as a function of temperature. (*After Barrett*, 1966.)

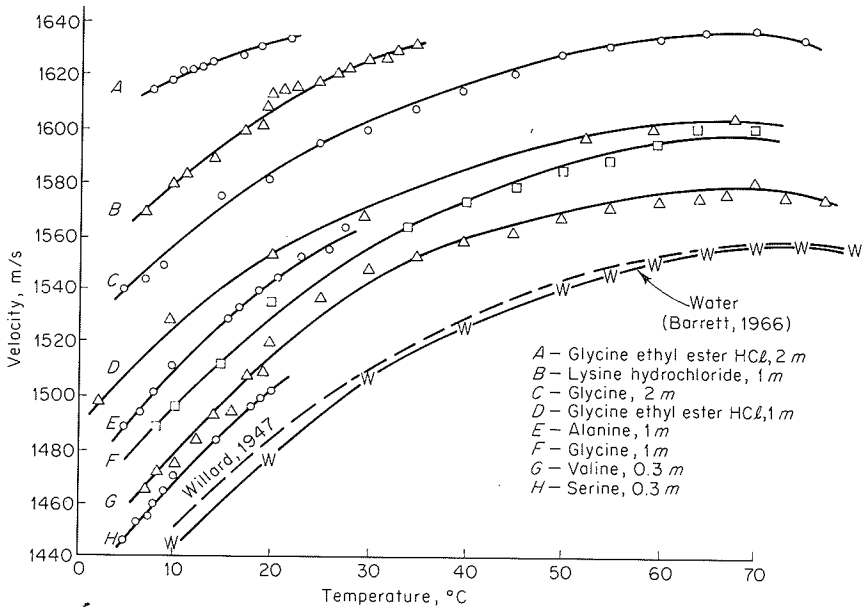

compounds and carbon disulfide, exhibit very high absorption coefficients for ultrasound—two or three orders of magnitude larger than that expected for classical (viscous) absorption. They are therefore particularly unsuitable as solvents in liquid systems for which comparatively small changes in the absorption coefficient must be detected, measured, and interpreted in terms of the properties of a solute species. However, some measurements on solutions of polypeptides in chloroform have been carried out by Zana, Candau, and Cerf [1963].

The cause of the high absorption coefficient for the unassociated liquids is the mechanism of energy transfer between translational states and internal vibrational modes of the molecules (Kneser, 1947*b*). Transitions between states of rotational isomerism may also cause significant contributions to the absorption coefficient of organic solvents (de Groot and Lamb, 1957). Good agreement is found between the vibrational specific heat and the magnitude of the absorption below the relaxation frequency, and also between the magnitudes of barrier heights to rotation calculated from ultrasonic and other techniques.

Hexane and similarly saturated hydrocarbons exhibit free rotation and correspondingly small values of absorption.

Acetic and propionic acids also exhibit extremely high absorption-coefficient values at frequencies below about 50 MHz. In this case the mechanism responsible is thought to be the dissociation of the dimer species which is present in the liquid state (Freedman, 1953; Lamb, 1965).

The absorption coefficients of many organic solvents are tabulated by Heasell and Lamb [1956*a*] and Schaafs [1967].

Solutions

Nonelectrolytes

Alcohols can associate with water by hydrogen bonding, and therefore a small mole fraction of alcohol in water causes serious disruption of the water structure, with consequent influence on the value of the absorption coefficient. The concentration dependence of the absorption of a mixture of water and ethyl alcohol displays a peak at 0.25 mole fraction alcohol (Storey, 1952). Evidently a solution of this composition yields a maximum concentration of a reacting species such as that resulting from the association of one ethyl alcohol molecule with four water molecules. The absorption parameter α/f^2 increases in magnitude on approaching 0°C from higher temperatures, and as the frequency decreases in the frequency range 10 to 100 MHz. Similar results have been found for methyl, propyl, isopropyl, and tertiary butyl alcohols in water (Burton, 1948) and in aqueous solutions of amines (Andreae, Edmonds, and McKellar, 1965). A maximum value is also found in the concentration dependence of the velocity of propagation.

This maximum occurs at lower concentrations of the solute species than the maximum in absorption, and is caused by the rapid breakdown in water structure and consequent minimum value in the product of density and compressibility caused by introduction of the solute. Association by hydrogen bonding between solute and water at unpaired electron sites on nitrogen and oxygen atoms is believed to produce a mechanism for the relaxational absorption observed in all these cases.

Hammes and Knoche [1966] studied mixtures of water and dioxane over the entire composition range at 10 to 25°C, and over the frequency range 10 to 200 MHz. The data were consistent with the supposition that hydrogen-bonded complexes of dioxane and water were participating in the equilibria perturbed by the ultrasonic wave. The two-step mechanism, $2W + D \rightleftharpoons DW_2$, $D + DW_2 \rightleftharpoons D_2W_2$, where $D \equiv$ dioxane and $W \equiv$ water, was analyzed and yielded standard volume and enthalpy changes for both reactions of approximately ± 1 cm^3/mole and ± 1 kcal/mole.

Hammes and Lewis [1966] have performed measurements on aqueous solutions of polyethylene glycol (molecular weight 20,000) and have observed absorption attributed to hydrogen bonding and conforming to a single relaxation process located at 21 MHz for a 1.20 *m* solution at 10°C. Further work by Hammes and Schimmel [1966] disclosed that the relaxation time decreases sharply if urea is added to the solution in concentrations between 2.0 and 4.0 *m*. The change is attributed to cooperative breakdown in the local water structure around the polymer molecules, probably accompanied by increased solvation. Aqueous solutions of urea alone show no relaxational behavior at concentrations up to 8.0 *m*.

The hydrogen bond energies associated with such reactions are smaller than the often-quoted value of about 5 kcal/mole (Pauling, 1940), since in the cases under consideration the solvent and the solute species are competing for the formation of hydrogen bonds (Klotz, 1960, 1962). Schellman [1955] deduced a value of 1.5 kcal/mole for the net enthalpy of formation of the hydrogen bond in the backbone of proteins in an environment of water. This value has been used by Némethy, Steinberg, and Scheraga [1963] in their study of hydrogen-bonding interactions of side chains of proteins.

Nonaqueous miscible liquids

Nonaqueous mixed solvent systems have occasionally been used. The behavior of the mixture in an ultrasonic absorption experiment depends primarily on the tendency of the liquid species to associate. Mixtures of two unassociating liquids exhibit an absorption coefficient at all intermediate concentrations which is less than the linearly interpolated value between the absorption coefficients of the pure constituent liquids. This reduction in absorption is due to the increased efficiency of transferring energy between

translational and vibrational modes, which is characteristic of collisions between unlike molecules in comparison with collisions between like molecules. Therefore the very high absorption coefficient of pure unassociated liquids may sometimes be reduced by adding an appreciable fraction of a second liquid with which it is miscible in all proportions, e.g., toluene to benzene, acetone to chloroform.

Some mixtures of associated liquids with highly absorbing unassociated liquids exhibit an initial increase in the value of the absorption coefficient with increased concentration of the associated liquid, a peak in the absorption value, and then a decrease with further addition of the associated liquid, e.g., phenol in carbon tetrachloride or cyclohexane.

For liquid mixtures that are not completely miscible in all proportions, phase separation is possible, and exceedingly high absorption is observed in the vicinity of the transition point (see page 297).

Some mixtures of highly associated liquids exhibit a minimum in the absorption coefficient as a function of concentration. These are probably systems for which the ultrasonic wave is perturbing a structural relaxation mechanism in one or both liquids, and the presence of a second molecular species increases the transition probabilities.

A comprehensive review of absorption in liquids and liquid mixtures has been presented by Sette [1961]. See also Schaafs [1967].

Aqueous electrolytes

Very extensive measurements of ultrasonic absorption and velocity of propagation have been made on electrolytic solutions, and the reader is referred to three reviews on the subject for detailed information (Stuehr and Yeager, 1965; Eigen and de Maeyer, 1963; Tamm, 1961). A qualitative summary of possible relaxational processes in electrolytes is called for, however, since these are fundamental for consideration of processes that may occur at charged sites on macromolecules. Introduction of simple ionic solutes into water causes disruption of the water structure and formation around the ions of hydration shells composed of water molecules experiencing electrostriction. The velocity of sound propagation normally increases with increasing concentration of ionic solute, but in exceptional cases of heavy metal salts, it may show an initial decrease and subsequent increase after passing through a minimum. The temperature dependence of the sound velocity shows a maximum that can be depressed as much as 25° below the value of 74°C characteristic of pure water. Measurement of the compressibility by a determination of sound velocity is one of several methods of estimating the number of water molecules that are bound to ions to form the hydrated structure (Conway and Bockris, 1954). The number of hydrating molecules thus determined depends rather critically upon the model and assumptions used. The lack of agreement among various methods is an

unsatisfactory feature of such calculations, making it desirable to restrict quantitative considerations to the primary hydration shell.

The absorption coefficient of electrolytic solutions is not significantly different from that of the solvent, water, in the cases of uni-univalent (1-1-) electrolytes of high ionic charge density. Electrolytes for which at least one of the ions is singly charged show negligible excess absorption at frequencies below 10 MHz. Electrolytes for which both the ions are multiply charged show excess absorption by as much as three orders of magnitude in the frequency range from 10 kHz to 100 MHz, and apparently continue to exhibit high absorption at higher and lower frequencies also. 2-2-Electrolytes have been most extensively investigated in connection with the cause of the high absorption of seawater, for which the magnesium sulfate content is primarily responsible. Tamm [1961] has also discussed the probable mechanism of the dissociation of nonhydrolyzing salts, associated with relaxation frequencies above 300 MHz. Figure 19 shows a summary of the extensive data obtained by Tamm and coworkers.

Reactions between ions are responsible for all the significant absorption processes in electrolytes, in contrast to reactions involving ions and the water molecules individually. This is the case since the process of simple hydration of a single ion proceeds too rapidly and would be common to all electrolytes, including those 1-1-electrolytes for which negligible excess absorption has been observed. Also, relaxation of the ionic atmosphere (Debye and Hückel, 1923) may be excluded since the contribution to the absorption was shown to be negligibly small by Eigen [1957].

The reactions occurring between ions, which are responsible for the absorption, have been classified as follows:

1. *Proton transfer processes.* (*a*) *Hydrolysis*, involving ionization of water and then association of either the hydrogen or hydroxyl ion, or both, with the solute species, with consequent partial or complete charge neutralization; (*b*) *ionization*, involving ionization of uncharged solute species or of charged ionic solute species to a higher degree of ionization.

   Such ionization and hydrolysis reactions are exhibited by solutions of weak acids and of salts of weak acids, respectively, and the reactions are coupled so that the equilibrium constants are related (Stuehr and Yeager, 1965). If K_I is the equilibrium constant for the hydrolysis reaction (I), K_{II} is the dissociation constant for water, and K_{III} is the dissociation constant for the weak acid HB, then

$$K_I = K_{II}/K_{III} \tag{94}$$

$$\begin{array}{ccc} \mathrm{HOH} + \mathrm{B^-} & \overset{\text{(I)}}{\rightleftharpoons} & \mathrm{OH^-} + \mathrm{HB} \\ \text{(II)}\ \diagdown\!\!\diagdown & & \diagup\!\!\diagup\ \text{(III)} \\ \mathrm{OH^-} + & \mathrm{H^+} & + \mathrm{B^-} \end{array}$$

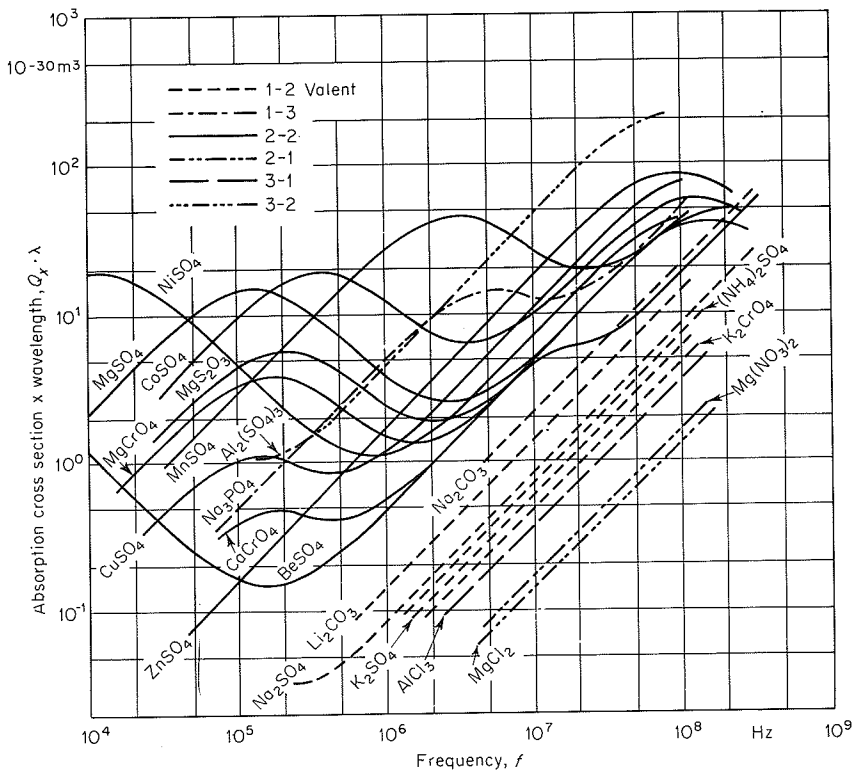

FIG. 19. Absorption cross section per wavelength for electrolytes. The ordinate is the intensity absorption coefficient per molecule $Q_a\lambda = 2(\alpha_r\lambda) \times (M_L/10c'N_L)$, where M_L is molecular weight and N_L is Avogadro's number. (*After Tamm, Kurtze, and Kaiser*, 1954.)

FIG. 20. Diagrammatic representation of complex ion formation in 2-2-electrolytes. (*a*) Complex of hydrated iron. (*b*) Intermediate structure. (*c*) Hydrated complexion. (*After Eigen.*)

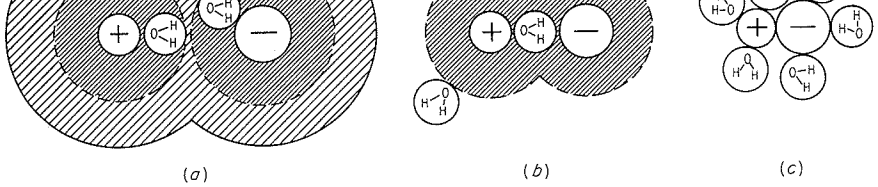

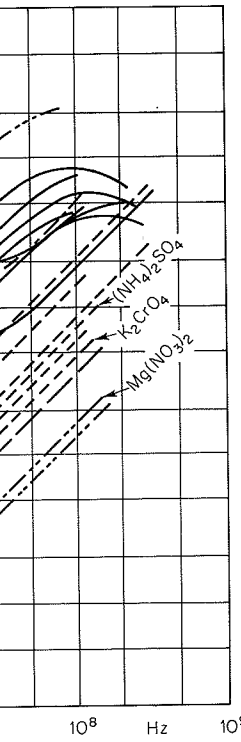

ctrolytes. The ordinate is
$\alpha_r\lambda) \times (M_L/10c'N_L)$, where
(After Tamm, Kurtze, and

formation in 2-2-electrolytes.
re. (*c*) Hydrated complexion.

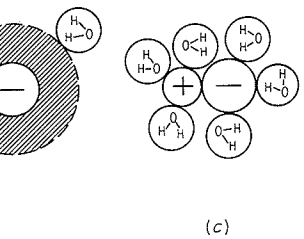

(*c*)

2. *Ionic association-dissociation processes.* On ionic association, intervening water molecules must be displaced with disruption of hydration shells but with retention of the identity of individual charged species in the formation of a complex ion pair. This process is responsible for the double relaxation observed in solutions of 2-2-electrolytes. It is illustrated symbolically by Eq. (95) and diagrammatically in Fig. 20 (Tamm, 1961). Additional experimental results for aqueous magnesium sulfate solutions, showing more detail than is apparent in Fig. 19, have been obtained by Smithson and Litovitz [1956] and by Atkinson and Kor [1965]. Their data exhibit relaxation frequencies at approximately 3 and 30 MHz, while Fig. 19 shows a third relaxation process to be operative at frequencies above 200 MHz. These results support the three-step mechanism shown in Eq. (95):

$$(M^{2+})_{aq} + (A^{2-})_{aq} \underset{k_{21}}{\overset{k_{12}}{\rightleftharpoons}} [M^{2+}(OH_2)(OH_2)A^{2-}]_{aq} \underset{k_{32}}{\overset{k_{23}}{\rightleftharpoons}} [M^{2+}(OH_2)A^{2-}]_{aq} \underset{k_{43}}{\overset{k_{34}}{\rightleftharpoons}} (M^{2+}A^{2-})_{aq} \quad (95)$$

Before reaction, the ions M^{2+} and A^{2-} are present as hydrated species, a state represented by the subscript *aq*. Water molecules beyond the first hydration shell will be associated comparatively loosely with the ions and will be displaced easily from the region between the approaching hydrated ions. This represents the diffusion-controlled first step, probably associated with the high-frequency relaxation in the neighborhood of 200 to 300 MHz, shown in Fig. 19 as an anticipated peak in the data at frequencies above 100 MHz. The second step involves the displacement of one of the water molecules from the primary hydration sheath of one ion with the production of a structure in which one water molecule is common to the primary sheaths of both anion and cation. The water molecule displaced would be expected to come from the hydration sheath of the anion since the interaction of the cation with surrounding water molecules is usually stronger than that of the anion. In magnesium sulfate solutions this reaction displacing the penultimate water molecule is almost certainly associated with the relaxation process exhibited at a frequency of about 30 MHz. The final stage in formation of the complex ion comprises removal of the last water molecule from the region of the primary sheath between the ions, and this step is related most probably to the low-frequency relaxation exhibited by 2-2-electrolytes, occurring in the frequency range near 3 MHz.

Other systems involving complex ion formation by means of chelation have been investigated by Eigen [1963] and Maass [1962].

In interpreting multistep relaxation processes of the type just described, it is important to note that the number of relaxation times corresponds to the number of steps, but each relaxation time does not necessarily correspond to a particular step. One-to-one correspondence between a step and a relaxation time can only be expected where the relaxation times are separated by two or more orders of magnitude. Association of one relaxation time with the fastest step in a sequential reaction scheme may be possible, but, in general, the relaxation times are related in a complex manner to the rate constants for individual steps. For example, in the general two-step case (Stuehr and Yeager, 1965),

$$X_1 \underset{k_{21}}{\overset{k_{12}}{\rightleftharpoons}} X_2 \underset{k_{32}}{\overset{k_{23}}{\rightleftharpoons}} X_3$$

the relaxation times are given by

$$\left.\begin{matrix}\tau' \\ \tau''\end{matrix}\right\} = 2[\zeta \pm (\zeta^2 - 4\chi)^{1/2}]^{-1} \tag{96}$$

where

$$\zeta \equiv k_{12} + k_{21} + k_{23} + k_{32}$$

$$\chi \equiv k_{12}k_{23} + k_{12}k_{32} + k_{21}k_{32}$$

and the k's are individual rate constants.

Extensive data on rate constants have been tabulated by Eigen et al. [1964] for many reactions of fundamental importance.

Amino acids and peptides

Amino acids will be considered first since they are elementary organic solute molecules of biological significance. When dissolved in water without additional ionic constituents to influence the state of charge of the amino acid, the solution exhibits a magnitude of the absorption parameter, α/f^2, which varies only slightly with frequency in the megahertz range, and differs only slightly from that of the solvent water (Barrett, 1966) (Fig. 21). If a a 0.5 M solution of glycine is brought to pH 10 by addition of sodium hydroxide, then the relaxational behavior which is observed can be described by a single relaxation frequency in the vicinity of 25 MHz. Figure 22 shows data taken at a temperature of 22°C (Maass, 1962; Eigen and Hammes, 1963). Table 10 shows numerical data for overall rate constants of association and dissociation taken from the review by Eigen et al. [1964]. The mechanism of relaxation in the solutions of glycine, dimethylglycine, and sarcosine (*N*-methylglycine) is attributed to the hydrolysis equilibrium, mentioned on page 277.

$$H^+RCOO^- + OH^- \rightleftharpoons RCOO^- + H_2O \tag{97}$$

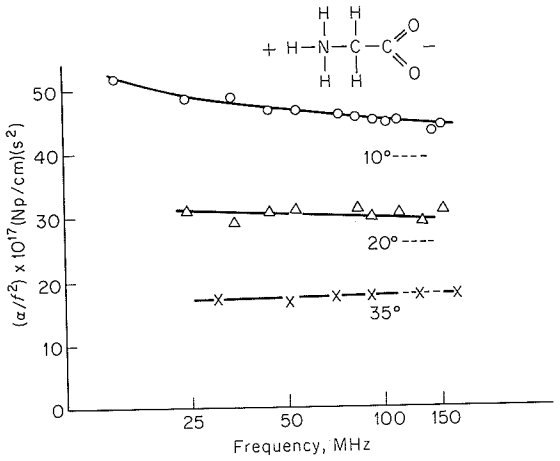

FIG. 21. Absorption parameter α/f^2 for glycine solutions (ionic strength = 0) as a function of frequency and temperature. 2.0 *m*: 10°C ○, 20°C △ (*after Barrett*, 1966); and 1.0 *m*: 35°C × (Edmonds, unpublished). The estimate of the uncertainty for each point is shown at the right. Dashed lines show the frequency-independent value for water at each temperature.

Such equilibria therefore constitute one of a number of mechanisms that may be effective in accounting for the ultrasonic absorption of more complicated macromolecules in aqueous solution when such macromolecules are composed of amino acid residues with side chains capable of participating in hydrolysis reactions. See also Parker et al. [1968].

FIG. 22. Molar absorption per wavelength of solutions of glycine and derivatives at 22°C. The parameter on the curves is the molar concentration. Ionic strength is 0.5. (*After Maass*, 1962, *and Eigen and Hammes*, 1963.)

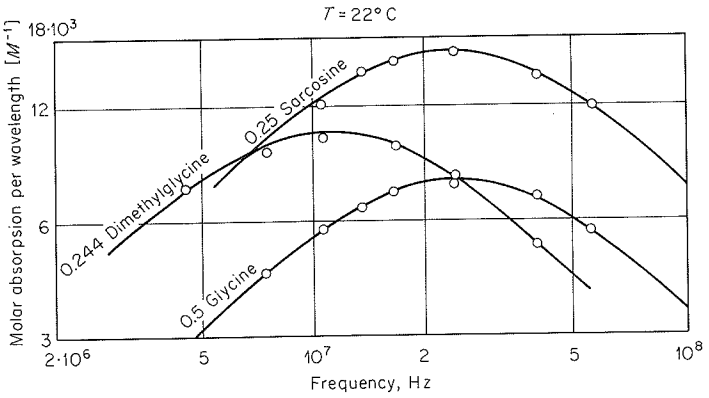

TABLE 10. RATE CONSTANTS OF HYDROLYSIS REACTIONS, 22°C (AFTER EIGEN et al., 1964 AND MAASS, 1962)

Material	*Ionic strength*[a]	$10^{-10}\,k_f$ (mole $^{-1}$ s^{-1})[b]	$10^{-5}\,k_b$ (s^{-1})[c]
Glycine	0.5	1.4	8.4
Sarcosine (*N*-methylglycine)	0.25	1.1	18.0
Dimethylglycine	0.25	0.73	6.5

[a] Ionic strength $= \frac{1}{2}\Sigma\, c_i z_i^2$, $c_i \equiv$ molar concentration of ith ion, $z_i \equiv$ valency of ith ion
[b] $k_f \equiv$ overall rate constant of association
[c] $k_b \equiv$ overall rate constant of dissociation

Amino acids in water solution may be considered also according to their action of structure making or breaking in the solvent. In neutral solution the amino acids are present as doubly charged molecules (zwitterions) and are susceptible to dissociation and recombination reactions on change of the environment. Hydrogen-bonding sites are located on both the amino and carboxyl groups, while the side chain may be acidic, nonpolar, or basic. The potentialities for breaking or making water structure in the vicinity of the solute molecules are therefore considerable.

Breaking the water structure will result in an increase in the concentration of less-bonded water molecules which form a closer-packed and less compressible structure, recognized by an increase in the velocity of sound propagation. Such an effect is observed for all the amino acids studied by Barrett, namely, glycine, alanine, serine, valine, glycine ethyl ester hydrochloride, lycine hydrochloride, and glutamic acid (Fig. 18). Other measurements of the velocity of propagation and, hence, of the compressibility, of aqueous solutions of amino acids have been made by Passynsky [1947], Gucker and Haag [1953], Goto and Isemura [1964], and Barrett [1966]. The presence of predominantly hydrogen-bonding solute species, for example, glycine, may increase the concentration of relatively unbonded water molecules in secondary hydration regions, and such molecules would become available to participate in the transition between icelike (bonded) and unbonded water:

$$(H_2O)_{\text{bonded}} \rightleftharpoons (H_2O)_{\text{unbonded}} \tag{98}$$

This mechanism suggested by Barrett could result in an increase in the measured absorption (supposedly due to the above transition), on the assumption that the presence of the glycine does not increase the transition probabilities of this reaction. An alternative approach is to consider that the transition probabilities and hence the rate constants of the reaction (Eq. 98) are affected by the presence of solutes (Stuehr and Yeager, 1965). If the transition probabilities were substantially influenced and reduced, then the relaxation frequency for the transition between bonded and unbonded water

would be increased with a consequent reduction in the absorption measured at much lower frequencies. Depression of the absorption coefficient below the value for water has been observed in aqueous solutions of potassium and sodium acetates, bromides, and iodides (Barrett, Beyer, and McNamara, 1954; Kurtze and Tamm, 1953) and in glycine ethyl ester hydrochloride (Barrett, 1966). The effect is evidently produced by the presence of anions of low charge density which have a small electrostrictive action on the surrounding water molecules.

These results for solutions that depress the value of the absorption coefficient at higher frequencies disclose the possibility of significant errors' arising in the interpretation of ultrasonic absorption data for other solutions. It is not justified to assume without qualification that the absorption attributable to the solvent phase of a solution is the same as that of the pure solvent, nor to derive under such assumption the "absorption coefficient" of the solute from a simple mixing formula. The potential error in ascribing the difference, $(\alpha\lambda)_{\text{solution}} - (\alpha\lambda)_{\text{solvent}}$, to absorption by the solute becomes progressively greater as the frequency increases. The preferred procedure, though more exacting experimentally, is to make measurements at sufficiently high frequencies so that $(\alpha/f^2)_\infty$ for the solution may be determined. Then the effective solute absorption at any lower frequency will be given by $\alpha/f^2 - (\alpha/f^2)_\infty$. This is discussed further on page 291.

Polypeptides

Ultrasonic absorption by an aqueous solution of a polypeptide may be related to any or all of four possible mechanisms: proton transfer, helix-coil transition, solvation, and relaxation of the shear viscosity. Major interest has tended to be focused on the helix-coil transition because of its significance as a constituent process in protein denaturation.

Accurate and comprehensive measurements of ultrasonic attenuation in polyglutamic acid solutions have been made by Burke, Hammes, and Lewis [1965]. Their measurements extend over the frequency range of 6 to 175 MHz and the pH range of 5.4 to 9.0 for a mixed solvent of aqueous sodium chloride and dioxane. Their data refer to 25°C and exhibit a distribution of relaxation times under all conditions, with a tendency to approach a single relaxation time at the highest value of pH. The molecular weight of their sample was 75,000, and the concentrations employed were 3 and 1.5 percent, corresponding to molalities of the monomer of 0.24 and 0.12, respectively (3.53 and 1.77 g monomer/100 ml). The accuracy of individual measurements of absorption was ±2 percent, except at lower frequencies where it was worse.

Typical data of ultrasonic absorption as a function of frequency in 3.53 g polyglutamic acid/100 ml solution in 2 parts 0.2 *M* NaCl (aqueous) + 1 part

dioxane at 25°C and various pH values are shown in Fig. 23, where they are compared with the dashed line based on a single relaxation time. The absorption values were smaller than the classical absorption calculated from shear viscosity at zero frequency, indicating that shear-viscosity relaxation had occurred at lower frequencies. A single value of the sound velocity, 1.59×10^5 cm/s, was reported for all values of pH and both concentrations. In this regard it should be noted that resolution of the very small velocity dispersion would not be expected.

The mechanism preferred by Burke, Hammes, and Lewis to account for the distribution of relaxation times is the interaction of solvent and polymer involving a breakdown of the water structure around the polypeptide and solvation of the latter by the water. Subsidiary experiments indicated that the solvating species was more probably water than dioxane. The alternative mechanisms of interest in this system, namely, helix-coil transition and protolytic reactions, were regarded as contributing only to a minor extent in the response to ultrasonic perturbation.

According to Schwarz [1965], the mean relaxation frequency for the helix-coil transition in polyglutamic acid might be expected to lie around 2 MHz, and so a broad spectrum of relaxation times centering around the value 8×10^{-8} s would be anticipated. However, a single relaxation function with *mean* relaxation time τ^* will approximate the behavior as long as the

FIG. 23. Absorption parameter α/f^2 as a function of frequency for 0.24 *m* poly-L-glutamic acid solutions at 25°C and various pH. The dashed curve corresponds to a single relaxation curve. (*After Burke, Hammes, and Lewis*, 1965.)

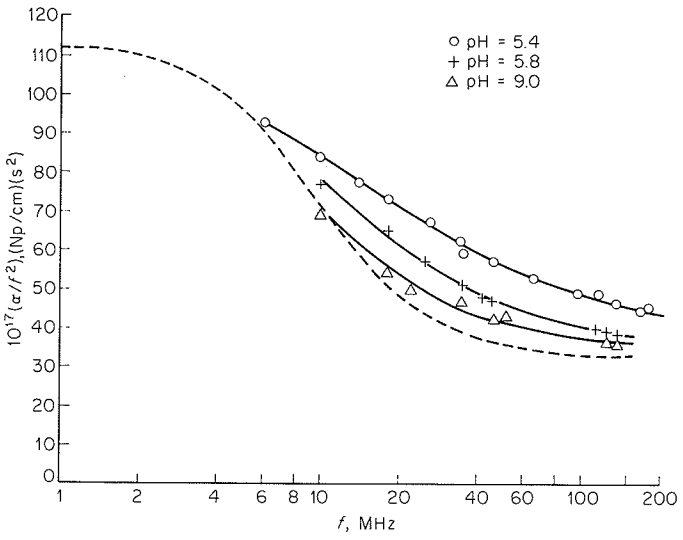

period of the perturbation is small compared to τ^*, e.g., for frequencies higher than about 20 MHz. The helix-coil transition is known to occur in the region pH $\simeq$ 6 (Doty, Wada, Yang, and Blout, 1957). Zana et al. [1963, 1966] have claimed its detection by an unorthodox ultrasonic technique at frequencies below 10 MHz. Wada, Sasabe, and Tomono [1967] have measured the complex shear viscosity, at 50 kHz, of polyglutamic acid in the same solvent as Burke, Hammes, and Lewis. Their results, shown in Fig. 24, indicate a substantial variation of the imaginary part of the shear viscosity near pH 6, which was attributed to the helix-coil transition. Their estimate of the *maximum* relaxation time was about 10^{-6} s, in rough agreement with a result calculated from Schwarz' theory. These authors consider compressional wave experiments in the megahertz frequency range to be inappropriate for investigation of the helix-coil transition mechanism, since they have observed solutions of polyglutamic acid and glutamic acid to behave similarly in such experiments. Glutamic acid can form neither helix nor coil configurations.

Nevertheless, Parker, Slutsky, and Applegate [1966, 1968] have obtained compressional wave data which they attribute to the helix-coil transition. Their measurements were made on solutions of poly-L-lysine of weight-average molecular weight 86,300 in 0.6 *M* sodium chloride (aqueous). Figure 25 shows their data at 35.8°C and at a polymer concentration of 2.0 g/100 ml. The data were fitted satisfactorily to curves described by single relaxation times. Each possible mechanism was examined for its ability to account for the observed absorption. The principal difference between solutions of polylysine and polyglutamic acid is the greater likelihood that proton transfer reactions would be significant in the former. The volume change for protonation of an amino group —NH_2 is considerably larger than

FIG. 24. Real and imaginary parts of complex shear viscosity at 50 kHz for a solution of polyglutamic acid at 22°C. Solvent viscosity = 2.6×10^{-2} poise. (*After Wada, Sasabe, and Tomono*, 1967.)

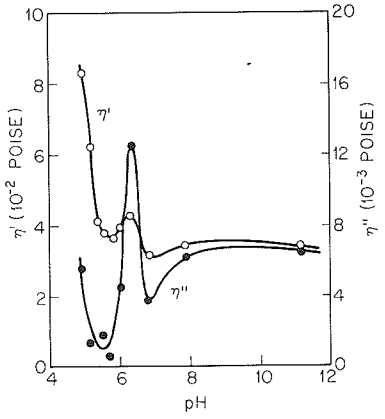

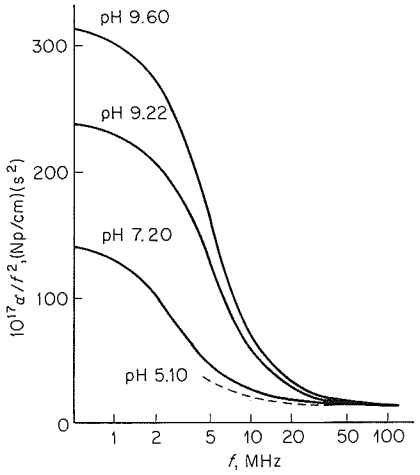

FIG. 25. Ultrasonic absorption as a function of frequency in 0.156 M (moles of monomer per liter) poly-L-lysine solutions in 0.6 M NaCl at 35.8°C and various values of pH. Solid lines are least-square fits to the single relaxation equation. The classical value of α/f^2 is 16.1×10^{-17} (Np/cm)(s^2). (*After Parker, Applegate, and Slutsky*, 1966.)

that for a carboxyl group COO^-. Nevertheless, this mechanism could be rejected because an unreasonably large volume change, associated with too small a backward rate constant, would have been required. The solvation mechanism could not be so conclusively eliminated, but evidence was presented to show that it was less satisfactory than the helix-coil mechanism. The volume changes deduced for the latter are given in Table 11. Figure 26 shows the fraction f_H of polymer present in the helical form as deduced from measurement of the optical rotation.

Measurements of absorption of polypeptides in nonaqueous solution have been carried out by Zana, Candau, and Cerf [1963] in the range of 1.7 to 20 MHz by the interferometric technique on solutions of poly-L-benzyl glutamate, poly-DL-benzyl glutamate and poly-L-benzyl aspartate in chloroform or a mixture of chloroform and dichloroacetic acid as solvents. Their

TABLE 11. ULTRASONIC ABSORPTION PARAMETERS FOR THE HELIX-COIL TRANSITION OF POLYLYSINE (AFTER PARKER et al., 1966)

pH	$10^8 A/\tau$ (s/cm)	$10^8 \tau$ (s)	ΔV (cm^3/mole)	f_H
9.60	8.82	3.39	6.2	0.146
9.22	6.90	3.21	7.6	0.068
7.20	2.27	5.66		<0.03

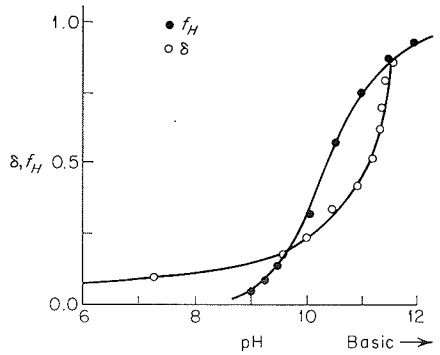

FIG. 26. Degree of dissociation (δ) and fraction of polymer present in helical form (f_H) for poly-L-lysine in 0.6 *M* sodium chloride solution at 25°C. (*After Parker, Slutsky, and Applegate*, 1968.)

data must be regarded as preliminary; the rapid decrease in absorption in the range 1.7 to 4 MHz is now subject to correction and reinterpretation as a normal relaxation process. Bauer and Haessler [1968] have attempted to verify similar effects reported by the same authors for solutions of polystyrene in benzene and have found orthodox relaxational behavior.

Proteins, particularly hemoglobin

Measurements of the acoustic properties of hemoglobin solutions have been more comprehensive than those on any other solution of biological significance. The most accurate data are those obtained by Carstensen and Schwan [1959*b*] in the frequency range of 0.3 to 10 MHz. At lower frequencies, data have been obtained by Gramberg [1956] at 35 and 82 kHz and at higher frequencies by Edmonds [1962] in the range of 32 to 232 MHz. More recent unpublished data are also included on Fig. 30. In the case of hemoglobin solutions there is therefore some hope that the major portion of the frequency range of relaxational absorption may have been covered by experimental measurement. However, it will be seen that ambiguities in interpreting the data still exist.

Carstensen and Schwan [1959*b*] reported data obtained by the use of their fixed-path pulse transmission apparatus which has been described briefly

on page 254. Their measurements of the absorption and velocity of sound were performed under a variety of conditions which enabled them to study the effects of temperature, concentration, pH, and the presence of neutral salts. The data relate to solutions of oxyhemoglobin with a possible impurity amounting to no more than 20 percent methemoglobin. A specific experiment designed to show any difference in the absorption by these two forms of the protein exhibited none. Samples were obtained originally from blood specimens of horse, cattle, sheep, and human beings, from which the hemoglobin was liberated by treatment with toluene followed by centrifugation. Slight differences in the absolute magnitude of the absorption and its temperature dependence were observed for hemoglobins derived from the different mammalian species. Where specific data are given in the following figures and text, they refer to bovine hemoglobin unless otherwise stated.

Figures 27 and 28 show respectively the absorption per wavelength and the velocity of propagation as a function of frequency at 25°C as measured by Carstensen and Schwan [1959*b*]. The concentration of hemoglobin in the solution is shown as the parameter on the curves. A correction has been applied to the absorption data by assuming a simple mixing formula and subtracting from the measured data a contribution that is attributed

FIG. 27. Absorption per wavelength for bovine hemoglobin solutions in water at 25°C as a function of frequency and concentration. Dashed curves show the residual absorption after correcting for the presence of the solvent by a simple mixing formula. (*After Carstensen and Schwan*, 1959*b*.)

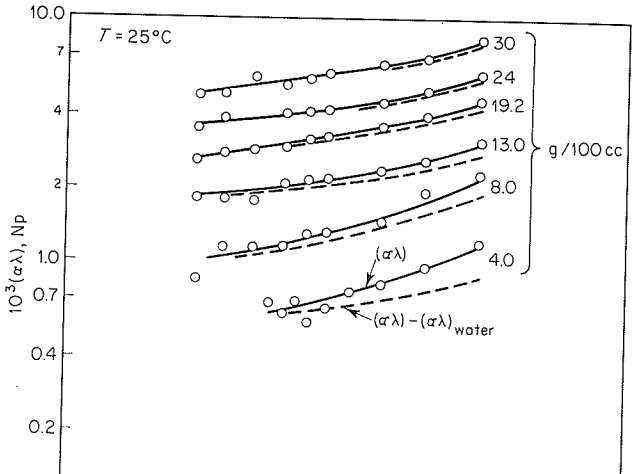

to the water alone
"simple water" an
of applying this co
the absorption attri
concentrations. Fu
to be proportional
higher concentratio
concentration, show
Hb/100 ml solution
it is reasonable to c
molecular species a
species in water. T
with the hypothesis
may be described in

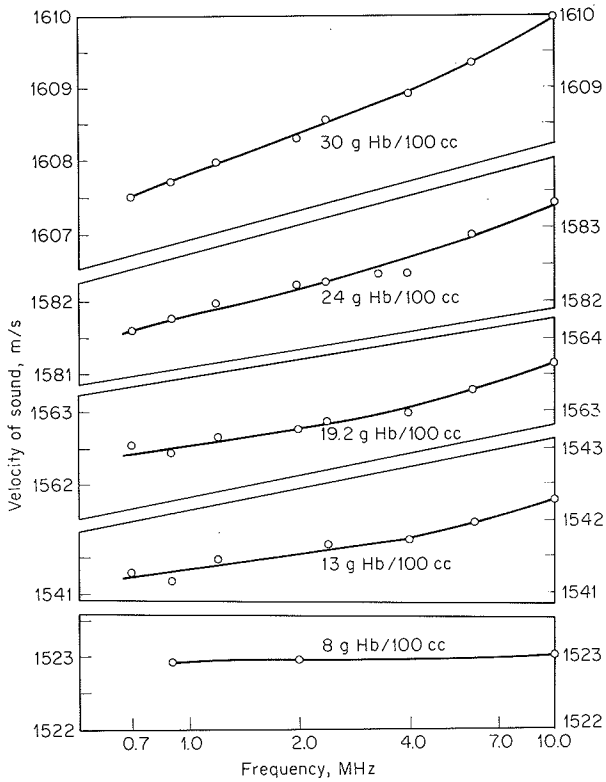

FIG. 28. Dispersion of the velocity in solutions of bovine hemoglobin in water at 25°C. (*After Carstensen and Schwan, 1959b.*)

to the water alone. The mixture is presumed to consist of the species "simple water" and the species "hydrated macromolecules." The result of applying this correction is to indicate that the frequency dependence of the absorption attributable to the hydrated macromolecule is the same at all concentrations. Furthermore, a reduced form of the data shows absorption to be proportional to concentration of hemoglobin up to 15 g/100 ml. At higher concentrations the absorption increases faster than linearly with concentration, showing a 20 percent excess at a concentration of 30 g Hb/100 ml solution. Therefore, to the limit of the linear proportionality, it is reasonable to discuss the absorption coefficient of the hydrated macromolecular species as though one were dealing with a dilute solution of the species in water. The dispersion of the velocity of propagation is consistent with the hypothesis that the excess absorption of the hydrated macromolecule may be described in terms of relaxation processes.

Since the solubility of hemoglobin in water is influenced by changes of pH, it was anticipated that the absorption should depend upon pH. However, no detectable effect was observed in the pH range from 6 to 9.4. Similarly, no detectable change in absorption was observed when the environment was a molar solution of NaCl or $(NH_4)_2SO_4$, neutral salts in which the solubility of hemoglobin is affected; these observations are similar to the behavior reported for glycine on page 280. Effects greater than the estimated experimental error of 5 percent would have been detectable, as is exemplified by the observed temperature dependence of absorption of hemoglobin solutions.

Figure 29 shows data obtained on human hemoglobin in a concentration of 16.5 g Hb/100 ml where the temperature varies from 7 to 35°C. It is apparent that the level of the plateau in absorption is shifted slightly to higher frequencies and lowered slightly on increase of temperature. Such a variation with temperature is consistent with the concept of a redistribution of relaxational processes, each exhibiting a temperature dependence determined by its energy of activation.

Two alternative procedures (instead of the application of a simple mixing formula) may be adopted in an attempt to isolate the relaxational contributions to the total measured absorption. One may either calculate the classical absorption coefficient from the static viscosity and the measured velocity of propagation, according to Eq. (30), and consider the classical absorption to be identical with the high-frequency absorption; or one may actually attempt to measure the absorption at sufficiently high frequencies to identify an asymptotic value. The former procedure assumes that relaxation of the viscous mechanism does not occur in the frequency range of interest, and at least in the case of polyglutamic acid, this assumption is invalid

FIG. 29. Influence of temperature change on solutions of human hemoglobin in water at concentration 16.5 g Hb/100 ml. (*After Carstensen and Schwan*, 1959*b*.)

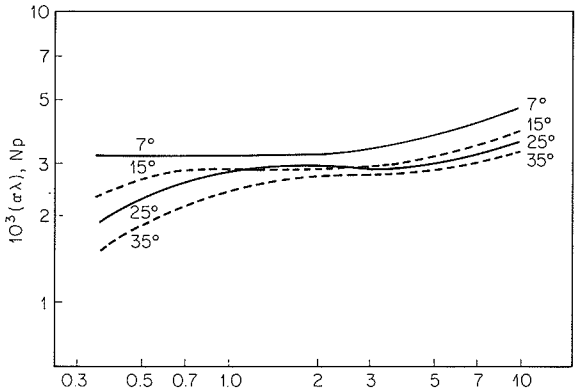

FIG. 30. Absorption
concentration 15 g H
measured value at hig

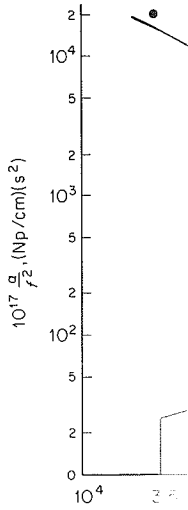

(Burke, Hammes,
Edmonds [1962]
(Np/cm)(s^2), appl
concentration of
value of α/f^2 has
470 MHz.‡ Thes
value (by subtrac
was made to deter
absorption. Afte
Fig. 31 results, wh
of concentration.
at high frequencie
spectrum at appro
on the magnitude
It must be borne
may possibly con
difficulties in the c

† Subsequent anal
nominally 15 g Hb, 10
in that communicati

‡ The authors are
University, Clevelan

FIG. 30. Absorption parameter α/f^2 for an aqueous solution of bovine hemoglobin at concentration 15 g Hb/100 ml and 25°C. The superscript ∞ refers to the asymptotic measured value at high frequencies and subscript v to Eq. (30).

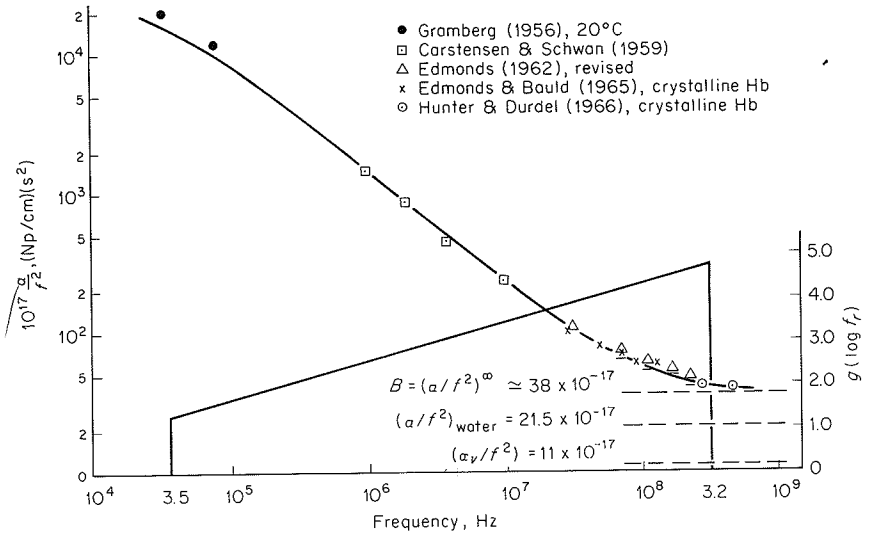

(Burke, Hammes, and Lewis, 1965). The latter procedure was adopted by Edmonds [1962] who obtained an asymptotic value of $\alpha/f^2 = 38 \times 10^{-17}$ (Np/cm)(s²), applicable to a solution of bovine hemoglobin in water at a concentration of 15 g/100 ml at a temperature of 25°C (Fig. 30).† This value of α/f^2 has been confirmed subsequently by measurements at 270 and 470 MHz.‡ These data are also shown in Fig. 30. Use of the asymptotic value (by subtraction from measured values of α/f^2 at lower frequencies) was made to determine the alleged relaxational contribution to the measured absorption. After conversion to absorption per wavelength, curve 1 of Fig. 31 results, where the data have also been reduced to become independent of concentration. Curve 1 shows a decreasing absorption per wavelength at high frequencies, and indicates an upper-frequency limit to the relaxation spectrum at approximately 300 MHz. However, curve 1 depends critically on the magnitude of the asymptotic high-frequency absorption that is chosen. It must be borne in mind that absorption due to any hysteresis mechanisms may possibly contribute at the highest frequencies, leading to additional difficulties in the determination of the upper limit of the relaxation spectrum.

† Subsequent analysis indicates that the concentration reported by Edmonds [1962] as nominally 15 g Hb/100 ml should have been 12 g Hb/100 ml. Other concentrations reported in that communication are changed in proportion.

‡ The authors are grateful to Dr. J. L. Hunter and Mr. Paul Durdel, John Carroll University, Cleveland, for carrying out these measurements.

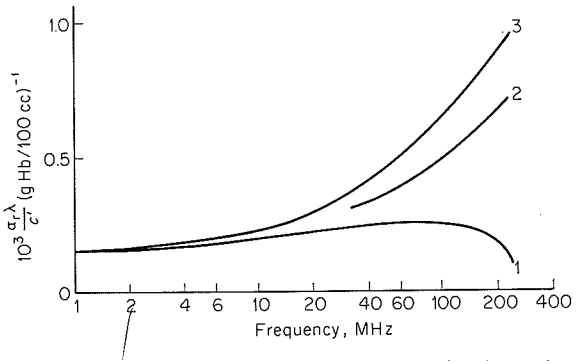

FIG. 31. Relaxational contribution to specific absorption per wavelength for bovine hemoglobin at 25°C. Computed from: (1) the value of $(\alpha/f^2)^\infty$ obtained by extrapolating from experimental data; (2) a simple mixing formula based on relative volumes; (3) $(\alpha/f^2)_v = B$, calculated from the static viscosity η^0. The superscript ∞ refers to the asymptotic measured value at high frequencies and subscript v to Eq. (30).

Curve 2 on Fig. 31 shows the result of correcting measured data by means of the simple mixing formula adopted by Carstensen and Schwan [1959*b*]. One would conclude from this curve that the distribution of shorter relaxation times was radically different from that predicted by curve 1. The third possibility is shown by curve 3 which was obtained by correcting measured data by subtracting the classical absorption due to viscosity. At low frequencies the differences in these possible interpretations are insignificant, and the results of Gramberg [1956] indicate that relaxation frequencies as low as 20 or 30 kHz are important.†

The absorption coefficient of a 12.5 g/100 ml solution of human serum albumin in water has been found to be indistinguishable from that of human hemoglobin in the same concentration (Carstensen, Li, and Schwan, 1953). These conclusions apply within the frequency range 0.8 to 3 MHz and the temperature range 10° to 40°C. The absorption data in these ranges were also coincident with the absorption values of red blood cells, when compared on the basis of reduced concentration, α/c'.‡

† Some further measurements on a solution of equine methemoglobin in water at approximately 6.7 g Hb/100 ml have been reported by Mayer and Vogel [1965]. Their data in the frequency range from 0.3 to 6 MHz are incompatible with Carstensen and Schwan's, and, furthermore, they report finding no dependence of the absorption on temperature and no dispersion of the propagation velocity. The experimental error reported by Mayer and Vogel at low frequencies is approximately 30 percent, whereas that of Carstensen was only 10 percent. We conclude that these data are less reliable than those that have been discussed above.

‡ See also Kessler [1968] for a study of bovine serum albumin solutions in water.

The absorption in gelatin solutions is approximately half that in hemoglobin and albumin and shows a similar frequency dependence in the frequency range 0.7 to 10 MHz. The absorption coefficient of a 20 g gelatin/100 ml solution in water shows a marked dependence on the state of charge of the protein (Fig. 32), indicating that solvation is a significant mechanism in determining the absorption coefficient (Pauly, 1957, Passynsky, 1947).

Carbohydrates

Hawley, Kessler, and Dunn [1965*a*, 1965*b*] have reported absorption data on aqueous solutions of dextran, a linear $\alpha(1 \rightarrow 6)$ anhydroglucose polysaccharide by-product of bacterial metabolism, which is commercially available in crystalline form. The molecular weights of the dextrans were 73,000, 186,000, 370,000, and 2,000,000. The absorption data for these polysaccharides—in the frequency range 3 to 69 MHz and concentration range 2.2 to 11.4 g/100 ml—have been compared with those for hemoglobin (molecular weight 68,000) in an endeavor to identify differences of ultrasonic absorption characteristics which might be due to differences in the molecular structure of proteins and polysaccharides, for example, the presence or absence of tertiary structure. The polysaccharide is primarily a linear structure with 5 to 10 percent glucose residues existing as branching elements, and it assumes random coil configurations in aqueous solution. In contrast, hemoglobin is a globular protein displaying a specifically folded structure, which is probably stabilized by hydrogen bonds and van der Waals forces (Kendrew, 1962; Braunitzer, Hilse, Rudloff, and Hilschmann, 1964).

FIG. 32. Absorption parameter (α/f^2) of a 20 percent solution of gelatin in water at 35°C and 5 MHz as a function of pH. (*After Pauly*, 1957.)

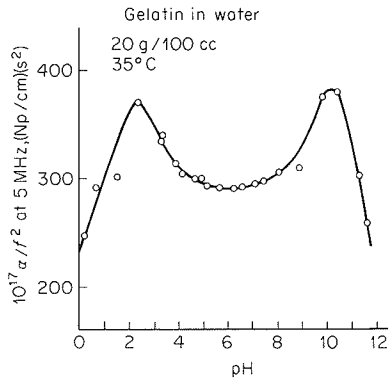

FIG. 33. Partial specific absorption parameter $\bar{\alpha}_2/f$ for aqueous solutions of bovine hemoglobin and polysaccharides.

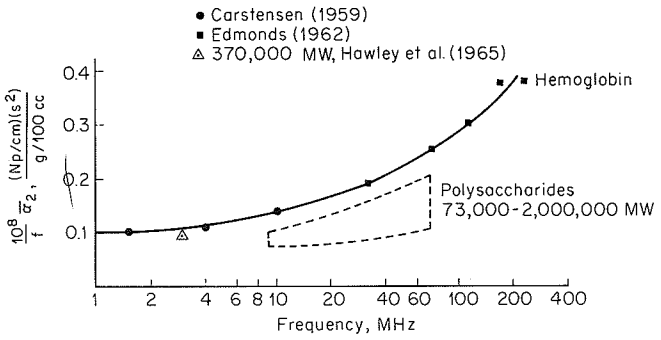

In view of the uncertainties in interpretation of data that were discussed on page 292, a simplified procedure for comparing the polysaccharides and hemoglobin is adopted. The partial specific absorption coefficient is defined as $\bar{\alpha}_2 = (\partial\alpha/\partial n_2)_{n_1,T,P,f}$, and the partial specific absorption per wavelength as $\bar{\alpha}_2 v/f$. These quantities are defined to be analogous to the partial specific volume $\bar{v}_2 = (\partial V/\partial n_2)_{n_1,T,P}$ where $n_1 \equiv$ concentration of solvent, and $n_2 \equiv c' \equiv$ concentration of solute. Therefore $\bar{\alpha}_2$ represents the incremental absorption at frequency f resulting from the addition of a small amount of solute to a solution. At lower concentrations (less than 10 g/100 ml approximately), the measured absorption coefficients are proportional to concentration for both polysaccharides and hemoglobin, indicating no interaction between solute molecules. At higher concentrations, $\bar{\alpha}_2$ increases, probably owing to interactions between the macromolecules (Carstensen and Schwan, 1959*b*).

The comparison of partial specific absorption per wavelength is shown on Fig. 33.† The data for polysaccharides lie below those for hemoglobin in all instances, although not by more than a factor 0.4. Therefore it is possible that the tertiary structure might be responsible for the excess incremental absorption of hemoglobin, as suggested by Hawley, Kessler, and Dunn [1965*a*]. The suggestion is supported by the absorption data for another protein, gelatin, which does not exhibit tertiary structure; α/c' is about half as great as that of hemoglobin at pH 6 to 7, although the dependence on pH indicates that solvation processes are of importance in determining the absorption in this case (Pauly, 1957). However, it is unlikely that this is the only cause of differences in the magnitudes of $\bar{\alpha}_2$, since protolytic reactions may also contribute to the excess absorption of hemoglobin.

† This figure supersedes that previously published by Hawley, Kessler, and Dunn [1965*b*].

Nucleic acids

Measurements of the absorption coefficient of calf thymus DNA have been reported by Lang and Cerf [1969]. They were obtained mainly by the interferometric method described briefly on page 258. The measurements were performed in the frequency interval of 3 to 58 MHz on samples of molecular weight $4.7 - 7.0 \times 10^6$ at concentrations 0.5–0.6 g/100 ml in an aqueous solution of 0.18 *M* sodium chloride and 0.02 *M* sodium citrate. The temperature was maintained at 5° and 25°C and the pH range was 6 to 12.5. The data at frequencies less than 27 MHz (Fig. 34) exhibit incipient relaxation and maxima at pH 11.9 attributable to alkaline denaturation. Thermal denaturation, followed by addition of formaldehyde to prevent renaturation, produced no change in specific absorption coefficient, α_{sp}/c', a quantity which is simply related to the partial specific absorption coefficient in cases where α is linearly related to concentration c' $(= n_2)$:

$$\frac{\alpha_{sp}}{c'} = \frac{\alpha - \alpha_0}{\alpha_0 c'} \xrightarrow[\delta c' \to 0]{} \frac{\bar{\alpha}_2}{\alpha_0} = \frac{\bar{\alpha}_2/f^2}{\alpha_0/f^2} \tag{99}$$

FIG. 34. Dependence of α/f^2 upon pH and frequency during alkaline denaturation of calf-thymus DNA in solution at 25°C and 0.3 g DNA/100 ml. (*After Lang and Cerf*, 1969.)

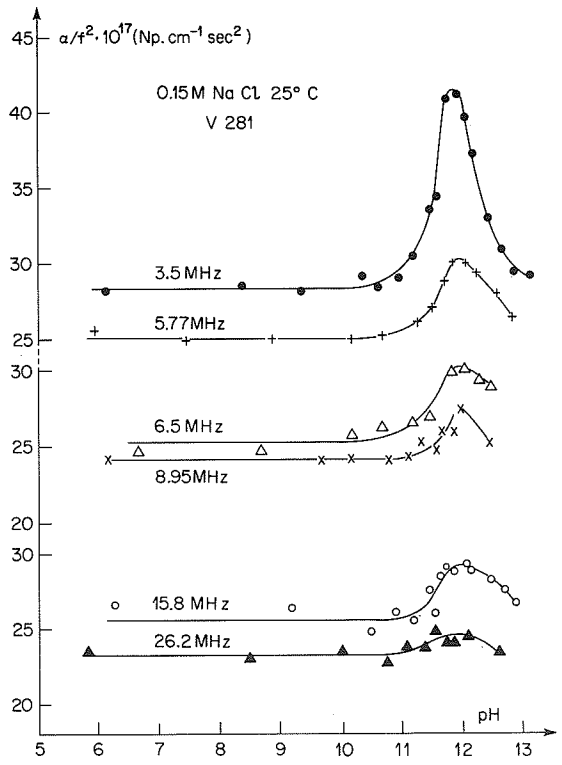

This work supersedes previous papers from the same laboratory, reporting a maximum in α/f^2 as a function of frequency for native DNA. A monotonic decrease with increasing frequency is now found under all conditions. The authors suggested that relaxation processes characterized by at least three states may account for this more reliable data. Consequently, it may not be necessary to utilize the theory of "stochastic resonance," developed by Cerf to include both relaxational and resonance behavior (Cerf, Candau, and Zana, 1962; Cerf, 1965*a*, 1965*b*). It is of interest to note here that Zana and Cerf [1964] have calculated the absorption to be assigned to viscosity in a solution of rigid ellipsoidal particles, representing DNA molecules.

Synthetic polymer solutions

The dynamic mechanical properties of solutions of synthetic polymers have been investigated extensively and have been reviewed by Philippoff [1965]. The molecular transitions involved in the response of long-chain polymers to mechanical stresses include those involving only a change of entropy ΔS with related change in free energy, $\Delta G = -T\,\Delta S$. The recovery of a state of ordering of lower free energy upon release of stress leads to the description of the rigidity modulus in terms of an "entropy elasticity." Rouse [1953] has developed expressions for $G'(\omega)$ and $G''(\omega)$—see Eq. (36)—for a model of a solution of isolated random-coil polymer molecules of N segments, each of which is permitted free rotation about a carbon-carbon bond. The hydrodynamical interactions between these segments are neglected in this model which therefore refers to a "free-draining" coiled molecule. For a concentration of n_2 molecules per unit volume, Rouse obtains

$$G'(\omega) = n_2 k_B T \sum_{p=1}^{N} \frac{\omega^2 \tau_p^{\,2}}{1 + \omega^2 \tau_p^{\,2}}$$

$$G''(\omega) = n_2 k_B T \sum_{p=1}^{N} \frac{\omega \tau_p}{1 + \omega^2 \tau_p^{\,2}} + \omega \eta_1 \tag{100}$$

where τ_p is the pth relaxation time, and η_1 is the viscosity of the solvent. When N is large, the generalization of the summation yields a continuous distribution of relaxation times, extending from τ_1 to τ_N.

The model has been refined by Zimm [1956] to include the effect of hydrodynamic interactions between the segments of the polymer molecule. Experimental data have shown that Zimm's theory describes the observed behavior of molecules of moderately high molecular weight ($\simeq$ 100,000) in viscous solvents, while even higher molecular weights ($\simeq 10^6$) lead to intermediate

results approaching the predictions of Rouse's theory (Ferry, Holmes, Lamb, and Matheson, 1966).

Lipids

No ultrasonic data relating specifically to lipids in isotropic liquid form are known to the authors. However, reference is made to cholesteryl benzoate on page 300.

Phase Transitions

Critical mixtures

An additional class of phenomena for which a distribution of relaxation times would be required to describe observed behavior is that of phase transitions. In the liquid state, phase transitions can occur in binary liquid mixtures when the constituent species are not mutually soluble in all proportions. The maximum or minimum temperature at which the phase transition occurs is the upper or lower critical solution temperature, and the necessary composition is the critical composition. Departures from simple behavior are most marked at the critical composition and temperature and are recognized by phenomena such as light scattering (turbidity, critical opalescence), anomalously high viscosity, and ultrasonic absorption. The variations of absorption and sound velocity at the critical composition with change of temperature display a cusplike maximum and branch point, respectively. Anomalous behavior may be observed at least 10°C on either side of the transition temperature in the case of triethylamine and water (Chynoweth and Schneider, 1951).

At temperatures within a few degrees of the transition temperature, the state of association of the liquid mixture is critically dependent on the temperature, and may therefore be perturbed by the temperature fluctuation in the sound wave. Response of the system necessitates diffusion of molecules in order for them to associate with one another to form a submicroscopic agglomerate. The reactions are therefore most probably diffusion-controlled. Their effect on the ultrasonic absorption coefficient is observable at low megahertz frequencies and below; but as yet no case has been studied over a sufficiently large frequency range to define a relaxation spectrum. The most comprehensive data available, on the system nitrobenzene-isoöctane by Anantaraman, Walters, Edmonds and Pings [1966], and on nitrobenzene-*n*-hexane by Singh, Darbari, and Verma [1966] are insufficient for this purpose. However, the results of the latter studies are in quite encouraging agreement with the theoretical predictions of Fixman [1962*b*].

The behavior of binary liquid mixtures at phase separation may be regarded as a model system which may help in the understanding of phase

transitions in solution from which micellar or liquid crystalline (mesomorphic) structures result. The latter are important in biological systems.

Micelles

Very few data are available on the ultrasonic behavior of micelle-forming systems. Mikhailov and Tarutina [1950] have reported some data obtained on the system gelatin in water at 25°C and at frequencies of 8.2 and 10.4 MHz over the concentration range 0 to 7 percent. Their data show a linear rise of the absorption coefficient to a concentration of 3 percent by weight, followed by a flattening and approximately constant absorption coefficient up to 7 percent. The similarity of their values of α/f^2 at the two frequencies indicates that their measurements were taken outside a relaxational region.

McKellar and Andreae [1962*b*] carried out more extensive measurements on the micelle-forming system *n*-octylamine and water. Their measurements of absorption extend over the range of 1.5 to 230 MHz, and the sound velocity was measured at 2 MHz. Their data show single relaxational frequency behavior in a region of isotropic solution at concentrations up to 0.3 mole fraction amine. The concentration-dependent relaxation frequency was found to lie in the range 15 to 27 MHz in this concentration interval. Figure 35 shows their comparison of data obtained on *n*-octylamine and *n*-amylamine at 20°C, expressed as the variation of the maximum absorption per wavelength with concentration. The data on the micelle-forming octylamine fall well below those for the non-micelle-forming amylamine and exhibit the approach to constancy. McKellar and Andreae [1962*b*] suggest that they may be observing the absorption due to hydrogen bonding between the water and unassociated octylamine, and that the reduction which they observe in the rate of increase of absorption per wavelength may be due to the progressive scavenging of single solute molecules by the formation of micellar structures. Relaxation associated with molecules in the micelle was imagined to occur at lower frequency. In the amylamine it has been proposed that the absorption is due to hydrogen-bonding mechanisms between the solute and water at the site of amino group (McKellar and Andreae, 1962*b*; Andreae, Edmonds, and McKellar, 1965). However, it is concluded in the latter paper that the hydrogen-bonding process is not always an isothermal process in aqueous solution, but becomes instead a thermal process, dominated by the enthalpy change ΔH rather than by the volume change ΔV, near concentrations for which $\alpha_r\lambda$ achieves maximum values. The argument is based on numerical calculations for three amine-water systems and the acetone-water system. See also Hammes and Knoche [1966].

An alternative explanation of the measurements on *n*-octylamine in water can then be developed in terms of a thermal relaxation. By forming micelles,

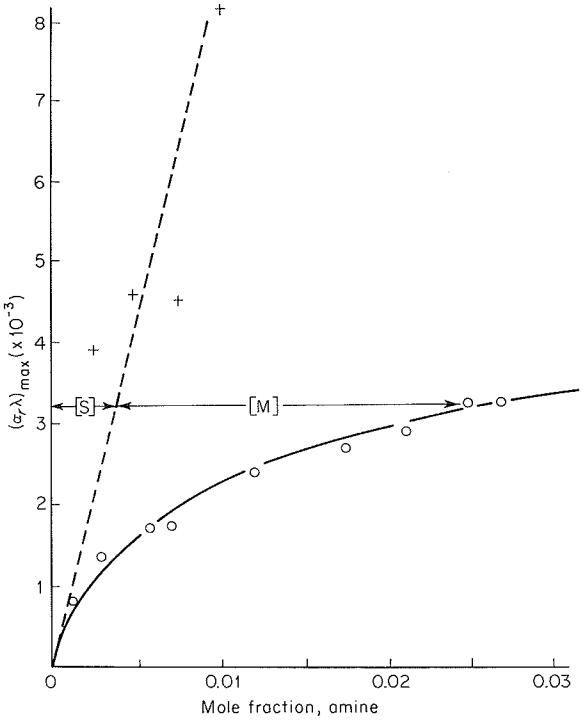

FIG. 35. Dependence of $(\alpha_r\lambda)_{max}$ on amine concentration for solutions of amylamine (+) and octylamine (○) in water at 20°C. $[M]$ and $[S] \equiv$ presumed concentrations of micelles and single molecules, respectively. Single relaxation analysis. (*After McKellar and Andreae*, 1962*b*.)

the solute might cause a smaller specific disturbance (per molecule) to the water structure than as single molecules, and the propagation of the sound wave might proceed nearly isothermally to appreciable concentrations of solute instead of only at low concentrations. This picture is favored by the absence of a peak in the curve of sound velocity versus concentration. The formation of micelles would therefore limit the absorption due to thermal processes and could lead to the observed flattening of the sound absorption curve. The explanation depends upon the formation of micelles, as before, but it avoids the postulate of a separate, lower-frequency relaxation process for solute molecules participating in the micelle. Data are at present inadequate to distinguish between these proposed interpretations.

Liquid crystals

At the transition temperature between a pure isotropic liquid phase and a liquid-crystalline (mesomorphic liquid) phase, the absorption increases

greatly to a cuspid maximum, and the velocity decreases to a cuspid minimum. Figure 36 shows the data obtained by Hoyer and Nolle [1956] for cholesteryl benzoate measured at 0.5 MHz. Below the transition temperature, the stable phase is the optically active cholesteric mesophase characterized by parallel alignment of molecules in sheets and helical stacking of the sheets (Fergason, 1964). Similar but less pronounced variations at the same transition region have been observed in the range of 2 to 15 MHz by Zvereva and Kapustin [1964] and Zvereva and Kapustin [1965] for cholesteryl caprate and cholesteryl caprinate, respectively. However, their data show a smooth transition from the cholesteric to the smectic mesophase which is stable at lower temperatures. One may speculate that relaxational effects associated with the latter transition may occur at lower frequency.

Mesomorphic phases in aqueous solution are exhibited in certain concentration ranges by such solutes as soaps and detergents, and phospholipids, e.g., lecithin (phosphatidylcholine) and cephelin (a mixture of phosphatidylserine and phosphatidylethanolamine). No ultrasonic measurements on such lyotropic mesophases are known to the authors.

The experimental and theoretical aspects of this topic have been reviewed by Edmonds and Orr [1966]. Further knowledge of the kinetic behavior of phospholipids in solution is necessary to permit more precise definition of the molecular interactions involved, and thereby to assist investigators studying such macromolecules in other situations, e.g., as structural components of biological membranes.

FIG. 36. Dependence of absorption coefficient α and velocity v on temperature near the isotropic-cholesteric transition in cholesteryl benzoate at 0.5 MHz. (*After Hoyer and Nolle*, 1956.)

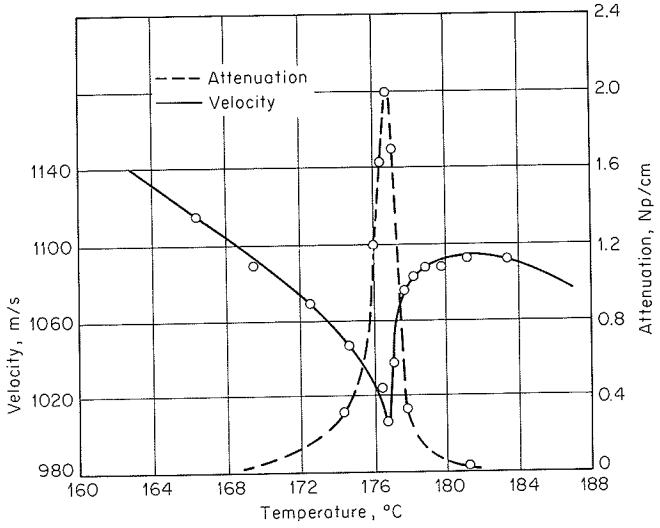

Gels

Gels correspo
particles or rand
of interaction b
modulus to the
as a suspending
material. Local
rubbers and gl
mesomorphic, li
to ultrasonic mea
ments of the co
trations ranging
greater than 2 g
[1951] has repor
as the temperatu
to 50°C, i.e., d
starch (20 to 40
the absorption c

Tissues

In this sectio
the ultrasonic ab
frequency and
concentration,
the eye, and lun
most soft tissu
separately. The
No formal theo
the ultrasonic
unusual acousti
sion is made t
upon specific p
known mechani
biological mate

Soft tissues

Frequency
the dependence
frequency. A
has been compi

Gels

Gels correspond to a state of high concentration of solutions of hydrated particles or randomly coiled long-chain polymer molecules, such that forces of interaction between the solute predominate and impart a finite rigidity modulus to the material at zero frequency. The solvent no longer functions as a suspending fluid medium but is dispersed throughout the semisolid material. Local ordering in a gel follows a statistical distribution as in rubbers and glasses rather than pseudocrystalline distribution as in the mesomorphic, liquid-crystalline phases. Sporadic attention has been given to ultrasonic measurements in gels. Passynsky [1947] has reported measurements of the compressibility and solvation numbers of gelatin at concentrations ranging from 0.2 to 9 g/100 ml. Gelation occurred at concentrations greater than 2 g/100 ml and did not influence the compressibility. Koinito [1951] has reported that the absorption coefficient at 1 MHz remains constant as the temperature of 1.2 to 4 g gelatin/100 ml solutions is varied from 12 to 50°C, i.e., during passage through the gelation region. Solutions of starch (20 to 40 g/100 ml) showed a slight reduction of the magnitude of the absorption coefficient on gelation.

Tissues

In this section the experimental data concerned with the dependence of the ultrasonic absorption coefficient of tissues on the acoustic field variables, frequency and wave amplitude, and the state variables, temperature and concentration, are reviewed. Several tissues, namely, refractive media of the eye, and lung, which exhibit absorption properties greatly different from most soft tissues, that is, fat, muscle, liver, nerve, etc., are discussed separately. The absorption properties of bone are also briefly described. No formal theory is presented for explaining the observed dependencies of the ultrasonic absorption coefficient; however, an interpretation of the unusual acoustic absorption properties of lung is mentioned briefly. Allusion is made to several of the dependencies of the absorption coefficient upon specific physical variables where they appear to resemble those of known mechanisms arising from the interaction of ultrasound and nonbiological materials.

Soft tissues

Frequency dependence. The literature is replete with data regarding the dependence of the ultrasonic absorption coefficient upon the acoustic frequency. A tabulation of the ultrasonic absorption and velocity data has been compiled by Goldman and Hueter [1956]. Figure 37, taken from

their paper, is a graphical representation of the acoustic amplitude absorption coefficient per wavelength for several mammalian tissues in the frequency range of approximately 200 kHz to 10 MHz. The scatter of the data, exhibited by the bands or broad shaded regions, results from the attempt to include all measurements (available at that time) by numerous investigators employing different experimental techniques. The appearance of the bands in Fig. 37 is not wholly surprising since many investigators neglect to give complete specifications of their experimental procedure and/or a description of the state of the specimen used. For example, it is known that the measurements represented in Fig. 37 were performed at different temperatures. However, it is not possible to determine from the literature the temperatures employed by the investigators reporting the data. (The influence of temperature on the absorption coefficient is discussed below.) It is, however, possible to discern several relatively simple relationships. For example, the absorption per cycle, α/f, is generally constant over the frequency range considered. For fat, α/f, increases slightly in the frequency range from 1 to 10 MHz. The experimental results for striated muscle and liver appear to exhibit a minimum in the neighborhood of 2 MHz. Fry [1952] has considered a viscous mechanism for the absorption of ultrasound in tissue, in which it is shown that the viscous forces acting between a suitable chosen distribution of suspended particles (or structural elements) and a suspending liquid can account for the experimentally observed linear relationship between acoustic absorption coefficient and ultrasonic frequency. The frequency band over which linearity obtains (in the model) is determined by the limits of the distribution of values for the parameters chosen to describe

FIG. 37. Acoustic amplitude absorption coefficient (in decibels per centimeter) per wavelength versus frequency for several mammalian tissues. (*After Goldman and Hueter*, 1956.)

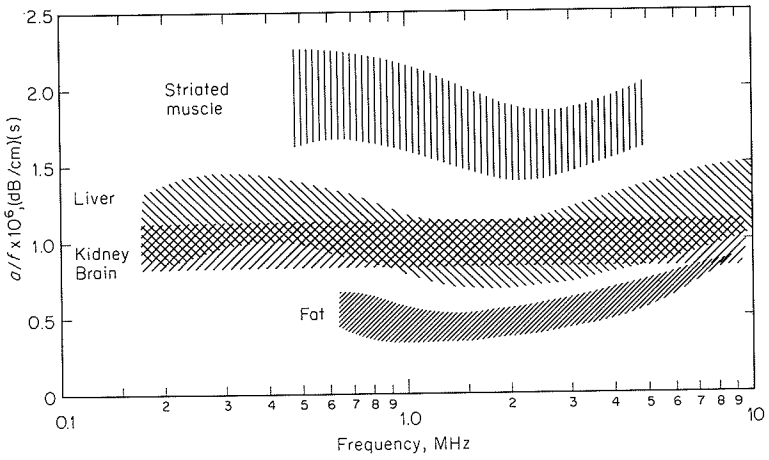

the structural elements. Below the linear range the theory predicts a quadratic dependence, in agreement with experiment.

Another way of presenting absorption data, prepared by Hueter [1958], which may be suggestive for the elucidation of mechanisms, is illustrated in Fig. 38. Here, the logarithm of the absorption coefficient is plotted as a function of the logarithm of the sound frequency, and the slopes of the resulting curves are examined (the slope is the exponent on frequency upon which the magnitude of the absorption coefficient depends). Figure 38 shows data for several materials of increasing biological complexity, and they exhibit corresponding graded complexity in absorptive behavior. The 10 M urea solution exhibits a slope of 2, indicative of classical viscous absorption for which $\alpha/f^2 = \text{constant}$. Homogenized milk, a suspension of fat particles and hydrated casein complexes, exhibits a slope of nearly unity from approximately 1 to 40 MHz. Behavior of this type cannot be explained in terms of simple viscosity or scattering theories. The curves for the absorption coefficients of egg albumin, brain tissue, liver, and striated muscle (not shown in Fig. 38) exhibit slopes between 1 and 2 in the neighborhood of 1 MHz and approach a slope of 2 at higher frequencies. Hueter [1958] has suggested that this type of frequency dependence can be described for specific muscle preparations by a double relaxation process in which the bulk (volume) viscosity of the tissue possesses a relaxation frequency near

FIG. 38. Acoustic amplitude absorption coefficient versus frequency for materials of different biological complexity. (*After Hueter*, 1958.)

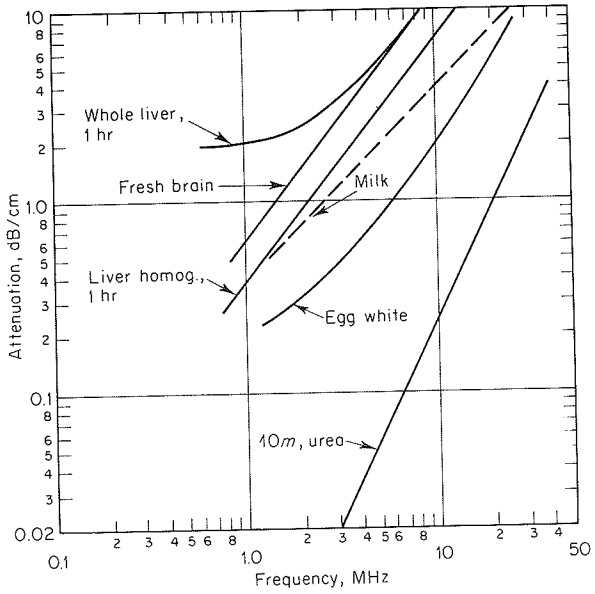

40 kHz, and the shear viscosity possesses a relaxation near 400 kHz. Although it is conceded that this is an oversimplification of a complicated process, it will be shown below that the temperature dependence of the acoustic absorption coefficient lends support to this view.

The dependence of the ultrasonic absorption coefficient upon the concentration of tissue components in solution is mentioned briefly below, and it is interesting to compare, as Hueter [1958] has done, the absorption in brain tissue, reported by numerous investigators, with the absorption of concentrated solutions of red cells, as shown in Fig. 39. The curve through the nerve-tissue data is drawn with a slope found for concentrated red cells (Carstensen et al., 1953). The figure suggests that nerve tissue behaves very much like a concentrated aggregate of protein with the absorption increased by approximately a factor of 2, perhaps due to the protein-protein interactions associated with the formation of tissue structure.

A study by Schwan et al. [1957] on liver and solutions of liver fractions has shown that tissue cell nuclei do not contribute significantly to tissue

FIG. 39. Ultrasonic absorption versus frequency for nervous tissue and solution of 85 percent red cells from human blood (protein curve). (*After Hueter*, 1958.)

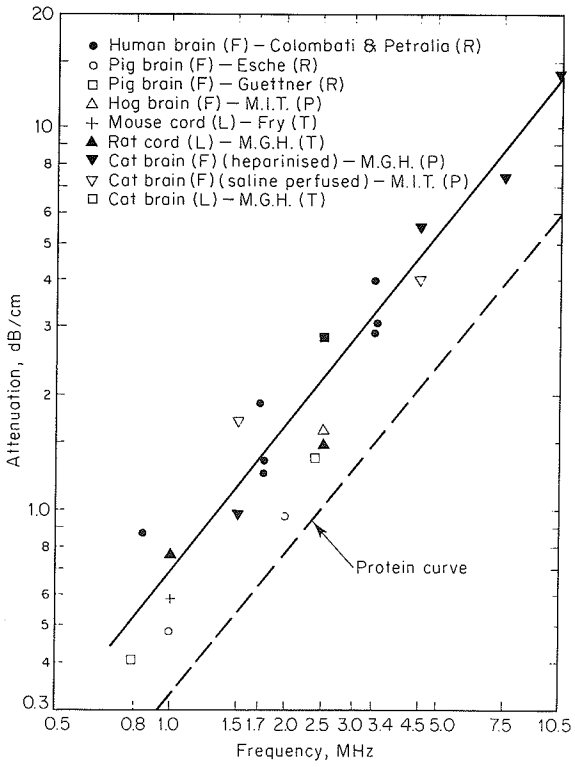

absorption. The fractions exhibit absorption spectra similar to those of tissues shown in Fig. 38. The study suggested that tissue absorption arises on a molecular level and is largely independent of architectural features. It was found that individual molecular constituents display somewhat different absorption coefficients which depend upon pH and molecular integrity. It is suggested that the tissue proteins may account for nearly 80 percent of the observed tissue absorption.

Temperature dependence. Only two studies dealing with the dependence of the ultrasonic absorption coefficient of biological materials upon temperature have been reported. The absorption coefficient of the spinal cord of young mice (approximately 24 hours after birth) has been measured in vivo by Dunn [1962, 1965] at the sound frequency of 1 MHz by employing the transient thermoelectric method (page 255). Figure 40 shows the acoustic intensity absorption coefficient versus temperature where it is seen to increase from 0.034 cm^{-1} at 2°C to 0.25 cm^{-1} at 45°C. The positive temperature coefficient of absorption eliminates shear viscosity as a possible mechanism. However, this variation does resemble the temperature dependence of the absorption coefficient of high-viscosity liquids above the main relaxation frequencies in the liquid (Litovitz and Lyon, 1954). Thus, the monotonic increase in the absorption coefficient as a function of temperature (at 1 MHz) of the spinal cord of young mice is considered to lend support to Hueter's [1958] suggestion, discussed above, that a double-relaxation process occurs, wherein both the bulk viscosity and the shear viscosity relax at frequencies well below the frequency of measurement.

Carstensen, Schwan, and coworkers [1953] have carried out an extensive study on the ultrasonic properties of blood and its components. In this work it was shown that the absorption properties of blood are determined largely by the protein content, and the value of the absorption coefficient was shown to be directly proportional to the protein concentration up to

FIG. 40. Acoustic intensity absorption coefficient versus temperature at 1 MHz for spinal cord of young mice. (*After Dunn*, 1962, 1965.)

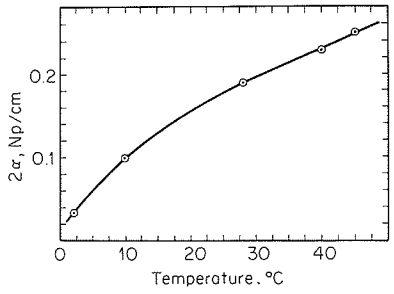

15 g Hb/100 ml in solution. Figure 41 shows their ultrasonic absorption data for hemoglobin solutions as a function of temperature at three acoustic frequencies. The negative temperature coefficient suggests that shear viscosity might play a role in the absorption mechanism, but the magnitude of the absorption coefficient shows that this mechanism alone is entirely inadequate.

The temperature dependence of the absorption coefficient, particularly that for young mouse spinal cord, illustrates the necessity for complete specification of the state of specimens when reporting experimental results. The data for the young mouse cord shows that a sevenfold increase in the absorption coefficient occurs in the temperature range from 0 to 45°C. Although the rate of change of the positive temperature coefficient appears to exhibit a marked decrease in the neighborhood of the normal temperature of adult mammals, namely, 37°C, it must be recalled that these measurements represent only one species and one tissue structure. Others may exhibit more or less pronounced temperature dependencies.

Amplitude dependence. The transient thermoelectric method (page 255) employed in obtaining the value of the absorption coefficient as a function of temperature of the young mouse spinal cord included exposure of each specimen to different acoustic intensity levels of incident sound energy (Dunn, 1962). Thus, the method made data available on the dependence of the acoustic absorption coefficient upon the sound amplitude. Equation (81), page 256, states that if the quantity $2\alpha/\rho_t c_p'$ is constant, the initial time rate of change of temperature, $(dT/dt)_0$, is a linear function of the acoustic intensity. Figure 42 shows that, in the range of incident acoustic intensities from a few watts per square centimeter to nearly 200 W/cm² and at three base temperatures of the animals, such linear relationships indeed obtain. On the assumption that the heat capacity per unit volume, $\rho_t c_p'$, is not dependent on the sonic intensity, it can be concluded that in the range

FIG. 41. Ultrasonic absorption versus temperature for hemoglobin solutions at three frequencies. (*After Carstensen et al.*, 1953.)

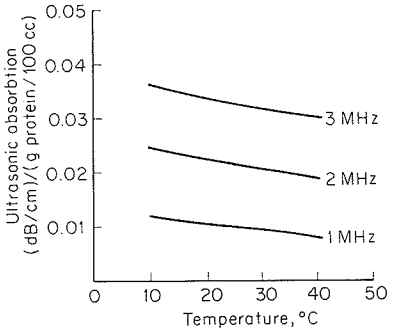

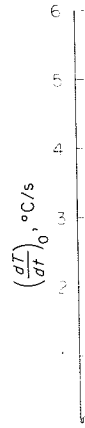

FIG. 42
produc
at thre

of intensities empl
intensity of the rac
here.

The following
of the value of t
intensity (for the
sound source via
5 cm in the expe
short in the salin
vibrating element
during propagatio
fundamental to t
of state of the li
negligible in this
wave incident on
frequency form.
state of tissue are
propagation dista
the transfer of en
is negligible withi

Absorption in bon

Bone is a tissue
from those of th

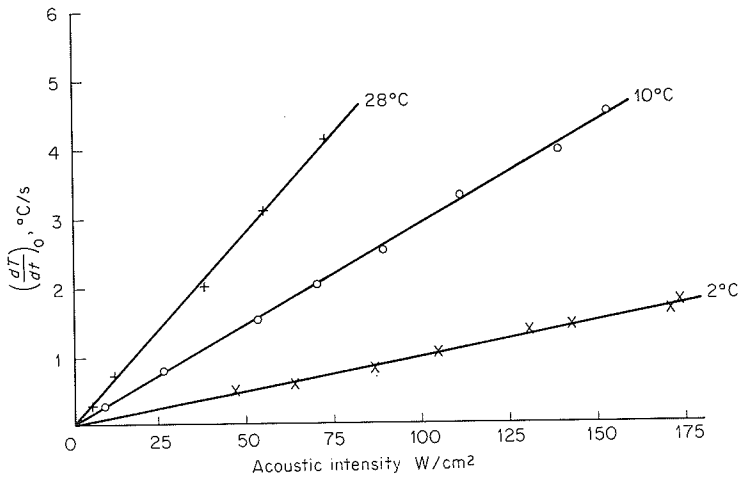

FIG. 42. Time rate of change of temperature in spinal cord of young mice produced by absorption of 1 MHz sound versus incident acoustic intensity at three temperatures. (*After Dunn*, 1962.)

of intensities employed here, the absorption coefficient is independent of the intensity of the radiation for the preparations employed in the study discussed here.

The following comments are of interest relative to the lack of variation of the value of the absorption coefficient of nerve tissue with the sound intensity (for the range of values indicated). The propagation distance from sound source via degassed mammalian saline to the tissue was approximately 5 cm in the experimental work of reference. This distance is sufficiently short in the saline so that initially monochromatic waves produced by the vibrating element (X-cut quartz plate) remain virtually monochromatic during propagation to the specimen; that is, the energy transferred from the fundamental to the harmonics, which results from the nonlinear equation of state of the liquid medium (see for example Fry and Dunn, 1962), is negligible in this path length at the highest intensities employed. Thus, the wave incident on the tissue is essentially undistorted from the initial single-frequency form. On the assumption that the coefficients in the equation of state of tissue are approximately the same as those of water, and since the propagation distance in the tissue is relatively short (approximately 0.5 mm), the transfer of energy from the incident fundamental wave to its harmonics is negligible within the specimen.

Absorption in bone

Bone is a tissue possessing acoustic propagation properties greatly different from those of the soft tissues discussed in the previous section. Hueter

[1952] has measured the acoustic absorption coefficient of specimens of fresh human skull in the frequency range of 0.6 to 3.5 MHz at temperatures between 25 and 30°C. These measurements show that the absorption coefficient of bone exhibits a quadratic dependence upon frequency (the classical viscous type) to approximately 2 MHz, followed by a transition to a lower power dependence at higher frequencies. The acoustic amplitude absorption coefficient per unit path length in bone is of the order of 1 Np/cm at 1 MHz, approximately an order of magnitude greater than that of most soft tissues at the same temperature and frequency.

Absorption in the refractive media of the eye

Begui [1954] has studied the acoustic properties of the refractive media of the eye in vitro. He determined the ultrasonic absorption coefficients of the aqueous and vitreous humors at 30 MHz and that of the lens at 3 MHz. The specimens were obtained from excised fresh calf eyes. At 30 MHz and 27.5°C, the aqueous and vitreous humors both exhibit an acoustic amplitude absorption coefficient of 0.35 Np/cm. Since this is approximately 50 percent greater than the absorption coefficient of dilute salt solutions, it suggests that the absorption coefficients of the humoral media of the calf eye possess a viscous-type dependence upon frequency; that is, the absorption coefficient probably increases as the square of the frequency.

The lens of the calf eye exhibits a value of 0.7 Np/cm for the acoustic amplitude absorption coefficient at 3 MHz and 28°C. Since the lens contains a relatively high concentration of protein, it is not unreasonable to assume, in the absence of further information, that the frequency dependence of the absorption coefficient of the lens resembles that of other soft tissue for which the absorption appears to be dominated by the protein content; i.e., it is probable that the absorption coefficient per unit path length of the lens varies approximately with the first power of the frequency.

Some investigators currently using ultrasonic methods for diagnosing disorders of the human eye feel that the lens absorption value given by Begui is larger than that for the human lens (in vivo). The possible discrepancy may result because of species differences. Indeed, Begui observed that the viscosity of the intraocular fluid of calf eyes is greater than the values normally stated for the fluid media of human eyes. Further, the specimens used by Begui were first stored (at temperatures in the neighborhood of 0 to 5°C) and were used for measurement purposes within a time interval of 10 days. Diagnostic procedures are, of course, performed in vivo. Some autolysis of the stored specimens may have occurred, although it is not immediately apparent that under such conditions the absorption coefficient should increase.

Lung tissue

The acoustic properties of excised dog lung have been investigated in two independent studies. The transient thermoelectric probe (page 255) was employed to determine the standing-wave pattern established between the lung sample and the acoustic source, due to the difference in acoustic impedance between lung tissue and the sound transmission fluid (saline), and to detect the amplitude of the sound waves propagating through the sample (Dunn and Fry, 1961). From the observed standing-wave ratio, the experimentally determined density of the lung samples (0.4 g/cm^3) and the acoustic impedance of the transmitting liquid (1.53×10^5 g/(cm^2)(s)), the speed of sound in lung tissue was found to be 6.5×10^4 cm/s. The frequency at which these measurements were made was 0.98 MHz, the temperature was 35°C, and the lung samples were excised in such a manner that the amount of gas remaining was considered to be somewhat in excess of the residual volume. The acoustic amplitude attenuation coefficient per unit path length was determined under the same conditions from a knowledge of the fraction of incident energy reflected at the two lung-saline interfaces, the thickness of the sample, and the relative acoustic intensity detected by the probe. The absorption value calculated from the data is 4.7 Np/cm.

In order to explain the unusually high absorption exhibited by lung tissue (more than an order of magnitude greater than that found for dry oxygen or nitrogen), an acoustic model based on the gross structure was postulated (Dunn and Fry, 1961). The very large number of spheroidal and cylindrical gaseous elements with dimensions comparable to the wavelength of sound in the lung at the frequency of measurement (0.98 MHz) suggests a model composed of a uniform distribution of spherical gas bubbles embedded in a liquidlike medium of high viscosity. It is considered that sound energy excites the bubbles to pulsate and that the bubbles dissipate their energy by radiating spherical sound waves. Dissipation attributed to viscous forces acting at the gas-liquid interface and to thermal conduction is negligible for the chosen numerical values of the parameters and for the frequency of 1 MHz. It is assumed that the embedding fluid has properties similar to those of water, except for viscosity, and that the gas has properties similar to those of air. The bubble radius chosen, 0.3 mm, is consistent with the dimensions of the gaseous elements of lung, and the bubble population consistent with the experimentally determined density is then 5.3×10^3 bubbles/cm^3. The relations presented on page 238, together with the numerical data presented in Table 12, yield a value for the absorption coefficient at 1 MHz of approximately 6 Np/cm. This value is in sufficiently good agreement with the experimental result to lend support to the view that the mechanism of ultrasonic attenuation in lung tissue is primarily the result of radiation of sound waves by pulsating gaseous inclusions.

TABLE 12. QUANTITIES FOR COMPUTATION OF ULTRASONIC ABSORPTION IN LUNG TISSUE

Quantity	*Definition*	*Numerical value*
ω	Angular frequency of sound field	6.28×10^6 rad/s
v	Acoustic velocity in liquid	1.5×10^5 cm/s
γ_g	Ratio of specific heats of gas	1.4
P_0	Static pressure	10^6 dyn/cm^2
ρ	Density of liquid	1.0 g/cm^3
ρ_g	Density of gas	1.29×10^{-3} g/cm^3
σ	Surface tension	75 dyn/cm
h_1	γ_g/ϵ	$1 < h_1 < \gamma_g$
c_p	Heat capacity at constant pressure of gas	0.24 cal/g
$\varkappa_g$	Thermal conductivity coefficient of gas	5.6×10^6 (cal/cm)(s)(°C)
η	Viscosity of liquidlike medium	1.5×10^2 poise (von Gierke et al., 1952)

More recently, a pulse transmission method has been employed to study the ultrasonic propagation properties of lung tissue (Reid, 1965). Excised dog lung was employed at a density of 0.26 g/cm^3; it contained therefore normal expiratory air, probably corresponding in amount to approximately the functional residual capacity. The speed of sound in lung tissue was determined by observing the change in time delay of the received pulse relative to that with the lung sample replaced by a transmitting fluid of known velocity. The method yielded only approximate values since the acoustic pulses emerging from the lung sample were distorted appreciably. The value of 5.8×10^4 cm/s was obtained at 1 MHz, which is considered to be in good agreement with that of the previous study. (A value of 3×10^4 cm/s was obtained at 390 kHz.) The insertion loss of the lung sample was determined by the change in attenuation required at the receiver-amplifier to produce a received signal with the sample in position equal to that observed when the sample was replaced with an acoustically transmitting liquid. Distortion of the received pulse and broadening of the beam shape are interpreted as evidence for scattering of the sound waves by the lung structures. Though it was not possible to determine a unique value for the attenuation coefficient of lung tissue, it is concluded that the attenuation is much greater than that of other nonosseous biological media, and in this regard the two studies are in agreement.

Analysis of Relaxation Spectra

Analytical procedures

Most of the specimens discussed on pages 283 to 310 exhibit relaxational absorption curves, $\alpha_r\lambda$ versus f, which do not conform to a single relaxation process. It is therefore necessary to consider the possible combinations of

two or more discrete relaxation processes, or the distribution function $g(\tau)$ in Eqs. (39) and (41), which could give rise to the observed behavior. Such attempts at analysis reveal considerable difficulties. In the first place, the distinction between discrete relaxation times and a continuous distribution of relaxation times can only be made if the discrete times differ by at least an order of magnitude. Recourse may be made to considering the probable mechanisms involved—slower chemical reactions will be associated with discrete times, while structural changes or diffusion-controlled reactions will sometimes be associated with continuous spectral distributions. In the case of discrete spectra with relaxation times differing by less than an order of magnitude, the validity of assuming superposition must be verified. In the second place, the observed dependence of the absorption coefficient on frequency is comparatively insensitive to the form of distribution function $g(\tau)$ chosen to describe it (Hiedemann and Spence, 1952). Hence, determination of the form of the distribution function is attended by such considerable uncertainty that the final function is of questionable value.

If a spectrum of discrete time constants is inadequate or implausible in any given case, then certain gross features of an adequate distribution function may be determined directly. For example, Schwan, Smith, and Kam Li [1957], and Carstensen and Schwan [1959], considered distributions represented by simple power functions—$g''(\tau) \equiv a_n''\tau_n$, where a_n'' is a constant independent of time or frequency. The equivalent distribution function for relaxation frequencies will be a similar power function $g(f_\tau) \equiv a_n\tau^{n+2}$, where the exponent $n + 2$ results from $\tau = \frac{1}{2}\pi f_\tau$ and $df_\tau \propto \tau^{-2}\,d\tau$. The corresponding distribution of activation energies is derived from Eq. (38) and the approximation $k_b \simeq 1/\tau$, $(k_f \ll k_b)$. Thus, $d(\Delta G^-) \propto \tau^{-1}\,d\tau$ and $g'(\Delta G^-) \equiv a_n'\tau^{n+1}$, where a_n' and a_n are appropriate constants. Several power functions were tested for their ability to reproduce the gently rising portion of the curve of $\alpha_r\lambda$ versus $\log f$ for hemoglobin solutions in the frequency range 0.3 to 10 MHz. Only the functions with $n = -1$ and a range of τ of at least $\tau_d/\tau_c = 1{,}000$ yielded adequately flat frequency dependence of the calculated $\alpha_r\lambda$, as shown in Fig. 43 for various ratios of the spectral limits, τ_c and τ_d. Functions with $n = 0$ or -2 yielded curves which were too sharply peaked. Extension of the experimental range confirmed this prediction of wide limits τ_c and τ_d and showed that the spectral range extended from $\tau_d \leq 8 \times 10^{-6}$ s to $\tau_d \geq 5 \times 10^{-10}$ s, i.e., $\tau_d/\tau_c > 10^4$ (Gramberg, 1956; Edmonds, 1962). An alternative method of predicting a constant value of $\alpha_r\lambda$ in a given frequency range is to use the "logarithmic box" function (Andrews, 1952). Edmonds [1962] carried out a forced fit to the hemoglobin data with a distorted "logarithmic box" function shown in revised form in Fig. 30, but the procedure appears to yield little of significance.

The similar problem of analyzing dielectric relaxation data has been considered in terms of other distribution functions (Davidson and Cole, 1950,

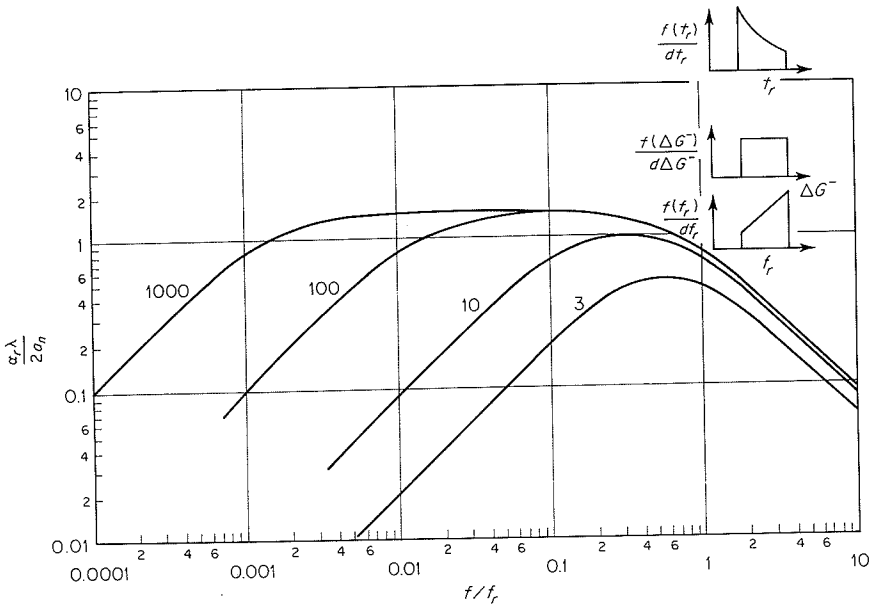

FIG. 43. Relative absorption per wavelength as a function of frequency for the power-function distribution $g(\tau) \propto \tau^{-1}$. The parameter on the curve is the ratio of the spectral limits τ_d/τ_c. (*After Schwan, Smith, and Kam Li*, 1957.)

1951). Burke, Hammes, and Lewis [1965] analyzed their ultrasonic data on poly-L-glutamic acid solutions in terms of the asymmetric distribution function of Davidson and Cole.

$$g_{DC}(\tau)\, d\tau = \frac{\sin \beta\pi}{\pi}\left(\frac{\tau/\tau_0}{1 - \tau/\tau_0}\right)^{\beta} d\left(\ln \frac{\tau}{\tau_0}\right) \quad \text{for } \tau < \tau_0$$
$$= 0 \qquad \text{for } \tau > \tau_0 \tag{101}$$

where the average relaxation time is given by

$$\bar{\tau} = \int_0^{\infty} \tau g_{DC}(\tau)\, d\tau \tag{102}$$

and

$$\frac{\alpha_r}{f^2} = A \int_0^{\infty} \frac{g_{DC}(\tau)\, d\tau}{1 + (\omega\tau)^2} \tag{103}$$

Values of the amplitude factor A, the asymmetry parameter β, and the average relaxation time $\bar{\tau}$ are given in Table 13. The values of β and $\bar{\tau}$ were found to be comparatively insensitive to changes in temperature while the magnitude A/c' decreased appreciably with increasing temperature. The insensitivity of relaxation time to temperature changes indicates a process involving negligible enthalpy changes. Thermodynamic analysis of the data on the assumption that only structural changes were involved led to an

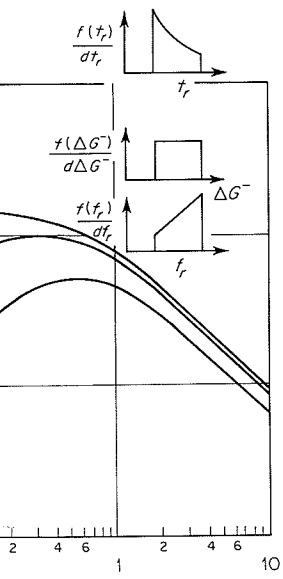

of frequency for the power-
rve is the ratio of the spectral

zed their ultrasonic data
asymmetric distribution

$\Big)$ for $\tau < \tau_0$

(101)

(102)

(103)

ry parameter β, and the
The values of β and $\bar{\tau}$
nges in temperature while
easing temperature. The
anges indicates a process
dynamic analysis of the
es were involved led to an

TABLE 13. ULTRASONIC ABSORPTION PARAMETERS[a] FOR POLYGLUTAMIC ACID (AFTER BURKE, HAMMES, AND LEWIS, 1965)

pH	$10^{15}\ A/c'$ s²/(cm)(m)	β	$10^8\bar{\tau}$ s	
5.4	2.80	0.48	0.7	0.240 m
5.6	2.90	0.58	0.9	
5.8	3.10	0.68	1.1	
6.0	3.25	0.70	1.2	
6.2	3.25	0.70	1.2	
9.0	3.25	0.73	1.8	
5.4	3.15	0.65	1.0	0.120 m
5.8	3.35	0.78	1.2	
6.2	3.45	0.80	1.4	
9.0	3.55	0.82	1.4	
9.0[b]	3.45	0.73	1.4	

[a] 2:1 0.2 *M* NaCl (*aq*)-dioxane, 25°C; $\beta = 31.0 \times 10^{-17}$ s²/cm.
[b] 2:1 4 *M* NaCl (*aq*)-dioxane, 25°C.

estimate of minimum volume change ΔV^0 of approximately ± 3 cm³/mole of monomer. This estimate comprises supporting evidence for the postulated relaxational mechanism, i.e., solvation of the macromolecule by water. The magnitude of ΔV^0 is as expected, and is smaller by a factor of 3 than the volume change accompanying ionization of acetic acid and larger by a factor of 3 than that for the helix-coil transition (Burke, Hammes, and Lewis, 1965).

Considerable attention has been given to the analysis of relaxation spectra in the study of the rheological properties of polymers and polymer solutions (Ferry, 1961; Gotlib and Salikhov, 1964). Among these extensively developed techniques of analysis is a numerical method of successive approximation which will be the subject of the next section. When materials are sufficiently viscoelastic to allow measurement of the complex shear modulus G^* to be performed in a separate experiment, then the procedure of analysis is facilitated. Shear-wave data may be interpreted without introduction of the complicating effects of the bulk viscoelastic properties, and with the valid consideration of only one distribution function $g_1(\tau)$ in Eq. (39). Consequently, experimental work should be designed to yield ultrasonic shear-wave *and* compressional-wave data on the same specimen over the same frequency range, whenever this can possibly be achieved (see Litovitz and Davis, 1965).

Numerical procedures

An approximate distribution function may be determined directly from the dependence of $\alpha_r\lambda$ on frequency. An expression equivalent to Eq. (37)

but referring to longitudinal compressional waves is

$$\frac{\alpha_l\lambda}{\pi} \simeq \frac{\alpha_r\lambda}{\pi} = \frac{\alpha_r v_l}{\pi f} = \frac{K''(\omega) + \frac{4}{3}G''(\omega)}{K'(\omega) + \frac{4}{3}G'(\omega)} \qquad \frac{\alpha_r\lambda}{\pi} \ll 1 \tag{104}$$

where it is assumed that the total absorption is due to relaxational processes. If it is also assumed that the magnitude of the velocity dispersion is negligible, then $K'(\omega)$ and $G'(\omega)$ can be considered independent of frequency. If, furthermore, the distribution functions, $g_1(\tau)$ and $g_2(\tau)$, which are used in the imaginary parts of Eqs. (39) and (41) to represent $G''(\omega)$ and $K''(\omega)$, respectively, are assumed to be the same and are written as $g(\tau)$, then the absorption per wavelength $(\alpha_r\lambda)$ will have the same functional dependence on frequency as $g_3(f_r)$, defined by the equation

$$g_3(f_r)\, df_r = g(\tau)\, d\tau \tag{105}$$

Hence, $\alpha_r\lambda$ plotted as a function of frequency can be regarded as a first approximation to a distribution function. If both shear and compressional wave-absorption data are available, then both $g_1(\tau)$ and $g_2(\tau)$ may be determined independently.

Exact expressions for evaluating a distribution function from experimental data have been given by Gross [1953], and approximate methods have been described by Alfrey [1948]. Barlow and Lamb [1959] have extended the technique to allow successive refinement of a distribution function. In the case of shear waves, they use the gradient of an experimental curve of $G'(\log f)$ to obtain a first approximation:

$$\frac{\partial G'(\log f)}{\partial(\log f)} = G^{\infty} g_4(\log p_r) \tag{106}$$

where $g_4(\log p_r)\, d(\log p_r) = g_1(\tau)\, d\tau$ and $p_r \equiv \tau/\tau_0$ is a dimensionless parameter, defined in terms of relaxation times τ, normalized with respect to an arbitrarily chosen relaxation time τ_0. The curve $G'(\log f)$ is recalculated from $g_4(\log p_r)$; the difference between calculated and experimental curves, $\delta G'(\log f)$, represents an incremental modulus which may be used in the same manner as $G'(\log f)$ in Eq. (106). The procedure is repeated until the reconstituted curve of $G'(\log f)$ agrees with the measured curve within experimental accuracy.

A similar procedure may be used if, instead of G', experimental curves of $\alpha_r\lambda$ or α_r/f^2 are available as functions of frequency.

5. CONCLUDING REMARKS

It can be concluded from the previous sections that current understanding of ultrasonic absorption processes in solutions of biologically interesting molecules and in tissues is unsatisfactory. Basic to such an understanding

is some knowledge of the fundamental steps involved in the chemical reactions that can and do occur. At present such knowledge regarding chemical reactions involving comparatively small molecules in solution is accumulating. A comprehensive theoretical treatment of chemical relaxational behavior for complex mechanisms has been published recently by Hammes and Schimmel [1966].

The unsatisfactory status of the field is due in part to an insufficiency of reliable data; in part to the complexity of the systems under consideration; and in part to the limitations imposed by the precision, volumetric requirements, and frequency range of current-measuring techniques. With the advent of Brillouin scattering methods, the available frequency range may be extended by two decades at the high-frequency end of the spectrum. However, normal Tyndall scattering of light by macromolecules in solution (which is employed to estimate molecular weights) may represent a restriction on the applicability of Brillouin techniques to specimens of high molecular weight. Additional exploitation of the thermoelectric method of measuring absorption-coefficient values of extremely small volumes of tissue promises to yield the essential information on individual tissue components. Further development of ultrasonic techniques capable of extending the study of small volumes of solutions at the low-frequency end of the spectrum is desirable, but presents considerable difficulties. Improvement in precision and accuracy can also be aided with the use of increasingly sophisticated electronic instrumentation and control circuitry.

Much of the earlier work dealing with the acoustic properties of tissues cannot be considered seriously because of the lack of adequate knowledge and control of the conditions under which the measurements were made. The necessity for comprehensive control and reporting of experimental conditions cannot be overemphasized. Knowledge is required of the temperature, density, viscosity, pH, and ionic strengths of solutions; the chemical purity, molecular weight, molecular weight distribution, and concentration of solutes; the source, age, preparative procedure, and physiological condition of tissue "samples" in vivo; and, in addition, the details of any preservative treatment employed for in vitro specimens.

Use of extensive computational facilities can be expected to allow investigators to compare their experimental data with predictions based on models of progressively increasing complexity. In this regard it is pertinent to observe that the analysis of ultrasonic absorption coefficient data [via Eq. (48)] offers a critical test of molecular models of liquids. Not only is $\alpha_r\lambda$ functionally related to the compressibility β_T and heat capacity C_p, which are second derivatives of the free energy G, but it is also explicitly related to the relaxational increments $\Delta\beta_T$ and ΔC_p, in these quantities via the difference between functions of these increments. Thus, a "liquid" model which adequately predicts the behavior of the ultrasonic absorption coefficient, as

TABLE 14. CLASSIFICATION OF POSSIBLE ABSORPTION MECHANISMS IN AQUEOUS SOLUTIONS OF MACROMOLECULES

System	*Mechanisms*	*References*	*Remarks*
I Homogeneous liquid continuum	(*a*) Shear viscosity and heat conduction	Stokes [1845] Kirchhoff [1868]	"Classical" absorption
	(*b*) Radiation and diffusion		Negligible magnitude
II Inhomogeneous liquid	(*a*) Scattering	Rayleigh	Diffraction phenomenon, results in absorption
	(*b*) Relative motion	Lamb, H. Epstein [1941]	Translational and rotational
III Intramolecular mechanisms (1) Water	(*a*) Flickering clusters	Hall [1948] Frank and Wen [1957] Némethy and Scheraga [1962] Marchi and Eyring [1964]	Structural mechanism + thermal mechanisms, possibly "revealed" by presence of solute if γ becomes significantly different from 1 (probably negligible)
	(*b*) Vacant lattice site	Samoilov [1946]	
	(*c*) Clathrates	Pauling and Marsh [1952]	
(2) Macromolecule	(*a*) Internal vibration	Kneser [1947]	Thermal mechanisms at primary, secondary, tertiary, and quaternary levels
	(*b*) Rotational isomerism	Lamb, J. [1965]	Thermal mechanisms at primary and secondary levels, e.g., disruption of secondary bonds while tertiary bonds remain intact (probably negligible)
	(*c*) Internal hydrogen bonding	Zana	
	(*d*) Cooperative phenomena	Zana et al. [1963]	e.g., Denaturation of protein
	(i) Helix-coil transition	Schwarz [1965] Zimm and Bragg [1959]	
	(ii) "Stochastic resonance"	Cerf [1965]	
	(*e*) Association-dissociation	Field and O'Brien [1955]	e.g., Dimerization
IV Intermolecular mechanisms (1) Ambient electrolyte	(*a*) Ionic association	Eigen [1963] Eigen, Kurtze and Tamm [1953]	Including complex ion formation
	(*b*) Ionic atmosphere	Debye and Hückel [1923] Eigen [1957]	Negligible magnitude
(2) Macromolecule–water interaction	(*a*) Hydrogen bonding	Klotz [1953]	Hydration
	(*b*) Hydrophobic bonding	Kauzman [1954]	Hydration
	(*c*) Local viscosity	Zimm [1956]	Modified viscosity
	(*d*) Proton transfer	Rouse [1953]	Free-draining model
	(*e*) Polyelectrolytic phenomena	Eigen and de Maeyer [1963]	Hydrolysis and ionization
	(i) Independent sites	Rice and Nagasawa [1961]	
	(ii) Interacting sites		
(3) Macromolecule–ambient electrolyte interaction	(*a*) Ionic atmosphere		Preferential hydration
	(*b*) Binding of small ions	Klotz [1953]	

well as the behavior of less demanding parameters, may be regarded with some degree of confidence.

Table 14 constitutes a tentative classification and selection of mechanisms which may prove relevant to the prediction of ultrasonic absorption coefficients from models of solutions of macromolecules. This table is no more than a provisional list compiled by the authors, and comprising topics that should be considered in attempts to postulate physical models. There is no intent to suggest that a comprehensive scheme of classification is presented. In assessing the probable significance of specific reaction mechanisms in any particular case, it is necessary to consider not only the energy of activation for the reaction but also the energy differences which determine the relative concentrations of the participating species. Obviously a reaction will not contribute appreciably to the measured absorption coefficient if one of the reacting species is present in negligible proportions.

IV Intermolecular mechanisms	(1) Ambient electrolyte	(*a*) Ionic association	Eigen [1963] Eigen, Kurtze and Tamm [1953]	Including complex ion formation
		(*b*) Ionic atmosphere	Debye and Hückel [1923] Eigen [1957]	Negligible magnitude
	(2) Macromolecule–water interaction	(*a*) Hydrogen bonding	Klotz [1953]	Hydration
		(*b*) Hydrophobic bonding	Kauzman [1954]	Hydration
		(*c*) Local viscosity	Zimm [1956] Rouse [1953]	Modified viscosity Free-draining model
		(*d*) Proton transfer	Eigen and de Maeyer [1963]	Hydrolysis and ionization
		(*e*) Polyelectrolytic phenomena (i) Independent sites (ii) Interacting sites	Rice and Nagasawa [1961]	
	(3) Macromolecule–ambient electrolyte interaction	(*a*) Ionic atmosphere		Preferential hydration
		(*b*) Binding of small ions	Klotz [1953]	

APPENDIX A

List of Symbols

		Eqs.
a	= radius of sound beam	78
a_1, a_2	= radii of spherical particles or bubbles	79
a_n, a_n', a_n''	= constants in power functions	311
a_s	= radius of sphere	56
A	= area (general)	69
A	= relaxational absorption parameter	52
A_c	= radiating area of transducer	87
b	= total dissipation parameter	62
b_t, b_r, b_v	= thermal, radiative, and viscous dissipation parameters	64, 65, 66
B_t	≡ coefficient	67
B	= classical absorption parameter	30
c	= concentration by volume of structured elements	55
c'	= concentration by weight of solute (g/100 ml)	295
c_p	= heat capacity of gas at constant pressure	61
C_p	= heat capacity of liquid at constant pressure, per mole	3
C_v	= heat capacity of liquid at constant volume, per mole	3
C_p'	= heat capacity of liquid at constant pressure, per gram	12
C_p^0	= heat capacity of liquid at constant pressure, zero frequency	48
ΔC_p	= molar increment in C_p (relaxational, $f = 0 \to \infty$)	48
c_i	= molar concentration of ith ion	Table 10
C	$= C_0 + C_L$	89
C_0	= static capacitance of transducer	88
C_L	= load capacitance	90
d	= piezoelectric coupling parameter	89

d_1	= distance between particles	79
$d(ka_s, \rho_s/\rho_0)$	= function	71
d_s	= deflection of sphere	70
D	= function in Table 5	69
$\mathscr{D}$	= diffusion coefficient	45
e	= base of Naperian logarithms	—
e	= piezoelectric constant	84
E	= voltage applied to or developed across transducer	84
E_0	= energy density	15
δE_0	= energy loss per unit volume per cycle	28
f	= frequency	6
f_r	= relaxation frequency (general)	52
f_R	= fundamental resonant frequency of transducer	85
$f_{1/2}$	= frequency of half-sensitivity	91
f_1	= relaxation frequency (shear viscosity)	36
$f(ka_s, \rho_s/\rho_0)$	≡ function	71
F	= force (general)	73
F_r	= radiation force	69
g	= gravitational constant	70
$g_1(\tau)$	= distribution function (shear)	39
$g_2(\tau)$	= distribution function (bulk)	41
$g_3(f_r)$	= modified distribution function	105
$g_4(\log p_r)$	= modified distribution function	106
g_{DC}	= Davidson-Cole distribution function	101
G	= shear modulus of elasticity	7
G	= Gibbs free energy	Fig. 3
G^*	= shear modulus (complex)	36
G^∞	= shear modulus (infinite frequency)	36
G'	= shear modulus (real part)	page 225
G''	= shear modulus (imaginary part)	page 225
g_R	≡ coefficient	59
G_1, G_2	= molar free energies of states 1 and 2	Fig. 3
ΔG	= molar change in free energy	Fig. 3
$\Delta G^\pm$	= free energies of activation	38
h	= Planck's constant	38
h_1	$= \gamma_g/\epsilon$	59
h_2	= coefficient	74
ΔH	= molar change in enthalpy	47
H	= molar enthalpy	47
Im	= imaginary part	42
I	= intensity	14
$I_\pm$	= intensity of waves traveling in $+ve$ and $-ve$ directions	Table 4
I_{1i}, I_{1r}	= intensities of incident and reflected waves in medium 1	Table 4
I_{2t}	= intensity of transmitted wave in medium 2	Table 4
$I_{1\pm,2\pm}$	= intensity of waves traveling in ± directions in media 1 and 2	20

j	= √−
J	= mech
k_B	= Boltz
k	= prop
$\mathbf{k}$	= prop
k_b	= back
k_f	= forw
k_{12}, k_{21}, etc.	= react
K	= bulk
K^*	= bulk
K^0	= bulk
ΔK^∞	= mola
$K_{\mathrm{I,II,III}}$	= equil
l	= path
L	= para
L_b	= leng
L_c	= thick
L_w	= leng
m	= mas
	m
m_s	= mas
M	= mas
M_e	= effec
M_L	= mol
n	= inte
n_R	= num
n_1, n_2	= con
$\mathbf{n}$	= unit
N	= num
N_L	= Avo
p	= inst
p_r	= nor
P	= amp
P_0	= amb
$P_\pm$	= pres
P_{1i}, P_{1r}	= pre
	i
P_{2t}	= pres
$P_{1\pm}$, $P_{2\pm}$	= pre
	t
$P_{\max}$, $P_{\min}$	= ma
P_r	= rad
q	= dur
Q	= am
Q_e	= elec
Q_m	= me

j	$= \sqrt{-1}$	—
J	= mechanical equivalent of heat	81
k_B	= Boltzmann's constant	38
k	= propagation constant	6
$\mathbf{k}$	= propagation vector, wave number	5
k_b	= backward reaction-rate constant	38
k_f	= forward reaction-rate constant	38
k_{12}, k_{21}, etc.	= reaction-rate constants	96
K	= bulk modulus of elasticity	40
K^*	= bulk modulus of elasticity (complex)	40
K^0	= bulk modulus of elasticity (zero frequency)	40
ΔK^∞	= molar change in bulk modulus (relaxational)	40
$K_{\mathrm{I,II,III}}$	= equilibrium constants	94
l	= path length in interferometer	82
L	= parallel tuning inductance	Fig. 16
L_b	= length of beam	78
L_c	= thickness of transducer	84
L_w	= length of suspension	70
m	= mass of fluid of equal volume as embedded element; molal (as unit)	57
m_s	= mass of sphere	70
M	= mass of embedded element; molar (as unit)	57
M_e	= effective mass of embedded element	55
M_L	= molecular weight	Fig. 19
n	= integer	22
n_R	= number of bubbles of radius R_R per unit volume	62
n_1, n_2	= concentration of solvent and solute	page 294
$\mathbf{n}$	= unit propagation vector	6
N	= number of segments in chain polymer molecule	100
N_L	= Avogadro's number	Fig. 19
p	= instantaneous acoustic pressure	10
p_r	= normalized relaxation time	106
P	= amplitude of acoustic pressure	Table 1
P_0	= ambient pressure	16
$P_\pm$	= pressure amplitudes for waves traveling in $+ve$ and $-ve$ directions	17
P_{1i}, P_{1r}	= pressure amplitudes of incident and reflected waves in medium 1	Table 4
P_{2t}	= pressure amplitude of transmitted wave in medium 2	Table 4
$P_{1\pm}$, $P_{2\pm}$	= pressure amplitudes of waves traveling in $\pm ve$ directions in media 1, 2	19
$P_{\max}$, $P_{\min}$	= maximum and minimum pressure in standing wave	18
P_r	= radiation pressure	69
q	= dummy acoustic field variable	1
Q	= amplitude of dummy acoustic field variable	1
Q_e	= electrical Q	page 269
Q_m	= mechanical Q	29

Q_x	= absorption cross section	Fig. 19
r	= general radial coordinate	5
r_c	= radius of transducer	page 262
$r_{2/1}$, $r_{3/1}$, $r_{2/3}$	= ratios of impedances of media 1, 2, 3	Table 4
R	= gas constant	38
R_c	= equivalent resistance of transducer	Fig. 16
R_f	= frictional force constant	55
$\mathscr{R}_a$	= amplitude-reflection coefficient	19
$\mathscr{R}_I$	= intensity-reflection coefficient	20
R_p	= parallel resistance of R_L and R_c	89
R_L	= load resistance	89
R_R	= radius of resonant bubble	58
Re	= real part	1
s	= instantaneous condensation	11
$s_{2/1}$	= ratio of second harmonic to fundamental amplitudes	75
S	= amplitude of condensation	Table 1
S	= entropy	47
ΔS	= molar change in entropy	47
SWR	= standing-wave ratio	18
$(SWR)_1$	= standing-wave ratio (case 1)	Table 4
t	= general time coordinate	1
$\mathscr{T}_a$	= amplitude transmission coefficient	19
$\mathscr{T}_I$	= intensity transmission coefficient	20
T	= ambient temperature (absolute)	12
t_D	= decay time	29
$\mathbf{T}$	= instantaneous stress	31
$\mathbf{T}_i$	= initial stress	page 224
$\mathbf{T}_f$	= final stress	page 224
U	= molar internal energy	47
$\dot{u}_i$	= shear strain rate (initial)	Fig. 1
$\dot{u}_f$	= shear strain rate (final)	Fig. 1
ΔU	= molar change in internal energy	47
U_m, U_M	= voltage minima and maxima	82
v	= phase velocity	1
v_c	= phase velocity in transducer	85
$v_{1,2,3}$	= phase velocity in media 1, 2, 3	Table 4
v_l	= phase velocity (longitudinal wave)	3
v_s	= phase velocity (shear wave)	37
v^0	= phase velocity (zero frequency)	48
v^∞	= phase velocity (infinite frequency)	48
Δv	= $v^\infty - v^0$, velocity dispersion	53*a*
v_f	= streaming flow velocity	78
V	= molar volume	47
ΔV	= molar volume change	47
ΔV^0	= standard molar volume change	page 313
x	= general spatial coordinate	1
x_3	= thickness of medium 3	Table 4

$X_{1,2,3}$	= reac
y	= gen
Y_e	= elec
Z_i	= vale
Z_0	= cha
$Z_{1,2}$	= cha
Z_e	= elec
α	= amp
α_l	= amp
α_s	= amp
α_r	= amp
α_t	= amp
α_v	= amp
α_{sp}	= amp
α_X, α_Y	= amp
α_0	= amp
α_2,$\alpha_{2,X}$,$\alpha_{2,Y}$	= atte
$\bar{\alpha}_2$	= par
β	= Da
β_S	= adia
β_T	= isot
β_S^0	= adia
$\Delta\beta_T$	= mol
β_2	= fun
γ	= rati
γ^0	= rati
γ_c	= para
γ_g	= ratio
Δ'	= loga
ϵ	= coef
ϵ_c	= rela
ϵ_0	= diel
η	= shea
η_1	= visc
η_v	= bulk
η^*	= shea
η^0	= shea
θ	= ther
ϑ	= inst
Θ	= inst
$\theta_{1,2}$	= ang
$\varkappa$	= ther
$\varkappa_g$	= ther
κ	= $A_c R$
λ	= wav
λ_3	= wav
μ	= inte

$X_{1,2,3}$	= reacting species	96
y	= general variable in diffusion equation	45
Y_e	= electric input admittance	Fig. 14
Z_i	= valency of ith ion	Table 10
Z_0	= characteristic acoustic impedance	13
$Z_{1,2}$	= characteristic acoustic impedances of media 1 and 2	19
Z_e	= electrical input impedance of transducer	87
α	= amplitude absorption coefficient (general)	27
α_l	= amplitude absorption coefficient (longitudinal waves)	43
α_s	= amplitude absorption coefficient (shear waves)	37
α_r	= amplitude absorption coefficient (relaxational)	48
α_t	= amplitude absorption coefficient (thermal conduction)	46
α_v	= amplitude absorption coefficient (viscosity)	30
α_{sp}	= amplitude absorption coefficient (specific)	page 295
α_X, α_Y	= amplitude absorption coefficient (liquids X and Y)	83
α_0	= amplitude absorption coefficient (solvent)	page 295
$\alpha_2, \alpha_{2,X}, \alpha_{2,Y}$	= attenuation coefficient (liquids X and Y)	82
$\bar{\alpha}_2$	= partial specific absorption coefficient	page 294
β	= Davidson-Cole distribution parameter	101
β_S	= adiabatic compressibility	2
β_T	= isothermal compressibility	3
β_S^0	= adiabatic compressibility (zero frequency)	48
$\Delta\beta_T$	= molar change in isothermal compressibility	48
β_2	= function	82
γ	= ratio of specific heats of liquid	3
γ^0	= ratio of specific heats of liquid (zero frequency)	48
γ_c	= parameter on Fig. 13	86
γ_g	= ratio of specific heats of gas	58
Δ'	= logarithmic decrement	29
ϵ	= coefficient	60
ϵ_c	= relative dielectric constant of transducer material	88
ϵ_0	= dielectric constant of free space	88
η	= shear viscosity	30
η_1	= viscosity of solvent	100
η_v	= bulk viscosity	42
η^*	= shear viscosity (complex)	34
η^0	= shear viscosity (zero frequency)	31
θ	= thermal expansion coefficient	12
ϑ	= instantaneous acoustic temperature	12
Θ	= instantaneous acoustic temperature amplitude	Table 1
$\theta_{1,2}$	= angles of incidence and refraction	Table 4
$\varkappa$	= thermal conductivity of liquid	46
$\varkappa_g$	= thermal conductivity of gas	61
κ	= $A_c R_c / L_c$	93
λ	= wavelength	6
λ_3	= wavelength in third medium	22
μ	= intensity absorption coefficient	page 222

ξ	= instantaneous particle displacement	2
$\dot{\xi}$	= instantaneous particle velocity	Table 1
$\dot{\xi}$	= local fluid velocity	73
$\ddot{\xi}$	= instantaneous particle acceleration	Table 1
ξ_x	= component of ξ in direction x	10
Ξ	= amplitude of particle displacement	Table 1
$\dot{\Xi}$	= amplitude of particle velocity	2
$\ddot{\Xi}$	= amplitude of particle acceleration	Table 1
$\Xi_{\pm}$	= amplitude of particle displacement in $\pm ve$ directions	5
ρ	= instantaneous density	11
ρ_0	= mean density of liquid	2
$\rho_{1,2,3}$	= densities of media 1, 2, 3	Table 4
ρ_e	= density of embedded elements	55
ρ_g	= density of gas	61
ρ_s	= density of sphere	71
ρ_t	= density of tissue	81
σ	= surface tension	59
τ	= relaxation time (general)	39
τ_0	= normalizing relaxation time (arbitrary)	101
τ_1	= relaxation time (shear modulus)	31
τ_2	= relaxation time (bulk modulus)	40
τ_3	= relaxation time (general thermodynamic)	48
τ_4	= relaxation time (structural)	49
τ_5	= relaxation time (thermal)	50
$\tau_a, \tau_b, \tau_c, \tau_d$	= limits of relaxation-time spectrum	39, 41
τ_p	= pth relaxation time for a segmented, coiled polymer molecule	100
τ', τ''	= relaxation times	96
τ^*	= mean relaxation time	page 284
$\bar{\tau}$	= average relaxation time	102
ϕ	= scalar displacement potential	8
φ	= angle of lag of response to perturbation	29
$\varphi_{2/1}$	= phase angle of second harmonic relative to fundamental	75
Φ	= coefficient	61
$\boldsymbol{\Phi}$	= vector displacement potential	8
ψ	= scalar velocity potential	9*b*
Ψ_t	= transition probability factor	38
ω	= angular frequency	1
ω_0	= R_f/M_e	55
ω_R	= resonant angular frequency of bubble	58
ω_{eR}	= resonant angular frequency of transducer	page 269

BIBLIOGRAPHY

Ackerman, E., and W. Holak: Ceramic Probe Microphones, *Rev. Sci. Instr.*, **25**:857 (1954).

Aldes, J. H.: The Indications and Contraindications for Ultrasonic Therapy in Medicine,

in E. Kelly (ed.), "Ultrasound in Biology and Medicine," p. 66, American Institute of Biological Science, Washington, D.C., 1957.

Alfrey, T.: "Mechanical Behavior of High Polymers," Interscience Publishers, Inc., New York, 1948.

Anantaraman, A. V., A. D. Walters, P. D. Edmonds, and C. J. Pings: Absorption of Sound near the Critical Point of the Nitrobenzene-*iso*-octane System, *J. Chem. Phys.*, **44**:2651 (1966).

Andreae, J. H., and P. D. Edmonds: Two Megacycle Ultrasonic Interferometer, *J. Sci. Instr.*, **38**:508 (1961).

Andreae, J. H., and J. Lamb: Ultrasonic Relaxation Theory for Liquids, *Proc. Phys. Soc. London*, **B69**:814 (1956).

Andreae, J. H., R. Bass, E. L. Heasell, and J. Lamb: Pulse Techniques for Measuring Ultrasonic Absorption in Liquids, *Acustica*, **8**:131 (1958).

Andreae, J. H., P. D. Edmonds, and J. F. McKellar: Ultrasonic Studies of Aqueous Solutions of Non-electrolytes, *Acustica*, **15**:74 (1965).

Andreae, J. H., and P. L. Joyce: 30 to 230 mc Pulse Technique for Ultrasonic Absorption Measurements in Liquids, *Brit. J. Appl. Phys.*, **13**:462 (1962).

Andrews, R. D.: Correlation of Dynamic and Static Measurements on Rubberlike Materials, *Ind. Eng. Chem.*, **44**:707 (1952).

Angerer, O. A., G. Barth, and W. Güttner: Über den Wirkungsmechanismus biologischer Ultraschallreaktionen, *Strahlentherapie*, **84**:601 (1954).

Atkinson, G., and S. K. Kor: The Kinetics of Ion Association in Manganese Sulphate Solutions, I, *J. Phys. Chem.*, **69**:128 (1965).

Barlow, A. J., and J. Lamb: The Visco-elastic Behaviour of Lubricating Oils under Cyclic Shearing Stress, *Proc. Roy. Soc. London*, **A253**:52 (1959).

Barrett, R. E., R. T. Beyer, and F. L. McNamara: Ultrasonic Absorption in Acetate Solutions, *J. Acoust. Soc. Amer.*, **26**:966 (1954).

Barrett, R. E.: Personal communication (1966).

Bass, R.: Diffraction Effects in the Ultrasonic Field of a Piston Source, *J. Acoust. Soc. Amer.*, **30**:602 (1958).

Bauer, H.-J., and H. Haessler: Determination of the Rotational Potential of Polystyrene by Sound Absorption Measurements in Solutions, *Rep. 6th Int. Congr. Acoustics*, p. J-69, Tokyo, 1968.

Begui, Z. E.: Acoustic Properties of the Refractive Media of the Eye, *J. Acoust. Soc. Amer.*, **26**:365 (1954).

Benedek, G. B., J. B. Lastovka, K. Fritsch, and T. Greytak: Brillouin Scattering in Liquids and Solids Using Low-Power Lasers, *J. Opt. Soc. Amer.*, **54**:1284 (1964).

Bernal, J. D., and R. H. Fowler: A Theory of Water and Ionic Solution, with Particular Reference to Hydrogen and Hydroxyl Ions, *J. Chem. Phys.*, **1**:515 (1933).

Beyer, R. T.: Nonlinear Acoustics, in W. P. Mason (ed.), "Physical Acoustics," vol. 2, part B, chap. 10, p. 231, Academic Press Inc., New York, 1965.

Blackstock, D. T.: Further Report on the Transient Solution for Sound in a Viscous Fluid, *J. Acoust. Soc. Amer.*, **40**:1268 (1966).

Blake, F. G.: The Onset of Cavitation in Liquids, *Harvard Univ. Acoust. Res. Lab. Tech. Memo.* 12, 1949.

Brandt, O., H. Freund, and E. Hiedemann: Schwebstoffe im Schallfeld, *Z. Physik*, **104**:511 (1937).

Braunitzer, G., K. Hilse, V. Rudloff, and N. Hilschmann: The Hemoglobins, *Advan. Protein Chem.*, **19**:1 (1964).

Burke, J. J., G. G. Hammes, and T. B. Lewis: Ultrasonic Attenuation Measurements in Poly-L-glutamic Acid Solutions, *J. Chem. Phys.*, **42**:3520 (1965).

Burton, C. J.: A Study of Ultrasonic Velocity and Absorption in Liquid Mixtures, *J. Acoust. Soc. Amer.*, **20**:186 (1948).

Carome, E. F., and J. M. Witting: Theory of Ultrasonic Attenuation in Cylindrical and Rectangular Waveguides, *J. Acoust. Soc. Amer.*, **33**:187 (1961).

Carstensen, E. L.: Measurement of Dispersion of Velocity of Sound in Liquids, *J. Acoust. Soc. Amer.*, **26**:858 (1954).

Carstensen, E. L., and H. P. Schwan: Absorption of Sound Arising from the Presence of Intact Cells in Blood, *J. Acoust. Soc. Amer.*, **31**:185 (1959*a*).

Carstensen, E. L., and H. P. Schwan: Acoustic Properties of Hemoglobin Solutions, *J. Acoust. Soc. Amer.*, **31**:305 (1959*b*).

Carstensen, E. L., Kam Li, and H. P. Schwan: Determination of the Acoustic Properties of Blood and Its Components, *J. Acoust. Soc. Amer.*, **25**:286 (1953).

Cerf, R.: Sur l'Interféromètre ultrasonore à deux transducteurs et la spectroscopie à fréquence continûment variable, *Acustica*, **13**:417 (1963).

Cerf, R.: Sur la Résonance stochastique, *Rep. 5th Int. Congr. Acoustic*, p. c13, Liege, 1965.

Cerf, R.: *Compt. Rend.*, **260**:3910, 5225 (1965).

Cerf, R., S. Candau, and R. Zana: Sur les Anomalies des spectres d'absorption ultrasonores dans les solutions de hauts polymères: Essai d'interpretation, *Rep. 4th Int. Congr. Acoustics*, p. J13, Copenhagen, 1962.

Chiao, R. Y., and B. P. Stoicheff: Brillouin Scattering in Liquids Excited by the He-Ne Maser, *J. Opt. Soc. Amer.*, **54**:1286 (1964).

Chynoweth, A. G., and W. G. Schneider: Ultrasonic Propagation in Binary Liquid Systems near Their Critical Solution Temperature, *J. Chem. Phys.*, **19**:1566 (1951).

Chynoweth, A. G., and W. G. Schneider: Erratum: Ultrasonic Propagation in Binary Liquid Systems near Their Critical Solution Temperature, *J. Chem. Phys.*, **20**:760 (1952).

Clark, A. E., and T. A. Litovitz: Ultrasonic Measurement of Vibrational, Rotational Isometric, Structural and Shear Relaxation in Isobutyl Bromide, *J. Acoust. Soc. Amer.*, **32**:1221 (1960).

Claussen, W. F.: Suggested Structures of Water in Inert Gas Hydrates, *J. Chem. Phys.*, **19**:259 (1951*a*).

Claussen, W. F.: Erratum: Suggested Structures of Water in Inert Gas Hydrates, *J. Chem. Phys.*, **19**:662 (1951*b*).

Claussen, W. F.: A Second Water Structure for Inert Gas Hydrates, *J. Chem. Phys.*, **19**:1425 (1951*c*).

Collie, C. H., J. B. Hasted, and D. M. Ritson: The Dielectric Properties of Water and Heavy Water, *Proc. Phys. Soc. London*, **60**:145 (1948).

Davidson, D. W., and R. H. Cole: Dielectric Relaxation in Glycerine, *J. Chem. Phys.*, **18**:1417 (1950).

Davidson, D. W.: Dielectric Relaxation in Glycerol, Propylene Glycol and *n*-Propanol, *J. Chem. Phys.*, **19**:1484 (1951).

Debye, P. J. W., and E. Hückel: Zur Theorie der Elektrolyte: I, Gefrierpunktserniedrigung und Verwandte Erscheinungen, *Physik. Z.*, **24**:185 (1923); also in The Collected Papers of Peter J. W. Debye, p. 217, Interscience Publishers, Inc., New York, 1954.

Debye, P. J. W., and F. W. Sears: Scattering of Light by Supersonic Waves, *Proc. Natl. Acad. Sci.*, **18**:410 (1932).

de Groot, M. S., and J. Lamb: Ultrasonic Relaxation in the Study of Rotational Isomers, *Proc. Roy. Soc. London*, **A242**:36 (1957).

Del Grosso, V. A., E. J. Smura, and P. F. Fougere: Accuracy of Ultrasonic Interferometer Velocity Determinations, *Naval Res. Lab. Rep.* 4439 (1954).

Devin, C.: Survey of Thermal, Radiation, and Viscous Damping of Pulsating Air Bubbles in Water, *J. Acoust. Soc. Amer.*, **31**:1654 (1959).

Doty, P., A. Wada, J. T. Yang, and E. R. Blout: Polypeptides: VIII, Molecular Configurations of Poly-L-glutamic Acid in Water-Dioxane Solution, *J. Polymer Sci.*, **23**:851 (1957).

Dunn, F.: Temperature and Amplitude Dependence of Acoustic Absorption in Tissue, *J. Acoust. Soc. Amer.*, **34**:1545 (1962).

Dunn, F.: Ultrasonic Absorption by Biological Materials, in E. Kelly (ed.), "Ultrasonic Energy," p. 51, University of Illinois Press, Urbana, Ill., 1965.

Dunn, F., and J. E. Breyer: Generation and Detection of Ultrahigh-frequency Sound in Liquids, *J. Acoust. Soc. Amer.*, **34**:775 (1962).

Dunn, F., and W. J. Fry: Precision Calibration of Ultrasonic Fields by Thermoelectric Probes, *IRE Trans. Ultrasonic Eng.*, **UE-5**:59 (1957).

Dunn, F.: Ultrasonic Absorption and Reflection by Lung Tissue, *Phys. Med. Biol.*, **5**:401 (1961).

Dunn, F., and S. A. Hawley: Ultra-high Acoustic Waves in Liquids and Their Interaction with Biological Structures, in E. Kelly (ed.), "Ultrasonic Energy," p. 66, University of Illinois Press, Urbana, Ill., 1965.

Eckart, C.: Vortices and Streams Caused by Sound Waves, *Phys. Rev.*, **73**:68 (1948).

Edmonds, P. D.: Ultrasonic Absorption of Hemoglobin Solutions, *Biochim. Biophys. Acta*, **63**:216 (1962).

Edmonds, P. D.: Ultrasonic Absorption Cell for Normal Liquids, *Rev. Sci. Instr.*, **37**:367 (1966).

Edmonds, P. D., and T. J. Bauld: Unpublished results (1965).

Edmonds, P. D., and D. A. Orr: Ultrasonic Absorption and Dispersion at Phase Transitions in Liquid Crystalline Compounds, *Mol. Crystals*, **1**:803 (1966).

Edmonds, P. D., V. F. Pearce, and J. H. Andreae: 1.5 to 28.5 Mc/sec Pulse Apparatus for Automatic Measurement of Sound Absorption in Liquids and Some Results for Aqueous and Other Solutions, *Brit. J. Appl. Phys.*, **13**:550 (1962).

Eigen, M.: Determination of General and Specific Ionic Interactions in Solution, *Discussions Faraday Soc.*, **24**:25 (1957).

Eigen, M.: Fast Elementary Steps in Chemical Reaction Mechanisms, *Pure Appl. Chem.*, **6**:97 (1963).

Eigen, M., and L. de Maeyer: Relaxation Methods, in S. L. Friess, E. S. Lewis, and A. Weissberger (eds.), "Technique of Organic Chemistry," vol. 8, part 2, p. 895, Interscience Publishers, Inc., New York, 1963.

Eigen, M., and G. G. Hammes: Elementary Steps in Enzyme Reactions, *Advan. Enzymol.*, **35**:1 (1963).

Eigen, M., G. Kurtze, and K. Tamm: Zum Reaktionsmechanismus der Ultraschallabsorption in wässerigen Elektrolytlösungen, *Z. Elektrochem.*, **57**:103 (1953).

Eigen, M., W. Kruse, G. Maass, and L. de Maeyer: Rate Constants of Protolytic Reactions in Aqueous Solution, *Progr. Reaction Kinetics*, 285 (1964).

El'piner, I. E.: "Ultrasound: Physical, Chemical and Biological Effects," Consultants Bureau, New York, 1964.

Epstein, P. S.: On the Absorption of Sound Waves in Suspensions and Emulsions, in "Theodore v. Kármán Anniversary Volume," California Institute of Technology, Pasadena, Calif., 1941.

Esche, R.: Untersuchung der Schwingungskavitation in Flüssigkeiten, *Akust. Beih.*, **4**:208 (1952).

Fergason, J. L.: Liquid Crystals, *Sci. Amer.*, August, 1964, p. 77.

Ferry, J. D.: "Viscoelastic Properties of Polymers," John Wiley & Sons, Inc., New York, 1961.

Ferry, J. D., L. A. Holmes, J. Lamb, and A. J. Matheson: Viscoelastic Behavior of Dilute Polystyrene Solutions in an Extended Frequency Range, *J. Phys. Chem.*, **70**:1685 (1966).

Ficken, G. W., and E. A. Hiedemann: Simple Form of the "Sing-around" Method for the Determination of Sound Velocities, *J. Acoust. Soc. Amer.*, **28**:921 (1956).

Field, E. O., and J. R. P. O'Brien: Dissociation of Human Haemoglobin at Low pH, *Biochem. J.*, **60**:656 (1955).

Fixman, M.: Heat Capacity of Critical Mixtures, *J. Chem. Phys.*, **36**:1957 (1962*a*).

Fixman, M.: Absorption and Dispersion of Sound in Critical Mixtures, *J. Chem. Phys.*, **36**:1961 (1962*b*).

Fleury, P. A., and R. Y. Chiao: Dispersion of Hypersonic Waves in Liquids, *J. Acoust. Soc. Amer.*, **39**:751 (1966).

Flynn, H. G., Physics of Acoustic Cavitation in Liquids, in W. P. Mason (ed.), "Physical Acoustics," vol. 1, part B, chap. 9, p. 57, Academic Press Inc., New York, 1964.

Forgacs, R. L.: Precision Ultrasonic Velocity Measurements, *Electronics*, **33**:98 (1960).

Forslind, E.: A Theory of Water, *Acta Polytech.*, no. 115, *Chem. Met. Ser.*, **3**:no. 5 (1952).

Forslind, E.: Water Association and Hydrogels, *Proc. 2d Int. Congr. Rheol.*, 1954, pp. 50–63.

Fox, F. E., and V. Griffing: Experimental Investigation of Ultrasonic Intensity Gain in Water Due to Concave Reflectors, *J. Acoust. Soc. Amer.*, **21**:352 (1949).

Frank, H. S., and W. Wen: Structural Aspects of Ion-solvent Interaction in Aqueous Solutions: A Suggested Picture of Water Structure, *Discussions Faraday Soc.*, **24**:133 (1957).

Franklin, D. L., W. Schegel, and R. F. Rushmer: Blood Flow Measured by Doppler Frequency Shift of Back-scattered Ultrasound, *Science*, **134**:564 (1961).

Freedman, E.: On the Use of Ultrasonic Absorption for the Determination of Very Rapid Rates at Equilibrium, *J. Chem. Phys.*, **21**:1784 (1953).

Fry, W. J.: Mechanism of Acoustic Absorption in Tissue, *J. Acoust. Soc. Amer.*, **24**:412 (1952).

Fry, W. J.: Mammillary Complex of Cat Brain: Aspects of Quantitative Organization, *Anat. Record*, **154**:175 (1966).

Fry, W. J., and F. Dunn: Ultrasound: Analysis and Experimental Methods in Biological Research, in W. L. Nastuk (ed.), "Physical Techniques in Biological Research," vol. 4, chap. 6, p. 261, Academic Press Inc., New York, 1962.

Fry, W. J., and R. B. Fry: Determination of Absolute Sound Levels and Acoustic Absorption Coefficients by Thermocouple Probes: Theory, *J. Acoust. Soc. Amer.*, **26**:294 (1954*a*).

Fry, W. J., and R. B. Fry: Determination of Absolute Sound Levels and Acoustic Absorption Coefficients by Thermocouple Probes: Experiment, *J. Acoust. Soc. Amer.*, **26**:311 (1954*b*).

Fry, W. J., and R. B. Fry: Temperature Changes Produced in Tissue during Ultrasonic Irradiation, *J. Acoust. Soc. Amer.*, **25**:6 (1953).

Fry, W. J., and R. Meyers: Ultrasonic Method of Modifying Brain Structure(s), *Confinia Neurol.*, **22**:315 (1962).

Fry, W. J., J. M. Taylor, and B. W. Henvis: "Design of Crystal Vibrating Systems," Dover Publications, Inc., New York, 1948.

Goldman, D. E., and T. F. Hueter: Tabular Data of the Velocity and Absorption of High-frequency Sound in Mammalian Tissues, *J. Acoust. Soc. Amer.*, **28**:35 (1956); **29**:655 (1957).

Gotlib, Y. Y., and Salikhov, K. M.: Theory of Ultrasonic Absorption in Concentrated Polymeric Solutions, *Sov. Phys.-Acoust.*, **9**:246 (1964).

Goto, S., and T. Isemura: Studies of the Hydration and the Structure of Water and Their Roles in Protein Structure: IV, The Hydration of Amino Acids and Oligopeptides, *Bull. Chem. Soc. Japan*, **37**:1697 (1964).

Gramberg, H.: Doctoral dissertation, Johann-Wolfgang-Goethe Universität, Frankfurt, 1956.

Greenspan, M., and C. E. Tschiegg: Speed of Sound in Water by a Direct Method, *J. Res. Natl. Bur. Std.*, **59**:249 (1957).

Gross, B.: "Mathematical Structure of the Theories of Viscoelasticity," Hermann & Cie., Paris, 1953.

Gruber, G. J., and T. A. Litovitz: Shear and Structural Relaxation in Molten Zinc Chloride, *J. Chem. Phys.*, **40**:13 (1964).

Gucker, F. T., and R. M. Haag: Compressibility of Solutions: II, An Ultrasonic Study of Aqueous Solutions of Some Simple Amino Acids and Their Uncharged Isomers at 25°C, *J. Acoust. Soc. Amer.*, **25**:470 (1953).

Hall, L.: The Origin of Ultrasonic Absorption in Water, *Phys. Rev.*, **73**:775 (1948).

Hammes, G. G., and W. Knoche: Ultrasonic Absorption Measurements in Mixed Solvents: Water-Dioxane, *J. Chem. Phys.*, **45**:4041 (1966).

Hammes, G. G., and T. B. Lewis: Ultrasonic Absorption in Aqueous Polyethylene Glycol Solutions, *J. Phys. Chem.*, **70**:1610 (1966).

Hammes, G. G., and P. R. Schimmel, Chemical Relaxation Spectra: Calculation of Relaxation Times for Complex Mechanisms, *J. Phys. Chem.*, **70**:2319 (1966).

Hawley, S. A., J. E. Breyer, and F. Dunn: Fabrication of Miniature Thermocouples for uhf Acoustic Detectors, *Rev. Sci. Instr.*, **33**:1118 (1962).

Hawley, S. A., L. W. Kessler, and F. Dunn: Ultrasonic Absorption in Aqueous Solutions of High-molecular-weight Polysaccharides, *J. Acoust. Soc. Amer.*, **38**:521 (1965*a*).

Hawley, S. A., L. W. Kessler, and F. Dunn: Ultrasonic Absorption in Aqueous Solutions of High-molecular-weight Polysaccharides, *J. Acoust. Soc. Amer.*, **38**:1064 (1965*b*).

Hawley, S. A., R. M. Macleod, and F. Dunn: Degradation of DNA by Intense, Non-cavitating Ultrasound, *J. Acoust. Soc. Amer.*, **35**:1285 (1963).

Heasell, E. L., and J. Lamb: The Absorption of Ultrasonic Waves in a Number of Pure Liquids over the Frequency Range 100 to 200 Mc/sec, *Proc. Phys. Soc. London*, **B69**:869 (1956*a*).

Heasell, E. L., and J. Lamb: Ultrasonic Relaxation Processes in Liquid Triethylamine, *Proc. Roy. Soc. London*, **A236**:233 (1956*b*).

Herzfeld, K. F., and T. A. Litovitz: "Absorption and Dispersion of Ultrasonic Waves," Academic Press Inc., New York, 1959.

Hiedemann, E.: in *FIAT Rev. Ger. Sci.*, 1939–1946, part 1, 178 (1947).

Hiedemann, E., and R. D. Spence: Towards a Uniform Theory of Relaxation Phenomena, *Z. Physik.*, **133**:109 (1952).

Holmes, J. H.: Medical Ultrasonic Diagnostic Techniques, in W. E. Murray and P. F. Salisbury (eds.), "Biomedical Sciences Instrumentation," vol. 2, p. 11, Plenum Press, New York, 1964.

Howry, D. H.: Techniques Used in Ultrasound Visualization of Soft Tissues, in E. Kelly (ed.), "Ultrasound in Biology and Medicine," p. 49, American Institute of Biological Sciences, Washington, D.C., 1957.

Hoyer, W. A., and A. W. Nolle: Behavior of Liquid Crystal Compounds near the Isotropic-Anisotropic Transition, *J. Chem. Phys.*, **24**:803 (1956).

Hubbard, J. C.: The Acoustic Resonator Interferometer: I, The Acoustic System and Its Equivalent Electric Network, *Phys. Rev.*, **38**:1001 (1931).

Hueter, T. F.: Messung der Ultraschallabsorption in menschlichen Schädelknochen und ihre Abhängigkeit von der Frequenz, *Naturwissenschaften*, **39**:21 (1952).

Hueter, T. F.: Viscoelastic Losses in Tissues in the Ultrasonic Range, *WADC Tech. Rep.*, 57–706 (1958).

Hueter, T. F., and R. H. Bolt: "Sonics," John Wiley & Sons, Inc., New York, 1955.

Hunter, J. L., and H. D. Dardy: Ultrahigh-frequency Ultrasonic Absorption Cell, *J. Acoust. Soc. Amer.*, **36**:1914 (1964).

Hunter, J. L., and P. Durdel: Personal communication (1966).

Kauzman, W.: Denaturation of Proteins and Enzymes, in W. D. McElroy and B. Glass (eds.), "The Mechanism of Enzyme Action," p. 70, Johns Hopkins Press, Baltimore, 1954.

Kavanau, J. L.: "Water and Solute Water Interactions," Holden-Day, San Francisco, 1964.

Kendrew, J. C.: Side-chain Interactions in Myoglobin, in "Enzyme Models and Enzyme Structure," *Brookhaven Symp. Biol.*, **15**:216 (1962).

Kessler, L. W.: The Absorption of Ultrasound in Aqueous Solutions of Bovine Serum Albumin and Polyethylene Glycol, Ph.D. Thesis, University of Illinois, Urbana, Illinois (1968).

Kirchhoff, G.: Über den Einfluss der Wärmeleitung in einem Gase auf die Schallbewegung, *Pogg. Ann. Phys.*, **134**:177 (1868).

Klotz, I. M.: Protein Interactions, *Proteins*, **1**(part B):727 (1953).

Klotz, I. M.: Noncovalent Bonds in Protein Structure, in "Protein Structure and Function," *Brookhaven Symp. Biol.*, No. 13:25 (1960).

Klotz, I. M., and J. S. Franzen: Hydrogen Bonds between Model Peptide Groups in Solution, *J. Amer. Chem. Soc.*, **84**:3461 (1962).

Kneser, H. O.: Zur Deutung der Schallabsorption in Wasser, *Naturwissenschaften*, **34**:53 (1947*a*).

Kneser, H. O.: Relaxation der Schwingungswärme als Ursache der Schallabsorption in Flüssigkeiten, *Naturwissenschaften*, **34**:54 (1947*b*).

Koinito, Y. M.: Change of the Ultrasonic Absorption in the Sol-Gel Transformation, *J. Chem. Soc. Japan*, **72**:904 (1951).

Lamb, H.: "Hydrodynamics," 6th ed., Dover Publications, Inc., New York, 1945.

Lamb, J.: Thermal Relaxation in Liquids, in W. P. Mason (ed.), "Physical Acoustics," vol. 2, part A, chap. 4, p. 203, Academic Press Inc., New York, 1965.

Lamb, J., and J. Richter: Anisotropic Acoustic Attenuation with New Measurements for Quartz at Room Temperature, *Proc. Roy. Soc.*, **A293**:479 (1966).

Lamb, J., and J. Richter: New Type of Cavity Resonator for Piezoelectric Surface Excitation of Acoustic Waves at Microwave Frequencies, *Electronics Letters*, **2**: (February, 1966).

Lang, J., and R. Cerf: Absorption ultrasonore dans des solutions d'acide désoxyribonucléique: étude de la dénaturation alcaline, *J. Chim. Phys.*, **66**:81 (1969).

Langevin, P.: Procédé et appareil d'emission et de reception des ondes elastiques sous-marines à l'aide des propriétés piezoélectrique du quartz, French Pat. 505703 (1918).

Lennard-Jones, J., and J. A. Pople, Molecular Association in Liquids: II, A Theory of the Structure of Water, *Proc. Roy. Soc. London*, **A205**:163 (1951).

Leonard, R. W.: The Attenuation of Ultrasonic Waves in Water, *J. Acoust. Soc. Amer.*, **20**:224 (1948).

Lieberman, L. N.: The Second Viscosity of Liquids, *Phys. Rev.*, **75**:1415 (1949).

Litovitz, T. A., and E. H. Carnevale: The Effect of Pressure on Sound Propagation in Water, *J. Appl. Phys.*, **26**:816 (1955).

Litovitz, T. A., and C. M. Davis: Structural and Shear Relaxation in Liquids, in W. P. Mason (ed.), "Physical Acoustics," vol. 2, part A, chap. 5, p. 282, Academic Press Inc., New York, 1965.

Litovitz, T. A., and T. Lyon: Ultrasonic Hysteresis in Viscous Liquids, *J. Acoust. Soc. Amer.*, **26**:577 (1954).

Litovitz, T. A., T. Lyon, and L. Peselnick: Ultrasonic Relaxation and Its Relation to Structure in Viscous Liquids, *J. Acoust. Soc. Amer.*, **26**:566 (1954).

Lucas, R., and P. Biquard: Propriétés optiques des milieux solides et liquides soumis aux vibrations élastiques ultra-sonores, *J. Phys. Radium*, **3**:464 (1932).

Maass, G.: Ph.D. thesis, University of Göttingen, 1962.

Maidanik, G.: Acoustical Radiation Pressure Due to Incident Plane Progressive Waves on Spherical Objects, *J. Acoust. Soc. Amer.*, **29**:738 (1957).

Maidanik, G., and P. J. Westervelt: Acoustical Radiation Pressure Due to Incident Plane Progressive Waves on Spherical Objects, *J. Acoust. Soc. Amer.*, **29**:936 (1957).

Marchi, R. P., and H. Eyring: Application of Significant Structure Theory to Water, *J. Phys. Chem.*, **68**:221 (1964).

Markham, J. J., R. T. Beyer, and R. B. Lindsay: Absorption of Sound in Fluids, *Rev. Mod. Phys.*, **23**:353 (1951).

Mason, W. P.: Viscoelasticity and Shear Elasticity Measurements of Liquids by Means of Shear Vibrating Crystals, *J. Colloid Sci.*, **3**:147 (1948).

Mason, W. P.: "Piezoelectric Crystals and Their Application to Ultrasonics," D. van Nostrand Company, Inc., Princeton, N.J., 1950.

Mason, W. P., and H. J. McSkimin: Attenuation and Scattering of High Frequency Sound Waves in Metals and Glasses, *J. Acoust. Soc. Amer.*, **19**:464 (1947).

Mason, W. P., W. O. Baker, H. J. McSkimin, and J. H. Heiss: Measurement of Shear Elasticity and Viscosity of Liquids at Ultrasonic Frequencies, *Phys. Rev.*, **75**:936 (1949).

Mayer, A., and H. Vogel: Ultraschallabsorption von Hämoglobinlösungen im MHz-Bereich, *Z. Naturforsch.*, **20b**:85 (1965).

Mayer, W. G.: Mode Conversion of Ultrasonic Waves at Flat Boundaries, *IEEE Trans.*, **SU-11**:1 (1964).

McKellar, J. F., and J. H. Andreae: Ultrasonic Relaxations in Aqueous Solutions of Aliphatic Amines, *Nature*, **195**:778 (1962*a*).

McKellar, J. F., and J. H. Andreae: Ultrasonic Relaxation in a Micellar System: *n*-Octylamine-water, *Nature*, **195**:865 (1962*b*).

McSkimin, H. J.: Method for Determining the Propagation Constants of Plastics at Ultrasonic Frequencies, *J. Acoust. Soc. Amer.*, **23**:429 (1951).

McSkimin, H. J.: Ultrasonic Methods for Measuring the Mechanical Properties of Liquids and Solids, in W. P. Mason (ed.), "Physical Acoustics," vol. 1, part A, chap. 4, p. 272, Academic Press Inc., New York, 1964.

McSkimin, H. J.: Velocity of Sound in Distilled Water for the Temperature Range 20°–75°C, *J. Acoust. Soc. Amer.*, **37**:325 (1965).

Mikhailov, I. G., and L. I. Tarutina: Absorption of Supersonic Waves in Gelatin Solutions, *Dokl. Akad. Nauk SSSR*, **74**:41 (1950); *Chem. Abstr.*, **45**:416 (1951).

Musa, R. S.: Two-crystal Interferometric Method for Measuring Ultrasonic Absorption Coefficients in Liquids, *J. Acoust. Soc. Amer.*, **30**:215 (1958).

Némethy, G., and H. A. Scheraga: Structure of Water and Hydrophobic Bonding in Proteins: I, A Model for the Thermodynamic Properties of Liquid Water, *J. Chem. Phys.*, **36**:3382 (1962).

Némethy, G., I. Z. Steinberg, and H. A. Scheraga: Influence of Water Structure and of Hydrophobic Interactions on the Strength of Side-chain Hydrogen Bonds in Proteins, *Biopolymers*, **1**:43 (1963).

Nolle, A. W., and J. F. Mifsud: Ultrasonic Wave Study of Swollen Buna-N Rubber, *J. Appl. Phys.*, **24**:5 (1953).

Nyborg, W. L.: Acoustic Streaming Due to Attenuated Plane Waves, *J. Acoust. Soc. Amer.*, **25**:68 (1953).

Nyborg, W. L.: Acoustic Streaming, in W. P. Mason (ed.), "Physical Acoustics," vol. 2, part B, chap. 11, p. 265, Academic Press Inc., New York, 1965.

Oestreicher, H. L.: Field and Impedance of an Oscillating Sphere in a Viscoelastic Medium with an Application to Biophysics, *J. Acoust. Soc. Amer.*, **23**:707 (1951).

Parker, R. C., K. R. Applegate, and L. J. Slutsky: Ultrasonic Study of the Helix-coil Transition in Poly-L-lysine, *J. Phys. Chem.*, **70**, 3018 (1966).

Parker, R. C., L. J. Slutsky, and K. R. Applegate: Ultrasonic Absorption and the Kinetics of Conformational Change in Poly-L-lysine, *J. Phys. Chem.*, **72**:3177 (1968).

Passynsky, A.: Solvation of Non-electrolytes and the Compressibility of Their Solutions, *Acta Physicochim. USSR*, **22**:137 (1947).

Pauling, L.: "The Nature of the Chemical Bond," Cornell University Press, Ithaca, N.Y., 1960.

Pauling, L., and R. E. Marsh: The Structure of Chlorine Hydrate, *Proc. Natl. Acad. Sci.*, **38**:112 (1952).

Pauly, H.: Unpublished data, 1957.

Pellam, J. R., and J. K. Galt: Ultrasonic Propagation in Liquids: I, Application of Pulse Technique to Velocity and Absorption Measurements at 15 Megacycles, *J. Chem. Phys.*, **14**:608 (1946).

Philippoff, W.: Relaxations in Polymer Solutions, Liquids and Gels, in W. P. Mason (ed.), "Physical Acoustics," vol. 2, part B, chap. 7, Academic Press Inc., New York, 1965.

Pinkerton, J. M. M.: The Absorption of Ultrasonic Waves in Liquids and Its Relation to Molecular Constitution, *Proc. Phys. Soc. London*, **B62**:129 (1949).

Raman, C. V., and N. S. N. Nath: The Diffraction of Light by High Frequency Sound Waves, I and II, *Proc. Indian Acad. Sci.*, **2**:406, 413 (1935).

Rayleigh, J. W. S.: "The Theory of Sound," vol. 2, 2d ed., Dover Publications, Inc., New York, 1945.

Redwood, M. R.: "Mechanical Waveguides," Pergamon Press, London, 1960.

Reid, J. M.: "Ultrasonic Diagnostic Methods in Cardiology," Ph.D. thesis, University of Pennsylvania, 1965.

Reid, J. M., and C. R. Joyner: The Use of Ultrasound to Record the Motion of Heart Structure, in E. Kelly (ed.), "Ultrasonic Energy," p. 278, University of Illinois Press, Urbana, Ill., 1965.

Rice, S. A., and Nagasawa, M.: "Polyelectrolyte Solutions," Academic Press Inc., New York, 1961.

Rouse, P. E.: A Theory of the Linear Viscoelastic Properties of Dilute Solutions of Coiling Molecules, *J. Chem. Phys.*, **21**:1272 (1953).

Samoilov, O. Y.: *Zh. Fiz. Khim.*, **20**:12 (1946).

Samoilov, O. Y.: A New Approach to the Study of Hydration of Ions in Aqueous Solutions, *Discussions Faraday Soc.*, **24**:141 (1957*a*).

Samoilov, O. Y.: In General Discussion, *Discussions Faraday Soc.*, **24**:216 (1957*b*).

Schaafs, W.: Molecular Acoustics, in Landolt-Börnstein, "Numerical Data and Functional Relationships in Science and Technology," New Series, Group II, vol. 5, Springer-Verlag, Berlin, 1967.

Schellman, J. A.: Thermodynamics of Urea Solutions and the Heat of Formation of the Peptide Hydrogen Bond, *Compt. Rend. Lab. Carlsberg, Sér. Chim.*, **29**:223 (1955).

Schneider, W. G., and C. J. Burton: Determination of the Elastic Constants of Solids by Ultrasonic Methods, *J. Appl. Phys.*, **20**:48 (1949).

Schwan, H. P., and E. L. Carstensen: Ultrasonics Aids Diathermy Experiments, *Electronics*, July, 1952, p. 216.

Schwan, H. P., A. E. Smith, and Kam Li: Acoustic Properties of Cell Nuclei, *WADC Tech. Rep.* (1957).

Schwarz, G.: On the Kinetics of Helix-coil Transition of Polypeptides in Solution, *J. Mol. Biol.*, **11**:64 (1965).

Sette, D.: Dispersion and Absorption of Sound Waves in Liquids and Mixtures of Liquids, in S. Flügge (ed.), "Handbuch der Physik," vol. XI/1, "Acoustics I," p. 275, Springer-Verlag OHG, Berlin, 1961.

Siegert, H.: Messung und Deutung der Konzentrationsabhängigeit der Ultraschall-absorption wässriger $CoSO_4$-Lösungen im Frequenzbereich 0.2 bis 2 MHz, *Acustica*, **13**:48 (1963).

Singh, R. P., G. S. Darbari, and R. P. Verma: Acoustical Behavior of Critical Mixtures, *Phys. Rev. Letters*, **16**:1150 (1966).

Smithson, J. R., and T. A. Litovitz: Absorption of Sound in Manganous Sulphate Solutions, *J. Acoust. Soc. Amer.*, **28**:462 (1956).

Stevenson, D. P.: On the Monomer Concentration of Liquid Water, *J. Phys. Chem.*, **69**:2145 (1965).

Stokes, G. G.: On the Theories of the Internal Friction of Fluids in Motion, and of the Equilibrium and Motion of Elastic Solids, *Trans. Camb. Phil. Soc.*, **8**:287 (1845).

Storey, L. R. O.: Ultrasonic Absorption in Mixtures of Ethyl Alcohol and Water, *Proc. Phys. Soc. London*, **B65**:943 (1952).

Strasberg, M.: Onset of Ultrasonic Cavitation in Tap Water, *J. Acoust. Soc. Amer.*, **31**:163 (1959).

Stuehr, J., and E. Yeager: The Propagation of Ultrasonic Waves in Electrolytic Solutions, in W. P. Mason (ed.), "Physical Acoustics," vol. 2, part A, chap. 6, p. 351, Academic Press Inc., New York, 1965.

Tamm, K.: Schallabsorption und -Dispersion in wässrigen Elektrolytlösungen, in S. Flügge (ed.), "Handbuch der Physik," vol. XI/1, "Acoustics I," p. 202, Springer-Verlag OHG, Berlin, 1961.

Tamm, K., and G. Kurtze: Absorption of Sound in Aqueous Solutions of Electrolytes, *Nature*, **168**:346 (1951).

Tamm, K., G. Kurtze, and R. Kaiser: Measurements of Sound Absorption in Aqueous Solutions of Electrolytes, *Acustica*, **4**:380 (1954).

von Gierke, H. E., H. L. Oestreicher, E. K. Franke, H. O. Parrack, and W. W. von Wittern: Physics of Vibration in Living Tissues, *J. Appl. Physiol.*, **4**:886 (1952).

Wada, Y., H. Sasabe, and M. Tomono: Viscoelastic Relaxations in Solutions of Poly-(glutamic acid) and Gelatin at Ultrasonic Frequencies, *Biopolymers*, **5**:887 (1967).

Westervelt, P. J.: The Theory of Steady Forces Caused by Sound Waves, *J. Acoust. Soc. Amer.*, **23**:312 (1951).

Willard, G. W.: Temperature Coefficient of Ultrasonic Velocity in Solutions, *J. Acoust. Soc. Amer.*, **19**:235 (1947).

Willard, G. W.: Ultrasonic Absorption and Velocity Measurements in Numerous Liquids, *J. Acoust. Soc. Amer.*, **12**:438 (1941).

Williams, M. L., R. F. Landel, and J. D. Ferry: Temperature Dependence of Relaxation Mechanisms in Amorphous Polymers and Other Glass-forming Liquids, *J. Amer. Chem. Soc.*, **77**:3701 (1955).

Zana, R., S. Candau, and R. Cerf: Mésures d'absorption ultrasonores dans les solutions de polypeptides, *J. Chim. Phys.*, **60**:869 (1963).

Zana, R., and R. Cerf: Absorption of Ultrasound by Solutions of Rigid Particles, *J. Chim. Phys.*, **61**:1203 (1964).

Zimm, B. H.: Dynamics of Polymer Molecules in Dilute Solution: Viscoelasticity, Flow Birefringence and Dielectric Loss, *J. Chem. Phys.*, **24**:269 (1956).

Zimm, B. H., and J. K. Bragg: Theory of the Phase Transition between Helix and Random Coil in Polypeptide Chains, *J. Chem. Phys.*, **31**:526 (1959).

Zvereva, G. E., and A. P. Kapustin: Measurement of the Ultrasonic Parameters of Liquid Crystals of Cholesteryl Caprate, *Soviet Phys. Acoust.*, **10**:97 (1964).

Zvereva, G. E., and A. P. Kapustin: Absorption of Ultrasound in Liquid Crystal Cholesteryl Caprinate, *Soviet Phys. Acoust.*, **11**:212 (1965).